

THESIS

MICHIGAN STATE UNIVERSITY LIBRARIES
3 1293 02058 6396

This is to certify that the

dissertation entitled

IN-SITU AND ON-LINE CHARACTERIZATION OF POLYMER SYSTEMS:

CURE MONITORING OF POLYMER COMPOSITES AND

SPECTROSCOPIC STUDIES OF CHEMICALLY AMPLIFIED PHOTORESISTS

presented by

Julie Lynne Pepper Jessop

has been accepted towards fulfillment of the requirements for

Ph.D. degree in Chemical Engineering

Mec B. Scrantor Major professor

Date 12/9/97

MSU is an Affirmative Action/Equal Opportunity Institution

O-12771

# LIBRARY Michigan State University

PLACE IN RETURN BOX to remove this checkout from your record.

TO AVOID FINES return on or before date due.

MAY BE RECALLED with earlier due date if requested.

DATE DUE	DATE DUE	DATE DUE
	•	

11/00 c:/CIRC/DateDue.p65-p.14

# IN-SITU AND ON-LINE CHARACTERIZATION OF POLYMER SYSTEMS: CURE MONITORING OF POLYMER COMPOSITES AND SPECTROSCOPIC STUDIES OF CHEMICALLY AMPLIFIED PHOTORESISTS

Ву

Julie Lynne Pepper Jessop

#### A DISSERTATION

Submitted to Michigan State University in partial fulfillment of the requirements for the degree of

**DOCTOR OF PHILOSOPHY** 

Department of Chemical Engineering

1999

#### ABSTRACT

# IN-SITU AND ON-LINE CHARACTERIZATION OF POLYMER SYSTEMS: CURE MONITORING OF POLYMER COMPOSITES AND SPECTROSCOPIC STUDIES OF CHEMICALLY AMPLIFIED PHOTORESISTS

Ву

### Julie Lynne Pepper Jessop

Spectroscopic techniques such as fluorescence and absorption are useful for *insitu* and on-line characterization of a variety of polymer systems. Two examples are discussed in this dissertation: monitoring of cure during polymerization of composite parts and characterization of acid mobility in chemically amplified photoresists.

In the field of radiation curing, there is a compelling need for inexpensive on-line sensors for the degree of cure. On-line monitoring techniques, which could be interfaced with an electronic control scheme, would significantly enhance the reliability of polymer and composites processing methods while reducing the cost. Fluorescence cure monitoring strategies based upon trace quantities of solvatochromic probes, such as pyrene and phenoxazone 660, do not lose sensitivity at the gel point and can be implemented using optical fibers. Therefore, this method is well suited to *in-situ* and online monitoring of cure in polymerization systems.

State-of-the-art microlithographic processes used to make features smaller than 0.25 microns are based upon deep-UV lithography and chemically amplified resists. In these resists, photoacid generated during exposure initiates cascading deprotection reactions during post exposure bake (PEB) to form a developable image. Reaction may not be limited to the illuminated areas since the photo-generated protons may diffuse

of pho of sen

out

life

dur

mul

red

tech situ

affe

outside this region; therefore, it is important to understand the diffusional characteristics of the photoacid. In order to obtain this information, molecular probes were added to the photoresist, and measurements were carried out *in situ* on quartz substrates. The photoacid generation during exposure was characterized using acid-sensitive fluorescence of fluorescein, and the acid concentration was quantified during PEB using the acid-sensitive absorption of crystal violet. To measure the microscopic free-volume changes during PEB, ground-state recovery measurements of crystal violet, whose excited-state lifetime increases as the local free volume decreases, were used. The macroscopic reduction of free volume due to the relaxation of polymer chains was measured using multi-wavelength interferometry. The further application of these experimental techniques will provide a systematic study of free-volume evolution and acid mobility *in situ* during PEB. For a given resist, a more thorough understanding of the factors that affect these parameters will allow improved microlithographic pattern generation.

For God, my husband and my parents

di lis

Iv

Ki

Ale

res

onl

to e

nick

Pad

conv

the o

me

add: ass:

tedi

coll

# **ACKNOWLEDGMENTS**

I have many people to thank for their support and assistance in completing this dissertation, both the research and the manuscript. This is definitely not an all-inclusive list, but I could not print this document without acknowledging a few names. First of all, I would like to thank my graduate committee: Drs. Kris Berglund, Gary Blanchard, John Klier, and Robert Ofoli. I appreciate that you have always been available to me as resources of guidance and advice. I would especially like to thank my major advisor, Dr. Alec Scranton, who modeled for me the qualities I wish to possess as a professor (not only in research, but also in teaching) and who provided me with so many opportunities to expand my graduate education. I could not ask for a better mentor!

Secondly, I want to thank the members of our research group, affectionately nicknamed ABSLab: Kiran Baikerikar, Bernhard Drescher, Khanh Nguyen, and Kathryn Padon. I have enjoyed our group lunches, group meetings (complete with snacks) and conversations in the office. I value our camaraderie and friendship, and you made life in the office a lot more interesting and fun! Furthermore, I am grateful to Katy for infecting me with the quilting bug, which gave me a creative outlet during times of stress. In addition, I would like to mention Saleha Mohamedulla, my undergraduate research assistant, who helped me so much the semester I taught by capably working through the tedium of the Filmetrics experiments. I also want to acknowledge Scott Goldie, my colleague in chemistry, who was a tremendous driving force in the crystal violet

exp

whe

Fou Earl

on n

prov

coul

Mari

How

and !

great

faith ever

in ]

hon

experiments. Your enthusiasm and energy were much appreciated, especially on days when the samples and equipment refused to cooperate!

Next, I would like to acknowledge gratefully support from the National Science Foundation in the form of a graduate fellowship. I am also thankful for the Amelia Earhart Fellowship from Zonta International, without which I would still be typing away on my 386 without Windows.

Of course, I am extremely thankful for the love, encouragement and prayers provided by my family throughout my college education. It was important for me to know that they were behind me every step of the way and that they were proud of me. I could not ask for a better cheering section! Most of all, I am so thankful for my husband Mark, who suffered through these many years of my education. I know sometimes that it must have seemed like an eternity to him, especially when it was his turn to cook. However, he shared fully and willingly in each of my joys and sorrows during this time, and I could not imagine having accomplished this without him by my side. We make a great team, and I am looking forward to what the future holds for us together!

Finally, I would like to thank my Lord and Savior, Jesus Christ. His love and faithfulness have been an anchor in my life, and I have begun to understand that "I can do everything through him who gives me strength" (Philippians 4:13). I echo Paul's words in I Timothy 1:17—"Now to the King eternal, immortal, invisible, the only God, be honor and glory for ever and ever. Amen."

LIST O

LIST O

1. BAC 1.1. 1.2. 1.3.

1 1 1.4. (

1.5. 1

2. OBJJ 2.1. ( 2.2. (

3. IN-SI USIN 3.1. In 3.2. E

3.3. R 3.3. 3.3.

# **TABLE OF CONTENTS**

LI	ST OF TABLES	X
LI	ST OF FIGURES	xi
1.	BACKGROUND AND MOTIVATION	1
	1.1. Introduction	
	1.2. Spectroscopic background	
	1.3. Cure monitoring of polymer composites	
	1.3.1. Advantages of fluorescence	
	1.3.2. Advantages of optical fibers	
	1.3.3. Fluorescence-based cure monitoring techniques	
	1.4. Characterization of chemically amplified photoresists	
	1.4.1. Introduction	
	1.4.1.1. Semiconductor manufacturing	
	1.4.1.2. Photoresist systems	
	1.4.1.3. Advantages of chemically amplified resists	
	1.4.1.4. Issues for the advancement of chemically amplified resists	
	1.4.1.5. Motivation for research on chemically amplified resists	
	1.4.2. Background	
	1.4.2.1. General properties of chemically amplified resists	
	1.4.2.2. Microlithography for processing of microelectronic devices	
	1.4.2.3. Current models for chemically amplified resists	
	1.4.2.4. Utility of molecular probes	
	1.5. References	24
2.	OBJECTIVES	
	2.1. Cure monitoring of polymer composites	
	2.2. Characterization of chemically amplified photoresists	28
3.	IN-SITU CURE MONITORING FOR COMPOSITES PROCESSING	
	USING FLUORESCENCE SENSORS	30
	3.1. Introduction	30
	3.2. Experimental	32
	3.2.1. Materials	32
	3.2.2. Measurements	33
	3.2.2.1. Fluorescence measurements	33
	3.2.2.2. Thermocouple measurements	33
	3.3. Results and discussion	34
	3.3.1. Fluorescent probe molecules	34
	3.3.2. Fluorescence measurements	
	3.3.3. Thermocouple measurements	37

	3.3.4. Sensitivity and interpretation of fluorescence response	37
	3.3.4.1. Effect of temperature on fluorescence response of probes	
	3.3.4.2. Comparison of probe responses during polymerization	
	3.3.4.3. Effect of polarity on fluorescence response of phenoxazone	
	660	39
	3.3.4.4. Effect of oxygen on fluorescence response of pyrene	40
	3.3.4.5. Effect of temperature and initiator concentration on intensity	
	ratio of phenoxazone 660	
	3.3.4.6. Effect of phenoxazone 660 concentration on intensity ratio	
	3.3.5. Equipment design	
	3.4. Conclusions	
	3.5. References	60
4.	IN-SITU MONITORING OF ACID CONCENTRATION IN CHEMICALLY AMPLIFIED PHOTORESISTS	<b>61</b>
	4.1. Introduction	
	4.1.1 Utility of molecular probes	
	4.1.2. Studies of acid concentration in CARs	
	4.2. Experimental	
	4.2.1. Materials	
	4.2.2. Methods	
	4.2.2.1. Absorption and Fluorescence Measurements	
	4.2.2.2. Steady-state fluorescence measurements with photoresist	
	films during exposure	
	4.2.2.3. Steady-state absorption measurements with photoresist films	
	during processing	
	4.3. Results and discussion	
	4.3.1. Probe molecule selection.	
	4.3.2. Acid-sensitivity of fluorescein	
	4.3.3. Study of photoacid generation during exposure in photoresist films	07
	using steady-state fluorescence	67
	4.3.4. Acid-sensitivity of crystal violet	
	4.3.5. Study of photoacid concentration during processing in photoresist	
	films using steady-state absorption	
	4.3.6. Effect of probe presence on photoacid concentration during	
	processing in photoresist films using steady-state absorption	72
	4.4. Conclusion	74
	4.5. References	
5.	FREE VOLUME IN CHEMICALLY AMPLIFIED PHOTORESISTS	90
	5.1. Introduction	<b>9</b> 0
	5.1.1. Utility of molecular probes	
	5.1.2. Studies of free volume evolution in CARs	
	5.2. Experimental	
	5.2.1. Materials	

5. 5.

6. Co

6.2

6.3

A. API A.1. A.2. A.3.

	5.2.2. Methods	92
	5.2.2.1. Ground-state recovery measurements with photoresist films	
	during processing	
	5.2.2.2. Multi-wavelength interferometry	94
	5.3. Results and discussion	
	5.3.1. Study of microscopic free volume changes in photoresist films using	
	ground-state recovery	
	5.3.2. Multi-wavelength interferometry	97
	5.4. Conclusions	
	5.5. References	
5.	CONCLUSIONS AND RECOMMENDATIONS	. 113
	6.1. Summary of results	. 113
	6.1.1. Cure monitoring of polymer composites	113
	6.1.2. Characterization of chemically amplified photoresists	114
	6.2. Suggestions for future work	115
	6.2.1. Cure monitoring of polymer composites	115
	6.2.2. Characterization of chemically amplified photoresists	118
	6.2.2.1. 248-nm resists	
	6.2.2.2. 193-nm resists	120
	6.3. References	123
4.	APPENDIX	
	A.1. Determination of equilibrium constants	125
	A.2. Determination of alpha plots	
	A 2 Defendance	

Table

Table

Table :

Table 4

# LIST OF TABLES

# Chapter 3

Table 3.1.	Comparison of solvent polarity and phenoxazone 660 emission maximum.	39
Table 3.2.	Effects of temperature and initiator concentration upon the time to polymerization and final intensity ratio plateau for phenoxazone 660 in styrene with AIBN	41
Table 3.3.	Dependence of fluorescence peak emission wavelength and final cure monitoring ratio of phenoxazone 660 in Derakane® 470-45 with 0.75 wt.% AIBN upon probe concentration	42
	Chapter 4	
Table 4.1.	Comparison of the absorbance ratio at 278 nm for the neat Apex-E 2408 DUV photoresist film to that of the crystal violet doped films during various stages of processing	74

Fig

Figu

Figu Figu

Figu

Figu

Figur

Figur

Figure

Figure

Figure

Figure

Figure :

# LIST OF FIGURES

# Chapter 1

Figure 1.1.	Jablonski diagram for a molecule showing the pathways for activation and deactivation: absorption (a), vibrational relaxation (b), fluorescence (c), external conversion (d), intersystem crossing (e), and phosphorescence (f)	. 22
Figure 1.2.	Deprotection of PTBOC in DUV photoresist	. 23
	Chapter 3	
Figure 3.1.	General chemical structure of the Derakane® vinyl ester resins	. 45
Figure 3.2.	Chemical structures of phenoxazone 660 (a) and pyrene (b)	. 46
Figure 3.3.	Spectral shift of phenoxazone 660 associated with curing Derakane <sup>®</sup> 411-C50 (with AIBN as initiator)	. 47
Figure 3.4.	Blue-shift in phenoxazone 660 peak emission as the cure of Derakane® 411-C50 (with AIBN as initiator) progresses	. 48
Figure 3.5.	Change in phenoxazone 660 fluorescence intensity ratio in curing styrene with AIBN as initiator	. 49
Figure 3.6.	Fluorescence response of pyrene in MMA with AIBN as initiator	50
Figure 3.7.	Change in pyrene fluorescence intensity ratio in curing MMA with AIBN as initiator	51
Figure 3.8.	Change in pyrene fluorescence rolling time ratio at 378 nm in curing MMA with AIBN as initiator	. 52
Figure 3.9.	Comparison between thermocouple () and phenoxazone 660 intensity ratio (■) data in curing Derakane® 411-C50 with AIBN as initiator	. 53
Figure 3.10.	Change in pyrene fluorescence intensity ratio in tri(ethylene glycol) divinyl ether with increasing (□) and decreasing (●) temperature	54
Figure 3.11.	Change in pyrene fluorescence intensity ratio (—) and phenoxazone 660 fluorescence intensity ratio (…) in curing Derakane® 470-45 with AIBN as initiator	55

1

Fi

Fig Fig

Figu Figu

Figur

Figur

Figure

Figure

Figure .

Figure 4

Figure 4

Figure 4.

Figure 4.

Figure 3.12.	Change in pyrene fluorescence intensity ratio in curing MMA with V-70 as initiator: without oxygen	56
Figure 3.13.	Change in pyrene fluorescence intensity (top) and rolling time ratio (bottom) at 378 nm in curing MMA with V-70 as initiator: without oxygen (□) and with oxygen (●)	57
Figure 3.14.	Diagram of in-situ monitoring instrument	58
Figure 3.15.	Change in intensity ratio of phenoxazone 660 emission in curing Derakane® 411-C50 with AIBN as initiator monitored by <i>in-situ</i> apparatus	59
	Chapter 4	
Figure 4.1.	Experimental setup for <i>in-situ</i> fluorescence experiments to determine photoacid generation during exposure	76
Figure 4.2.	Absorption (abs), excitation (ex) and emission (em) characteristics of Apex-E 2408 DUV photoresist	. 77
Figure 4.3.	Molecular structure of fluorescein	78
Figure 4.4.	Absorption and emission characteristics of fluorescein in Apex-E 2408 DUV photoresist	. 78
Figure 4.5.	Change in fluorescein fluorescence emission in Apex-E 2408 DUV photoresist upon addition of sulfuric acid: before acid addition (—) and after acid addition (…)	. 79
Figure 4.6.	Fluorescence spectra of fluorescein in Apex-E 2408 DUV photoresist film as a function of increased exposure time	. <b>8</b> 0
Figure 4.7.	Intensity ratio at 525 nm and 560 nm of fluorescein in Apex-E 2408 DUV photoresist film as a function of increased exposure time	. 81
Figure 4.8.	Protonation/deprotonation equilibria for crystal violet. The corresponding spectra are shown in Figure 4.11	. 82
Figure 4.9.	Absorption and emission characteristics of crystal violet in Apex-E 2408 DUV photoresist	. 83
Figure 4.10.	Absorption and emission characteristics of crystal violet in bulk acidic (top) and basic (bottom) solutions	. 84
Figure 4.11.	Absorption spectra of crystal violet in aqueous solution. [H <sup>+</sup> ] for the solution spectra are indicated on the plot	. 85

Fi

Fi

Fig

Fig

Fig

Fig

Figu

Figu

Figui

Figur

Figure

Figure

Figure 6

Figure 6.

Figure 4.12.	Absorption spectra of crystal violet in Apex-E 2408 DUV photoresist film during and after processing
Figure 4.13.	Effect of 0.3 wt.% crystal violet in Apex-E 2408 DUV photoresist film upon the absorbance spectrum before and after processing
	Chapter 5
Figure 5.1.	Experimental setup for ground state recovery experiments to determine microscopic free volume in the photoresist films
Figure 5.2.	Experimental setup for dynamic film thickness measurements to observe macroscopic free volume evolution
Figure 5.3.	Molecular structure of crystal violet
Figure 5.4.	Schematic representation of the transient change in ground state absorption of crystal violet in response to excitation by a pump laser pulse
Figure 5.5.	Instrumental response function (····) and experimental ground state recovery data (—) for crystal violet in the Apex-E 2408 DUV photoresist film
Figure 5.6.	Linear calibration curve relating the short time constant, $\tau_1$ , from the ground state recovery experiments of viscous liquids doped with 0.1 wt.% crystal violet to the matrix viscosity
Figure 5.7.	Instrumental response function (····) and experimental ground state recovery data (—) for crystal violet in glycerol
Figure 5.8.	Change in Apex-E 2408 DUV photoresist film thickness as a function of bake time at 100°C for unexposed (top) and exposed (bottom) films
Figure 5.9.	Change in thickness of Apex-E 2408 DUV photoresist film as a function of exposure dose and post exposure bake time
Figure 5.10.	Change in thickness of UV5-0.6 positive DUV photoresist film as a function of exposure dose and post exposure bake time
	Chapter 6
Figure 6.1.	Differential scanning calorimetry plots for polymerization of Derakane® 411-C50 at 70°C: heat of reaction (top) and conversion (bottom)
Figure 6.2.	Chemical structure of the latest 193-nm resist formulation

Figur

Figur

Figur

# Appendix

Figure A.1.	Change in absorption spectrum of crystal violet with increasing acid concentration in buffered solution series	. 128
Figure A.2.	Extrapolation of extinction coefficients for CV <sup>+</sup> (violet species, top) and H <sub>2</sub> CV <sup>3+</sup> (yellow species, bottom) based upon reported literature values.	. 129
Figure A.3.	Change in relative amounts of $CV^+$ ( $\alpha_2$ ), $HCV^{2+}$ ( $\alpha_1$ ) and $H_2CV^{3+}$ ( $\alpha_0$ ) with decreasing acid concentration	. 130

situ an process comple in-situ : be discreparts ar amplific probe remonitor sensitiv method Informa

the und

addition

the pho

often li

# Chapter 1

### **BACKGROUND AND MOTIVATION**

#### 1.1. INTRODUCTION

The ability to make improvements and advancements in chemical processes is often limited by the unavailability of *in-situ* information on the state of the system. *In*situ and on-line information is often difficult to obtain, and many quality control or process optimization efforts are based upon off-line measurements after the process is complete. Spectroscopic techniques such as fluorescence and absorption are useful for in-situ and on-line characterization of a variety of polymer systems. Two examples will be discussed in this dissertation: monitoring of cure during polymerization of composite parts and characterization of the deprotection reaction after the exposure of chemically amplified resists. In the first instance, by adding small amounts of a solvatochromic probe molecule to a system, it is possible to use spectroscopic techniques to gather pertinent processing information in a quick and timely manner. Fluorescence cure monitoring strategies based upon trace quantities of solvatochromic probes do not lose sensitivity at the gel point and can be implemented using optical fibers. Therefore, this method is well suited to in-situ and on-line monitoring of cure in polymerization systems. Information about the concentration and mobility of photo-generated acids is critical for the understanding and optimization of deep-UV chemically amplified resists. The addition of carefully selected probe molecules to the resist matrix enables the detection of the photoacid and its diffusion during the post exposure bake cycle using lifetime,

absorp change picture

and dif

diagram
molecul
energy s
This act
then dis
such as the term
of 10-11

state, wh

on a tim:

the first

which th

scale of

using a

absorption and fluorescence measurements. In addition, correlation of the free volume changes within the photoresist with diffusion of the photoacid present a more complete picture of the changes occurring during resist processing.

#### 1.2. SPECTROSCOPIC BACKGROUND

Spectroscopic techniques are especially amenable to the investigation of reaction and diffusion mechanisms due to the variety of methods available and to the short time scales which allow resolution of these polymer processes. Figure 1.1 shows the Jablonski diagram enumerating possible pathways of activation and deactivation for a molecule. A molecule may be promoted from a low energy state (i.e, the ground state S<sub>0</sub>) to a higher energy state (e.g., the first excited singlet state S<sub>1</sub>) through the absorption of a photon. This activation process typically occurs on the order of 10<sup>-15</sup> seconds. The molecule may then dissipate this energy by one of several means. There are non-radiative pathways, such as rotational motions of the molecule or collisions with other molecules, denoted by the term external conversion. These deactivation processes typically occur on the order of 10<sup>-11</sup> seconds. There are also radiative pathways, which involve the emission of a photon of light. If this process occurs between a singlet excited state and the ground state, wherein both electronic states are spin-paired, it is termed fluorescence and occurs on a time scale of 10<sup>-9</sup> seconds. If this process occurs between a triplet excited state (e.g., the first excited triplet state T<sub>1</sub>), in which the spin is unpaired, and the ground state, in which the spin is paired, it is termed phosphorescence and occurs on a much slower time scale of 10<sup>-4</sup> to 10<sup>4</sup> seconds. Thus, by tracking the electronic state of an excited molecule using absorption or fluorescence spectroscopy, whether steady-state or transient,

inform

and oth lack of control determine system respons

1.3.1.

minimiz

and from

numerou

Secondly rapid res

Since nu

quantur

signal a

of contin

information concerning the status of a system may be extracted depending upon the photo-responsive nature of the individual components.

#### 1.3. CURE MONITORING OF POLYMER COMPOSITES

In the field of composites processing, it has been widely recognized that the development of convenient, compact methods for on-line monitoring of degree of cure and other process variables would make an important impact on polymer systems. The lack of such techniques has led to off-line measurements forming the basis of quality control efforts. Unfortunately, time, materials and energy are wasted when it is determined that the product is unacceptable via this method. An on-line monitoring system would allow a feedback control system that could manipulate process variables in response to changes in the system. In this way, an on-line monitoring method would minimize defect-related losses.

## 1.3.1. Advantages of fluorescence

The use of fluorescence to create an *in-situ* or on-line monitoring system has numerous advantages. First of all, excitation and emission lights can be easily routed to and from the system using optical fibers. This is especially attractive in systems like those for free radical polymerization which must be blanketed in a nitrogen atmosphere. Secondly, the short intrinsic time scale of fluorescence (10<sup>-9</sup> seconds) provides extremely rapid response and makes it suitable to follow the changing variables in polymer systems. Since numerous probe molecules are available with large absorptivities and fluorescence quantum yields, it is easy to obtain measurements with high signal-to-noise ratios without signal averaging. Finally, fluorescence monitoring can be applied to the on-line control of continuous processes using feedback control systems.

samp

comm

the as

and the

of the [

### 1.3.2. Advantages of optical fibers

Optical fibers provide a versatile method of transmitting radiation, either to the sample surface or its interior, retrieving the modulated light and transmitting it to the detection system via total internal reflection. Because optical fibers are flexible, they are easily incorporated in and around many system geometries. They also transmit light signals over large distances, which means the sample need not be positioned right next to the detection unit. In addition, commercial optical fibers designed for optical communications are attractive for monitoring studies because the fibers themselves and the associated fiber couplers, manipulation devices, optical components, and related instrumentation are readily available.

# 1.3.3. Fluorescence-based cure monitoring techniques

In the past several years, many research groups have devoted their time and energy in an effort to use fluorescence and fluorescent probes in the cure monitoring of polymers and composites. The majority of these methods are based on the sensitivity of probe molecules to the change in viscosity due to the polymerization. However, the major drawback to these methods is the loss of this sensitivity at the gel point where the viscosity diverges. Several of these methods are described in the following paragraphs.

F.W. Wang et al. have used 1,3-bis-(1-pyrene) propane (BPP) as an excimer-forming probe in polymerizing methyl methacrylate<sup>2</sup> and epoxy resin mixtures.<sup>3</sup> BPP forms excimers when an excited state molecule associates with another molecule in its ground state. The probability of this excimer formation is related to molecular mobility and the microviscosity of the environment around the probes. By taking an intensity ratio of the BPP monomer fluorescence (used as the internal standard) with respect to BPP

excimer fluorescence, it is possible to monitor the crosslinking reaction of the epoxy (i.e., as the viscosity of the system increases, so does the intensity ratio). O. Valdes-Aguilera et al. have similarly used the excimer-forming property of pyrene to monitor the cure of methyl methacrylate. By monitoring the ratio of excimer to monomer fluorescence, they are able to determine the rate of polymerization at low conversions.

A second cure monitoring method developed by F.W. Wang *et al.* uses 1-(4-dimethylaminophenyl)-6-phenyl-1,3,5-hexatriene (DMA-DPH) as a viscosity-sensitive probe in epoxy resin mixtures.<sup>3</sup> DMA-DPH exhibits an increase in fluorescence intensity as the viscosity of the local environment increases. By taking an intensity ratio of DMA-DPH fluorescence with respect to 9,10-diphenylanthracene (used as the viscosity-insensitive internal standard), the crosslinking reaction of the epoxy may be monitored by observing the increasing intensity ratio.

F.W. Wang and E.S. Wu also experimented briefly with using fluorescence recovery after photobleaching (FRAP) to monitor the cure of epoxy resins.<sup>5</sup> Using 1,1'-dihexyl-3,3,3',3'-tetramethylindocarbocyanine perchlorate [DilC<sub>6</sub>(3)], the rate of recovery of fluorescence intensity was measured to determine the diffusion coefficient. This diffusion coefficient decreases as the viscosity increases, enabling the study of crosslinking progression. However, this method is too slow to use practically in an industrial process setting.

S.F. Scarlata and J.A. Ors have used derivatives of 4-aminonaphthalimide to monitor the cure of bisphenol-A-epoxy-acrylated resin mixtures.<sup>6</sup> The fluorescence polarization of the non-reactive probe in the curing epoxy mixture is measured, since the probe molecule depolarizes light as it rotates. Therefore, an increase in the polarization

due

incre

impl

optro

obser

The 1

have

increa

decay

fluore

metho

such a

Two fl

a spect

recently

probe

solvatoc

also ada

molecu

have by

due to a decrease in the rotational freedom of the dye is observed as the viscosity increases during the cure. This method is not particularly amenable to on-line implementation either due to the expense of the monitoring equipment.

R.L. Levy and S.D. Schwab have specially built and patented a fluorescence optrode cure sensor to monitor the cure of epoxy resins. With this instrument, they observed changes in the resin fluorescence and the wavelength of its maximum emission. The fluorescence emanating from the resin has been attributed to resin impurities that have yet to be isolated. However, it is postulated that the fluorescence of these molecules increases with increasing viscosity because molecular motion leading to fast non-radiative decay is inhibited by the crosslink structure of the epoxy. Because the exact origin of the fluorescence response is not known and is thought to be intrinsic to the system, this method is not a good candidate for widespread industrial use.

J.C. Song *et al.* have been working with intramolecular charge transfer molecules such as dansyl amide and its derivatives to monitor the polymerization of acrylates.<sup>8,9</sup> Two fluorescence peak intensities characteristic of the dye molecule used are ratioed, and a spectral blue shift of the ratio is observed as the polymerization proceeds. Until just recently, this shift has been attributed to increases in the microviscosity surrounding the probe molecule as the polymer cures; however, D.C. Neckers has cited the solvatochromic nature of these probes as the reason for spectral changes.<sup>10</sup> They have also adapted a fiber optic attachment for *in-situ* monitoring of the polymerizations.

In an effort to circumvent the problem of sensitivity loss with viscosity-sensitive molecular probes, other methods that use self-quenching probes or solvatochromic probes have been developed. For example, K.E. Miller *et al.* have used ethyl (2-fluorenyl)

polymon polymon quence the measurements.

epoxy involve

diamir

proces

cure. 13

during

allows works v

apply to

nitrosti. resin. 14

the sen

also de

methacrylate (FLEMA) as a self-quenching comonomer/molecular probe in the radical polymerization of methyl methacrylate.<sup>11</sup> The fluorescence due to fluorene is quenched by the C=C in acrylate monomers; however, after this bond is broken during the polymerization for incorporation into the polymer backbone, the fluorescence ceases to be quenched. Therefore, the emission intensity from the fluorene is directly proportional to the monomer conversion. Again, this method is system specific, and it entails an extra synthesis to create a polymerizable probe molecule, which may limit its use in industrial processes.

- H.J. Paik and N.H. Sung have exploited the intrinsic fluorescence of aromatic diamine curing agents such as diaminodiphenyl sulfone (DDS) to monitor the cure of epoxy resins.<sup>12</sup> Prior to this research, Sung et al. had used an extrinsic method that involved adding a reactive label and an internal standard to the reaction system to monitor cure.<sup>13</sup> However, in this system, the progressive red shift of the amine hardener's fluorescence peak is simply monitored as it is changed from a primary to a tertiary amine during the crosslinking reaction. They have also developed a fiber optic attachment that allows them to perform *in-situ* measurements of the epoxy cure cycle. This method works very well for systems containing the diamine curing agents; however, it does not apply to the broader spectrum of polymer composites.
- D.L. Woerdeman and R.S. Parnas have used 4-(N,N-dimethylamino)-4'nitrostilbene (DMANS) as a polarity-sensitive probe to monitor the cure of an epoxy
  resin. A fluorescent wavelength shift to the blue is observed as the resin cures due to
  the sensitivity of the probe to the changing polarity of the reaction mixture. They have
  also developed an evanescent wave sensor to monitor the cure *in-situ* using a standing

M.S

ex

Ma

ma

imp that

shov

need

syste

proce

1.4.1.

the inf

people

product

reason

manufa

chipma

industr<sub>i</sub>

billion/

wave at the fiber/resin interface that propagates into the medium and decays exponentially.

As can be seen, there has been an assortment of methods developed in an effort to make use of fluorescent probe molecules to monitor the cure of polymers and composites. Many groups have also realized the utility of *in-situ* techniques in commercial implementation of the monitoring methods. Of all the methods discussed above, those that do not rely upon some viscosity-dependent characteristic of the probe molecules show the most promise in revealing the entire cure profile. However, there is a definite need for the development of a method that can be used in a wide variety of polymer systems and yet can be simply and cost-effectively incorporated in an industrial processing scheme.

## 1.4. CHARACTERIZATION OF CHEMICALLY AMPLIFIED RESISTS

## 1.4.1. Introduction

Semiconductors provide the enabling technology for the Information Age. Today, the information technology sector accounts for 11 percent of our gross domestic product and one-fourth of our manufacturing output. This sector employs more than 4.2 million people with wages nearly double those of the average manufacturing worker. The productivity gains made possible by information technology are the most important reason why America has the world's most competitive economy. The US semiconductor manufacturers supply some 40 percent of the world's output of microchips, and US chipmakers derive more than half of their sales from international markets. The chip industry reached \$132 billion in annual sales in 1996 and is projected to exceed \$232 billion worldwide in the year 2000. 16

cleanl enviro

These

with th

damage

deposit

insulati

spin coa

photore

placed)

Next, t

photore

and har exposed

photom.

pattern

reaction

the cast

develor

the  $de_{\S}$ 

# 1.4.1.1. Semiconductor manufacturing

Semiconductor manufacturing is a complex process marked by its attention to cleanliness and purity. Great lengths are taken to provide dust- and lint-free environments in which the microchips are constructed. The manufacture itself begins with the creation of a single silicon crystal ingot that is sliced into thin silicon wafers. These wafers are lapped to remove mechanical defects and etched to remove surface damage. They are then polished and cleaned to provide a smooth, planar surface for deposition. Finally, a thin layer of silicon dioxide is formed over the wafer as an insulation against electrical charge.<sup>17</sup>

Once the silicon wafer has been thus prepared, it is coated with a liquid photoresist formulation. Typically, the deposition of the resist is accomplished using a spin coater which rotates the wafer (in the middle of which a puddle of the resist has been placed) at approximately 3,000 rpm to produce an even film about one micrometer thick. Next, the wafer undergoes a prebaking process which eliminates solvent from the photoresist film, increases the adhesion between the film and the silicon dioxide layer, and hardens the film to promote damage resistance. After the prebake, the resist is exposed to ultraviolet (UV) light which penetrates through the quartz areas of a photomask onto the photoresist but is blocked by the chromium areas, and a circuit pattern is created. The photons impinging upon the photoresist initiate a chemical reaction that results in the degradation (in the case of positive resists) or crosslinking (in the case of negative resists) of the exposed photoresist. The photoresist is subsequently developed by rinsing off the degraded or unreacted portions with base or acid to reveal the desired pattern. The wafer with the remaining photoresist is then postbaked to

increase pinhole resistance and surface adhesion, as well as to eliminate any volatiles remaining and to increase the chemical resistance of the resist.<sup>18</sup>

When the desired pattern has been formed in the photoresist, a buffered oxide etch is used to remove the exposed areas of silicon dioxide. Metals are then deposited onto the silicon surface to provide the conductive pathways of the microchip. The photoresist is selectively removed from the substrate after the completion of the pattern using a process called ashing where plasma is used to strip off the photoresist without damaging the other layers on the chip. This process involving the photoresist is repeated numerous times using various patterns to form the complex circuitry layers. Once the circuit pattern is complete, it is tested with a "needle-like" probe to ensure the connections are operating properly. Since there are many individual components created on one silicon wafer, it is now sliced to separate each chip. Each functional chip is placed on a lead frame, and ultra-thin wires are attached from the lead frame to the connection points of the circuit. Finally, the device is encapsulated in a polymer to protect the circuit and its connections from physical and chemical damage.<sup>17</sup>

## 1.4.1.2. Photoresist systems

One of the key elements in the formation of a desired image on the semiconductor chip is the photoresist. Photoresist technology grew out of the printing industry where patterns were first etched on copper in the 1800s using gelatin which had been sensitized with a dichromate salt. Improvements were subsequently made in the process in the 1930s by replacing the natural colloids with synthetic polymers. By the 1950s, the circuit board industry was experiencing rapid growth, and the resist formulations of the time did not offer the processing ease and accuracy needed for "advanced" circuit integration. At

this time, Kodak introduced a photoresist based on cinnamic acid derivatives which revolutionized circuit board processing and led to the formulation of more sophisticated photoresists as used in the microelectronics industry today.<sup>18</sup>

Although the photoresists contain the same elements (photosensitizer, resin, and additives in a solvent), there are basically two types of photoresists used to etched the circuit patterns in chips: negative and positive. In a negative resist, the area exposed to the light undergoes crosslinking or cyclization to render it insoluble in the developing solution. Thus, when the resist is washed with solvent, the exposed regions remain to form the pattern while the unexposed region is removed by the developing solution. <sup>19</sup> One example is the polyvinyl cinnamate photoresist developed by Kodak that undergoes extensive crosslinking when exposed to light. Another class is the isoprenoid resins that form an insoluble cyclized rubber when illuminated. <sup>18</sup> In a positive resist, the irradiated area undergoes degradation or solubilization. Here, when the resist is washed with solvent, the exposed regions are removed to form the image while the rest remains. An example of this is the degradation of poly(methyl methacrylate), specifically about the acrylic portion of the molecule, upon light exposure. <sup>19</sup>

# 1.4.1.3. Advantages of chemically amplified resists

Although these photoresist systems have allowed the microelectronics industry to make great strides in computing technology, they now pose a barrier to state-of-the-art semiconductor processes. In order for smaller feature sizes to be etched onto chips, thereby allowing more circuitry to be placed onto one chip at a time, shorter wavelengths of light must be used. However, the sensitizers used in the photoresist mixtures are usually activated by visible or near-UV light, 18 not the deep-UV light necessary for

advancing to the next generation of microchips. Moreover, since one photon yields only one photo-event in these systems, it is difficult to provide enough light to initiate the reactions which will result in pattern formation because the photon count from standard light sources is generally quite low in the deep-UV area of the spectrum.

To address these shortcomings of normal photoresists, a specialized group of photoresists called chemically amplified resists (CARs) was developed in the early 1980s.<sup>20</sup> These positive-resist systems have risen to the forefront of semiconductor manufacturing and are most promising for the further advancement of semiconductor technology. In a CAR system, one photon induces the dissociation of the photoinitiator that generates an acid. This acid reacts with a functional group on a nearby polymer chain, cleaving off the long pendant chain and regenerating the acid. Thus, one photon initiates many deprotection events, and it is this multiplicative process by which the system is characterized as amplified.<sup>21</sup>

With this new photoresist technology, it is then possible to utilize the deep-UV light to decrease the sizes of patterns etched into the photoresist. First of all, the photoinitiators used in CAR systems undergo photolysis with deep-UV light (i.e., wavelengths on the order of 250 nm). Secondly, the reaction-diffusion process of the CARs provides high sensitivity to the impinging deep-UV photons. Due to the amplification nature of the resist, it only takes a small number of photons to begin a chain of deprotection reactions that will propagate to form a pattern as the photoacid diffuses throughout the medium.

# 1.4.1.4. Issues for the advancement of chemically amplified resists

Although chemically amplified resists offer many advantages to the semiconductor manufacturing process, there are several issues that have vet to be addressed in order to apply this technology more successfully. The first and foremost issue deals with resolution and line-width control when etching patterns in the photoresist.<sup>20,22</sup> Due to the regenerative nature of the photoacid, diffusion of a photoacid molecule into an unexposed region during the post exposure bake may lead to a pattern in the resist which is different than that which is on the mask by beginning a cascade of deprotection reactions in an unintended area. Therefore, it is imperative to understand and control the diffusion and mobility of the photoacid in the resist. However, this leads into a second issue concerning CAR technology: the accepted models are geared toward normal resists in which there is only one deprotection reaction for every photo-event. In such resist systems, optical principles may be applied to develop a model that will predict the appearance of the end product given a certain photomask. Furthermore, attempts to develop new models specifically designed for the CAR systems have been unsuccessful because the chosen parameters do not accurately predict the diffusion and reaction of the photoacid. Therefore, there is a compelling need to fit realistic parameters to the CAR systems so that the technology may be used with even shorter wavelengths.

## 1.4.1.5. Motivation for research on chemically amplified resists

The key to utilizing chemically amplified resists to their fullest potential lies in tracing the lifetime and activity of the photoacid. Without a clear understanding of photoacid diffusion and mobility during illumination and postbake of the photoresist, it will be difficult to extend semiconductor processing technology into the next generation

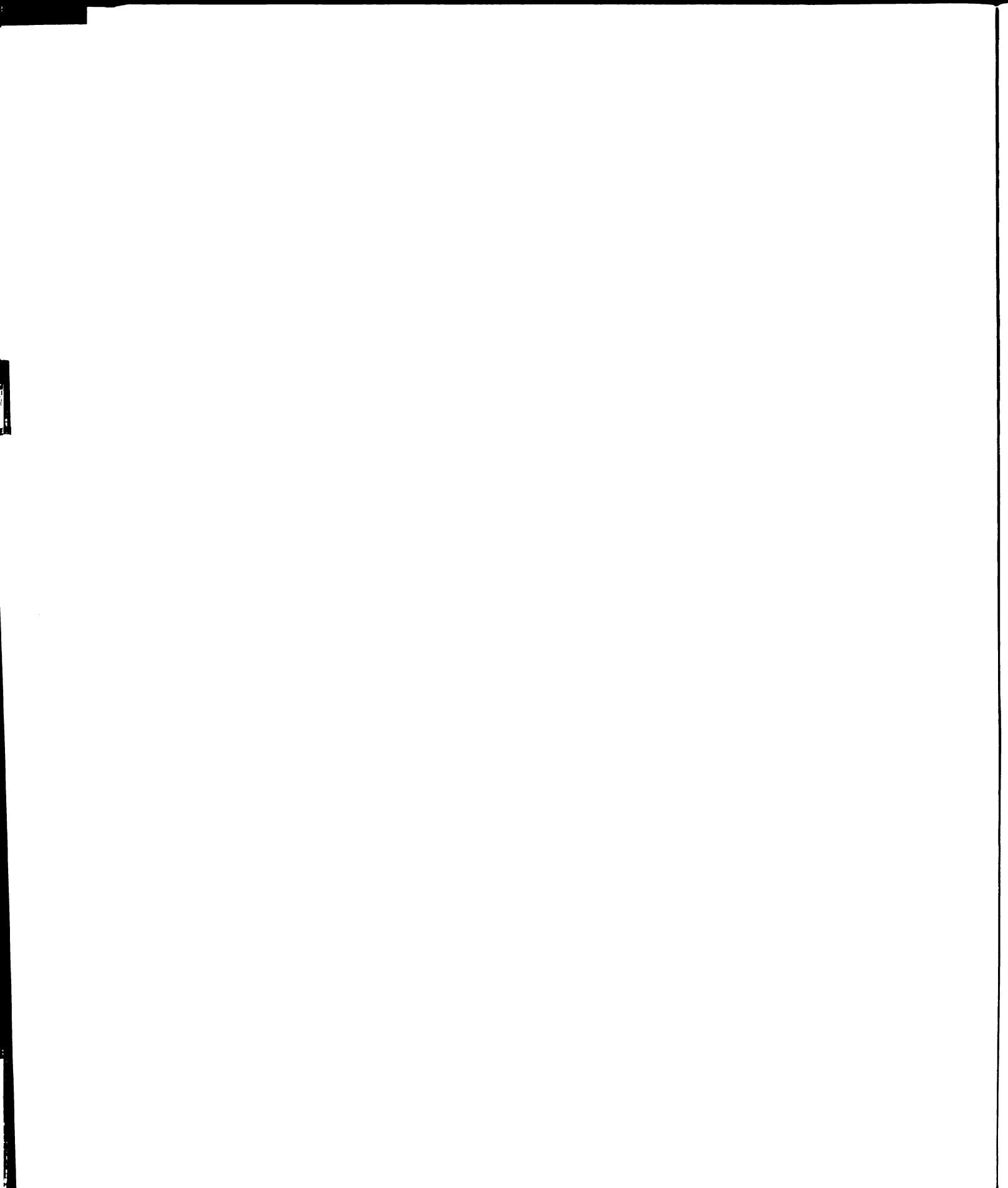
using chemically amplified resists. Furthermore, current photoresist models must be improved to encompass these concepts such that suitable parameters are obtained, thereby allowing accurate prediction of the end result from a given pattern upon a CAR.

Once an understanding of the diffusion and mobility of the photoacid in chemically amplified resists is obtained, then strides may be taken to improve semiconductor technology. The direct repercussions will include smaller feature sizes and increased circuit density. This would result in more compact and faster processing units for microelectronics users everywhere.

# 1.4.2. Background

# 1.4.2.1. General properties of chemically amplified resists

Positive chemically amplified resists were first developed by Ito and coworkers to meet the technological initiative to produce microelectronic devices with increased circuit density. Their system incorporates onium salts (e.g., diphenyliodonium hexafluoroarsenate) which are widely used in the photocuring of coatings. These cationic photoinitiators dissociate upon absorption of deep-UV light to yield a cation radical and a Bröndstedt acid. The polymer used to form the basis of the photoresist is poly(p-t-butoxycarbonyloxystyrene), also known as PTBOC, which consists of long chains with bulky pendant groups. The acid formed during the photo-event cleaves off the pendant chain, thereby deprotecting the polymer chain and regenerating the acid. Figure 1.2 shows an example of the deprotection reaction that takes place. A small number of deprotection events occur during the illumination of the photoresist; however, the majority of the deprotection reactions occur during poste xposure bake at elevated temperatures. The deprotected chains are then rendered soluble in base and may be



washed away when the photoresist is developed, while the chains that are still protected remain to form the pattern.

## 1.4.2.2. Microlithography for processing of microelectronic devices

The most critical semiconductor technology is the microlithographic process used to define the features on an integrated circuit chip. There is a continual drive to produce devices with smaller feature sizes, since smaller sizes allow for more transistors to be packed onto a single chip while simultaneously increasing performance and reliability. Reduced feature sizes are obtained by using higher energy or shorter wavelength light to pattern the resist, and, at the leading edge, the industry is undergoing a transition from 365-nm to 248-nm technology. At these higher energies the photon flux is greatly reduced, and in order to increase throughput, deep-UV resists are "chemically amplified" where the effect of a photo-generated acid is multiplied by a chemical chain reaction. The state-of-the-art lithographic processes used to make features smaller than 0.25 microns are based upon deep-UV lithography and chemically amplified resists. The ability of CARs to produce nearly vertical sidewalls from a relatively low intensity light source has greatly extended the working resolution of optical lithography. Deep-UV chemically amplified resists rely on a photoinitiated reaction followed by a post exposure bake during which diffusion and chemical reaction (deprotection) form a developable image. In these resists, the photo-active compound reacts with light to produce acid, which, during the post exposure bake (PEB) process, diffuses and reacts in a chain reaction that degrades the polymer matrix (for a positive resist) and regenerates the acid. As the polymer matrix degrades, the viscosity in the vicinity of this reaction site (i.e., the local or microviscosity) is reduced. This reduced viscosity (or increased free volume)

results in an increase in the localized diffusion coefficient of the acid in the polymer. In its turn, the larger diffusion coefficient results in a higher acid concentration and accelerates the degradation of the exposed resist, thus forming a front. It is this non-linear phenomenon that produces sharp sidewalls, even in the presence of severe standing waves. While this interplay of diffusion and reaction forms sharp sidewalls, it also results in a steady increase in line width of about 30 to 50 nm/min. For the typical 90 second PEB, this would translate to a total increase in line width of 90 to 150 nm, a very significant fraction of critical dimensions (CDs) at small feature sizes.

Processing factors which have a dramatic effect on line width are post apply bake (PAB) temperature and time, exposure intensity, post exposure bake duration and temperature, as well as developer conditions such as the concentration of developer, temperature and time. Physically, the PAB temperature determines the viscosity of the resist prior to the PEB. Increasing the duration or temperature of the PAB will reduce the free volume and result in an increased viscosity of the resist. Higher PEB temperatures increase the sensitivity of the resist but also increase the mobility of the acid, making the process more susceptible to process variations. Both reaction and diffusion are very sensitive to temperature and time, and even slight non-uniformity on hot plates or a delay in reaching a cool plate (and therefore delay in quenching the reaction) can cause significant changes in CDs. These non-linear interactions between exposure light intensity, chemical reaction and a non-constant diffusion make optimizing and running a stable process a challenge.

# 1.4.2.3. Current models for chemically amplified resists

To date, there are no viable computer models for deep-UV chemically amplified resists. Current approaches to identifying model parameters rely on one of two methods. By far, the most common method is by performing a design of experiments (DOE) to sample CD variation as a function of PAB and PEB conditions. A second, less common method is FTIR spectroscopy that has been used to monitor acid formation during the PEB process. While the DOE approach allows for efficient sampling of a limited phase space, its results cannot be easily extended to regions outside this space. Therefore, this approach limits the utility of the model parameters and does not allow for efficient and reliable extrapolation. The other major problems with this approach arise from the fact that the results obtained are very dependent on the stability and sensitivity of the process. While the use of FTIR spectroscopy provides direct insight into the deprotection reaction, it does not provide any information on physical changes (such as viscosity, free volume, diffusivity, etc.). In addition, FTIR studies are complicated by the background noise from the resist and cannot be used as a tool to study changes occurring during resist development due to the very high absorbance of infrared by water.

Classical modeling approaches for non-chemically amplified resist are based on the use of an empirical correlation between the energy absorbed by the resist volume and the rate at which a resist dissolves into a given developer (dissolution rate curve). The strong dependency upon experimental conditions makes this modeling approach ill-suited for predictive studies where new process conditions need to be explored. The dissolution rate curve approach has severe limitations in the modeling of CARs, where no direct relation can be postulated between the exposure conditions and the final developed resist

profiles. In the case of CARs, the dissolution rate depends not only on the development process but also on the coupled effect of photoacid diffusion and thermally controlled catalytic reactions during PEB.

Current PEB models described in literature can be summarized in the following two coupled partial differential equations that describe the kinetics of the species involved in the chemical reactions and diffusion.<sup>24</sup>

$$\frac{\partial [M]}{\partial t} - k_{DP}[M]^{P}[H]^{Q} \tag{1.1}$$

$$\frac{\partial[H]}{\partial t} = -k_A[H]^m - \nabla[D(M)\nabla[H]]$$
 (1.2)

The first equation describes the reaction leading to the deprotection of the polymer sites. [M] and [H] refer to the concentrations of protected sites and photoacid respectively. The model parameter  $k_{DP}$  is the rate constant for the sites' deprotection, while p and q are the reaction orders for each species. The second equation describes the reaction and diffusion of photoacid (in time and space) during the PEB. [H] represents the photoacid concentration available for deprotection, m is an effective reaction order,  $k_A$  the photoacid loss reaction rate and D the photoacid diffusion coefficient (not necessarily constant). It is interesting to note that different reaction and diffusion mechanisms (and consequently different values for model parameters) have been used to describe the kinetics of deep-UV CARs. While some experimental work indicates that the diffusion coefficient varies exponentially with the photoacid concentration, 25 other papers assume that the process is characterized by a constant diffusion coefficient. 26.27

Based on the above discussion, it is clear that the applicability of these models is currently limited by the experimental resist process characterization, which translates into a lack of reliable parameter values. Typical experimental parameter extraction has been based on two techniques, namely FTIR spectroscopy and CD metrology. More powerful techniques that are capable of simultaneously monitoring the dynamics and evolution of several species over wide process ranges are badly needed, and developing such techniques is the focus of this research.

# 1.4.2.4. Utility of molecular probes

Luminescence (fluorescence and phosphorescence) techniques offer a unique method to study the kinetics of a number of reactions, especially diffusion-controlled reactions. For example, luminescence quenching and viscosity-sensitive fluorescence have been applied to various polymer systems to characterize initiation, polymerization and free volume on short time scales. Such approaches provide a basis for extracting similar parameters in chemically amplified resist systems.

# 1.4.2.4.1. Luminescence quenching

A very powerful and well-established technique for studying mobility and transport in polymer systems is luminescence quenching. The process of quenching results in a deactivation of the excited singlet or triplet state (S<sub>1</sub> or T<sub>1</sub>) by interaction with another molecule called a quencher, resulting in a radiationless transfer to the ground state. Dynamic quenching relies on a direct collision between an excited-state luminescent molecule and the quenching molecule. Therefore, reactions between the quencher and the luminescent molecule manifest themselves by a reduction in fluorescence and phosphorescence lifetimes. Since the rate of this type of reaction is diffusion-controlled, this process is very useful in characterizing other diffusion-controlled reactions in polymer systems. Phosphorescence quenching is typically more

useful in polymer systems where the diffusion times are relatively long. These techniques have been used to study diffusion-controlled reactions occurring due to polymer-small molecule interactions, <sup>28</sup> as well as due to interactions between small molecules in polymeric systems. <sup>29</sup>

Scranton and coworkers have investigated the rate of reaction between anthracene and iodonium salt in methanol by observing the change in emission lifetime of a fluorescent probe upon quenching.<sup>30,31</sup> The phosphorescence lifetimes of anthracene were quenched from  $9.55 \times 10^{-6}$  seconds in the absence of initiator to  $3.85 \times 10^{-7}$  seconds in the presence of 2.0 wt% initiator. These studies demonstrate the utility of this technique for characterizing rapidly changing systems.

# 1.4.2.4.2. Viscosity-sensitive fluorescence

In addition to measuring the rate of diffusion-controlled reactions, fluorescence can also be used to probe the local environment of the system. The addition of a small amount of a viscosity-sensitive probe can be used to measure the microviscosity or free-volume of the system. Many researchers have exploited this technique to gather such information in polymer systems.

For example, Moorjani and coworkers demonstrated the utility of fluorescence monitoring when dealing with diffusion-controlled reactions in media of different viscosity.<sup>32</sup> In their studies of a polymer system, they used the fluorescence of the photosensitizer anthracene to determine how the reaction rate changes as the polymer cures. As the viscosity increased, the rate of diffusion-controlled reaction dramatically decreased. Victor and Torkelson have also used molecular probes to measure the free volume available in a polymer structure.<sup>33</sup> The molecules chosen for their studies

(stilbene, azobenzene, m-azotolutene, etc.) undergo photoisomerization and require different free volumes in order to carry out this conformational change. By observing the fluorescence change of the probe molecules, it was possible to quantify the free volume distribution in the polymers. In addition, several methods developed to monitor cure in polymer systems and based upon viscosity-sensitive fluorescence were discussed previously in this chapter.<sup>2-9</sup> These methods also involve the addition of specially chosen probe molecules into the systems.

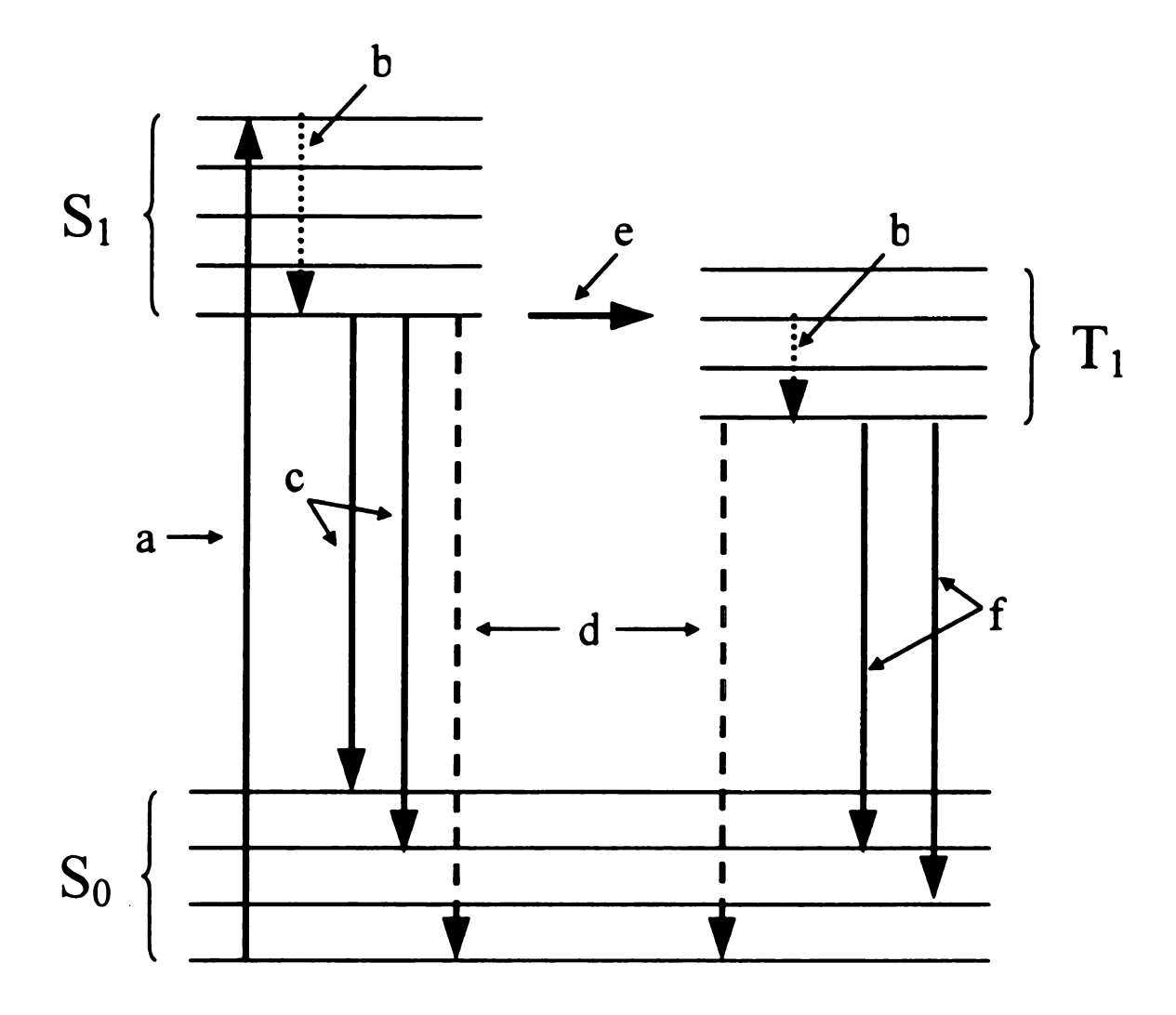


Figure 1.1. Jablonski diagram for a molecule showing the pathways for activation and deactivation: absorption (a), vibrational relaxation (b), fluorescence (c), external conversion (d), intersystem crossing (e), and phosphorescence (f).

$$\begin{array}{c} \begin{array}{c} \begin{array}{c} \\ \\ \\ \\ \\ \end{array} \end{array} \begin{array}{c} \\ \\ \\ \end{array} \begin{array}{c} \\ \\ \end{array} \begin{array}{c} \\ \\ \\ \end{array} \begin{array}{c} \\ \\ \\ \end{array} \begin{array}{c} \\ \\ \\ \end{array} \begin{array}{c} \\ \\ \\ \end{array} \begin{array}{c} \\ \\ \end{array} \begin{array}{c} \\ \\ \\ \end{array} \begin{array}{c} \\ \\ \\ \\ \end{array} \begin{array}{c$$

Figure 1.2. Deprotection of PTBOC in DUV photoresist.

## 1.5. REFERENCES

- 1. J.D. Ingle, Jr. and S.R. Crouch, *Spectrochemical Analysis*, Prentice Hall, New Jersey, 1988.
- 2. F.W. Wang, R.E. Lowry and W.H. Grant, "Novel excimer fluorescence method for monitoring polymerization: 1. Polymerization of methyl methacrylate," *Polymer*, 25(5), 690 (1984).
- 3. F.W. Wang, R.E. Lowry and B.M. Faconi, "Novel fluorescence method for cure monitoring of epoxy resins," *Polymer*, 27, 1529 (1986).
- 4. O. Valdes-Aguilera, C.P. Pathak and D.C. Neckers, "Pyrene as a Fluorescent Probe for Monitoring Polymerization Rates," *Macromolecules*, 23, 689 (1990).
- 5. F.W. Wang and E.-S. Wu, "Cure monitoring of epoxy resins by fluorescence recovery after photobleaching," *Polym. Commun.*, 28, 73 (1987).
- 6. S.F. Scarlata and J.A. Ors, "Fluorescence polarization: A method to monitor polymer cure," *Polym. Commun.*, 27, 41 (1986).
- 7. R.L. Levy and S.D. Schwab, "Monitoring the Composite Curing Process With a Fluorescence-Based Fiber-Optic Sensor," *Polym. Comp.*, 12(2), 96 (1991).
- 8. J.C. Song and D.C. Neckers, "A fluorescence probe method for characterization of photopolymerized networks," *PMSE*, 71, 71 (1994).
- 9. J.C. Song, Z.J. Wang, R. Bao, and D.C. Neckers, "Cure Montioring of UV Coatings Using a Fiber-Optic Fluorescence Technique," *PMSE*, 72, 591 (1995).
- 10. W.F. Jager, A.A. Volkers and D.C. Neckers, "Solvatochromic Fluorescent Probes for Monitoring the Photopolymerization of Dimethacrylates," *Macromolecules*, 28, 8153 (1995).
- 11. K.E. Miller, E.L. Burch, F.D. Lewis, J.M. Torkelson, "In Situ Monitoring of Free-Radical Polymerization by Fluorescence Quenching of Fluorene and Reactive Derivatives," J. Poly. Sci.: Part B, 32, 2625 (1994).
- 12. H.-J. Paik and N.-H. Sung, "Fiberoptic Intrinsic Fluorescence for *In-Situ* Cure Monitoring of Amine Cured Epoxy and Composites," *Polymer Engineering and Science*, 34(12), 1025 (1994).

- 13. N.-H. Sung, W. Dang, H.-J. Pail, C.S.P. Sung, "In-situ monitoring of epoxy cure by fiber-optic molecular sensors," 36<sup>th</sup> International SAMPE Symposium, 36, 1461, (1991).
- 14. D.L. Woerdeman, K.M. Flynn, J.P. Dunkers, R.S. Parnas, "The Use of Evanescent Wave Fluorescence Spectroscopy for Control of the Liquid Molding Process," *Journal of Reinforced Plastics and Composites*, 15(9), 922 (1996).
- 15. W.J. Sanders, III, SIA Washington Conference, Washington, D.C., March 11, 1997.
- 16. E.M. Kirschner, "Electronic Chemicals," Chemical & Engineering News, 75(47), 25 (1997).
- 17. Fullman Company, "The Semiconductor Manufacturing Process," on the Worldwide Web at http://www.fullman.com/semiconductors/, 1997.
- 18. W.S. DeForest, *Photoresist: Materials and Processes*, McGraw-Hill Book Company, New York, 1975.
- 19. G. Baker, CEM 956: Polymer Chemistry, Michigan State University, Fall 1996.
- 20. G. Wallraff, J. Hutchinson, W. Hinsberg, F. Houie, P. Seidel, R. Johnson, and W. Oldham, "Thermal and acid-catalyzed deprotection kinetics in candidate deep ultraviolet materials," J. Vac. Sci. Technol. B, 12(6), 3857 (1994).
- 21. H. Ito and C.G. Willson, "Applications of Photoinitiators to the Design of Resists for Semiconductor Manufacturing," *Polymers in Electronics*, edited by T. Davidson, American Chemical Society, Washington, D.C., 1984.
- 22. J. Nakamura, H. Ban, K. Deguchi, and A. Tanaka, "Effect of Acid Diffusion on Resolution of a Chemically Amplified Resist in X-Ray Lithography," *Japanese Journal of Applied Physics*, 30(10), 2619 (1991).
- 23. J.-P. Fouassier, *Photoinitiation, Photopolymerization, and Photocuring: Fundamentals and Applications*, Hanser Publishers, New York, 1995.
- 24. M. Zuniga, G. Walraff and A.R. Neureuther, "Reaction Diffusion Kinetics in Deep-UV Positive Tone Resist Systems," *Proceedings of SPIE*, 2438, 113 (1995).
- 25. M. Zuniga and A.R. Neureuther, "Post Exposure Bake Characterization and Parameter Extraction for Positive Deep-UV Resists through Broad-Area Exposure Experiments," *Proceedings of SPIE*, 2724, 110 (1996).
- 26. A.A. Krasnoperova, M. Khan, S. Rhyner, J.W. Taylor, Y. Zhu, and R. Cerrina, "Modeling and simulations of a positive chemically amplified photoresist for x-ray lithography," J. Vac. Sci. Technol. B, 12(6), 3900 (1994).

- 27. L. Capodieci, A. Krasnoperova, F. Cerrina, C. Lyons, C. Spence, and K. Early, "Novel postexposure bake simulator: First results," *J. Vac. Sci. Technol. B*, 13(6), 2963 (1995).
- 28. M.S. Gerbert and J.M. Torkelson, "Synthesis, characterization and photophysical properties of benzil-labelled polymers for studies of diffusion-limited interactions by phospherence quenching," *Polymer*, 31, 2402 (1990).
- 29. M.S. Gerbert, D.H.-S. Yu, and J.M. Torkelson, "Diffusion-Limited Polymer-Small Molecule Interactions: A Study of Phospherence Quenching," *Macromolecules*, 25, 4160 (1992).
- 30. E.W. Nelson, T.P. Carter and A.B. Scranton, "Kinetics of Cationic Photopolymerizations of Divinyl Ethers Characterized Using *In Situ* Raman Spectroscopy," *J. Poly. Sci., A: Polym. Chem.*, 34, 403 (1996).
- 31. E.W. Nelson, T.P. Carter and A.B. Scranton, "Fluorescence Monitoring of Cationic Photopolymerizations: Divinyl Ether Polymerizations Photosensitized by Anthracene Derivatives," *Macromolecules*, 27, 1013 (1994).
- 32. S.K. Moorjani, "Polymers From Renewable Resources: Cationic Photopolymerization of Epoxidized Natural Oils," Master's Thesis, Michigan State University, 1996.
- 33. J.G. Victor and J.M. Torkelson, "On Measuring the Distribution of Local Free Volume in Glassy Polymers by Photochromic and Fluorescence Techniques," *Macromolecules*, **20**, 2241 (1987).

# Chapter 2

# **OBJECTIVES**

## 2.1. CURE MONITORING OF POLYMER COMPOSITES

On-line monitoring of polymer cure is crucial for the prevention of losses due to defective samples. Fluorescence spectroscopy provides a clear advantage for the development of a cure monitoring technique in that it allows investigation on the time scale of the polymerization. However, judicious selection of molecular probes must be made in order to maintain sensitivity throughout the entire reaction, especially after the gel point. This, coupled with the necessity of simplicity and cost efficiency in order to incorporate the technique into industrial processing situations, poses a definite challenge.

The overall objective for this research has been to demonstrate the utility of solvatochromic fluorescence probes for an inexpensive, non-intrusive, portable means of cure monitoring for polymer composites using optical fibers. The specific research objectives by which this was accomplished are as follows: (i) to identify appropriate solvatochromic probes for the cure monitoring of polymers, (ii) to demonstrate the fluorescence cure monitoring technique with several model systems, and (iii) to investigate the underlying physicochemical origins of probe spectral response.

These objectives were fulfilled through the careful selection of two molecular probes, namely phenoxazone 660 and pyrene, whose fluorescence response is based on the polarity of their environments. This response was successfully demonstrated for three major polymer classes (acrylate, styrene and vinyl ether systems) and studied to

dete

con

the

of

pr

d

Π

determine the effects of oxygen, cure temperature, probe concentration, and initiator concentration. Finally, an optical fiber spectrometer was proposed and tested to confirm the utility of this *in-situ* technique.

# 2.2. CHARACTERIZATION OF CHEMICALLY AMPLIFIED PHOTORESISTS

It is clear from the discussion in the first chapter that a fundamental understanding of the reaction-diffusion mechanism is needed to optimize and extend the range of processes using deep-UV chemically amplified resists. Isolating and measuring each of the kinetic parameters and activation energies for the various steps of the reaction diffusion during the post exposure bake process will enable the development of an accurate model with predictive capabilities. However, spectroscopic techniques, which are powerful and fast, must first be designed to obtain various model parameters. This is a daunting task to perform in situ because the photoresist films are less than one micron thick, making it extremely difficult to obtain any optical signal from the sample. Therefore, careful selection of molecular probes and strategies for signal collection and analysis are paramount in order to acquire acid production, viscosity, diffusivity, and reaction kinetics as a function of temperature for a variety photoresist processing conditions (e.g., bake temperatures and exposure times) in the thin photoresist films.

The overall objective for this research has been to develop highly sensitive, timeresolved spectroscopic techniques to investigate the reaction-diffusion phenomena during chemically amplified photoresist processing with the aid of probe molecules. The specific research objectives by which this was accomplished are as follows: (i) to monitor acid generation during exposure, (ii) to quantify acid concentration throughout

pos exp

st:

,

post exposure bake, and (iii) to measure the evolution of free volume during post exposure bake.

These objectives were fulfilled through the development of several spectroscopic techniques especially tailored for the thin film photoresist system. First of all, steady-state fluorescence monitoring using the probe molecule fluorescein was applied to obtain information about photoacid generation during exposure to 248-nm light. Secondly, steady-state absorption of a second probe molecule crystal violet was applied to measure the proton concentration during post exposure bake. Finally, two techniques were used to measure the evolution of free volume in the resist. The first is a microscopic technique based on ground-state recovery measurements also using the probe molecule crystal violet. The second is a macroscopic technique that measures the dynamic film thickness using multi-wavelength interferometry. Each of these techniques was realized *in situ* with the one-micron thick photoresist films.

# Chapter 3

# IN-SITU CURE MONITORING FOR COMPOSITES PROCESSING USING FLUORESCENCE SENSORS

## 3.1. INTRODUCTION

In the field of radiation curing, there is a compelling need for the development of inexpensive on-line sensors for the degree of cure. On-line monitoring of photopolymerizations is extremely difficult since these reactions are typically carried out in high-speed, continuous processing formats. Due to the lack of appropriate on-line sensors for degree of cure, most quality control efforts rely on *ex-situ* measurements made after the polymerization is complete. Therefore, if a polymer has cured improperly, it is too late to make process adjustments and the entire run must be discarded. A similar situation exists for traditional polymer and composites processing methods. For example, the manufacture of polymer matrix composites involves a series of complex chemical and physical changes that must be adequately controlled to produce products with desirable properties. Again, due to the lack of appropriate on-line sensors for properties such as viscosity and degree of cure, most quality control efforts are based on off-line measurements made after the product has completed its cure cycle.

Clearly, on-line monitoring techniques, which could be interfaced with an electronic control scheme, would significantly enhance the reliability of polymer and composites processing methods while reducing the cost. The need for such sensors has been recognized widely, and the measurement of a variety of physical phenomena has

been explored, including dielectric constant and loss, acoustic and ultrasonic wave propagation, and optical techniques.<sup>1</sup> To date, none of these approaches has resulted in the development of an inexpensive on-line sensor.

Fluorescence techniques have been proposed for the development of on-line viscosity sensors due to the fact that the fluorescence behavior of a variety of molecular probes depends on the local viscosity. For example, many fluorescent probes exhibit enhanced fluorescence intensity with increasing viscosity due to decreased non-radiative energy transfer. Levy and Schwab<sup>2</sup> and Wang et al.<sup>3</sup> demonstrated that such an increase in fluorescence intensity can be used to monitor the viscosity increase during cure. The measurement of absolute fluorescence intensity, however, has some significant limitations. For example, the method has limited utility for monitoring the degree of cure above the gel point (limited dynamic range) and is subject to uncertainty due to variations in background fluorescence. Stroeks et al. investigated the use of viscosity-sensitive excimer formation to monitor degree of cure. In addition to the aforementioned limitations of the previous technique, the investigators concluded that apparent intensity changes in the excimer peak were actually dominated by changes in the intensity of the overlapping monomer peak (which was increasing because of reduced non-radiative transfer). Valdes-Aguilera et al. 5 have also utilized an excimer-forming probe to monitor cure at low conversions, using a ratio of the monomer to excimer fluorescence emission. which can be controlled by adjusting the probe concentration. Finally, Scarlata and Ors<sup>6</sup> have monitored an increase in fluorescence polarization that they attribute to a viscosityinduced decrease in the rotational mobility of the probe molecule. However, due to its

complexity, this technique is unlikely to form the basis for an inexpensive on-line sensor for polymer and composites processing due to its need to measure absolute quantities.

In this chapter, a novel fluorescence monitoring scheme utilizing a solvatochromic probe that exhibits a shift in fluorescence wavelength with increasing cure is reported. This research was motivated by the fact that the use of a solvatochromic probe avoids many of the problems and pitfalls associated with viscosity-sensitive fluorescence. First, the solvatochromic method is based upon the relative fluorescence intensity ratio of two interdependent peaks, thereby avoiding the problems (such as broadband background interference) associated with absolute fluorescence intensity measurements. In addition, unlike the viscosity-sensitive fluorescence probes, the solvatochromic probe does not lose sensitivity after the gel point (where the viscosity has diverged). One monitoring method based upon an oxazone probe and a second based upon a polycyclic aromatic hydrocarbon probe will be presented, and the advantages and limitations of these curemonitoring schemes will be discussed.

## 3.2. EXPERIMENTAL

#### 3.2.1. Materials

These studies were performed using commercial vinyl esters (Derakane<sup>®</sup>), methyl methacrylate (MMA) and styrene. Derakane<sup>®</sup> resins 411-C50 and 470-45, the general structure of which is shown in Figure 3.1, were obtained from Dow Chemical Company (Midland, MI), MMA and styrene were purchased from Aldrich Chemical Company Aldrich (Milwaukee, WI) and Polysciences, Inc. (Warrington, PA), respectively. The radical initiators, 2,2'-azobisisobutyronitrile (AIBN) and 2,2'-azobis(2,4-dimethyl-4-methoxy valeronitrile) (V-70), were purchased from Polysciences, Inc. and Wako Pure

Chemical Industries, Ltd. (Richmond, VA), respectively. The fluorescence probes, phenoxazone 660 and pyrene, were purchased from Exciton and Aldrich Chemical Company, respectively. All chemicals were used as received except the MMA, which was vacuum distilled before use to remove hydroquinone inhibitors, and the styrene, which was washed with Dehibit-100 (Polysciences, Inc.) before use to remove the inhibitor 4-tert-butylcatechol.

## 3.2.2. Methods

# 3.2.2.1. Fluorescence measurements

Derakane® 411-C50 samples with 0.75 wt.% AIBN and 10<sup>-4</sup> wt.% phenoxazone 660 were cured in an Aminco-Bowman Series 2 Luminescence Spectrometer at 70°C. The sample emission spectrum from 550 nm to 800 nm was recorded every five minutes using an excitation wavelength of 540 nm. Likewise, MMA samples with 0.5 wt.% AIBN and 10<sup>-3</sup> wt.% pyrene were cured in the spectrometer at 70°C, recording the sample emission spectrum from 350 nm to 600 nm every five minutes with an excitation frequency of 334 nm. Styrene samples with 0.78 wt.% AIBN and 10<sup>-3</sup> wt.% phenoxazone 660 were cured in the spectrometer at 70°C, recording the sample emission at 570 nm and 590 nm every ten seconds with excitation at 510 nm.

# 3.2.2.2. Thermocouple measurements

For some experiments, fluorescence and temperature measurements were taken simultaneously in the AB2 spectrometer. A thermocouple was placed in the middle of the cuvettes, away from the walls and out of the excitation and emission pathways. A second thermocouple was placed in the recirculating bath reservoir as a control. Temperature readings were taken every 1.8 seconds.

## 3.3. RESULTS AND DISCUSSION

## 3.3.1. Fluorescent probe molecules

The use of probe molecules to study chemical and/or physical phenomena hinges on the sensitivity of the probe molecule to some changing property of its local environment. Two such changes are the polarity of the local environment and its structural rigidity. In addition, for the probe molecule to be useful it must also have a large absorptivity and a moderately high fluorescence quantum yield, so that the information about its local environment can be measured efficiently. Phenoxazone 660 and pyrene (Figure 3.2) fulfill these requirements for the specific systems under study.

The oxazones are solvatochromic; their emission spectra are sensitive to the polarity of their local environment. The sensitivity of the phenoxazones to the polarity of their local environment arises from the non-bonding orbital associated primarily with the heterocyclic nitrogen. Interactions between this lone pair and its immediate surroundings (several Å) determine its energy with respect to the excited state of the molecule, and thus its coupling to the chromophore. This tunable degree of "delocalization" is highly selective for interactions with the ring-bound nitrogen. The fluorescence spectrum of pyrene is also sensitive to solvent polarity. The mechanism by which this polarity-dependence operates is now well understood and can be predicted from the energy-dependence of the linear response of these molecules. Imbedding these dyes in matrices undergoing polymerization allows the examination of both the polarity and structural changes associated with the curing cycle.

3.3

P

i

1

١

#### 3.3.2. Fluorescence measurements

Monitoring changes in a chemical system in real time and in the presence of potential background interferences places limits on the ways in which the measurement can be accomplished. Measuring an absolute quantity is practical only if the background is known and preferably constant in time. For this reason, absolute emission intensity is not likely to be a suitable quantity for long-term, on-line or process-control measurements. The probe molecule fluorescence lifetime is an absolute quantity that can be resolved from the background since measurement of this quantity depends on time registration introduced by the instrumentation (background interference will not be synchronous). Such a measurement is, however, technologically involved9 and not likely to be useful for practical chemical processing situations. A more practical approach for probe molecule-based monitoring is to measure the position or shape of the probe emission band as a function of environment. A particularly simple way to do this is to monitor two different emission wavelengths, as shown Figure 3.3, and take the ratio of the intensities at the two wavelengths. 10 Measuring the ratio rather than absolute intensities eliminates many uncertainties associated with macroscopic inhomogeneities and broadband background interferences such as scattered white light.

For Derakane<sup>®</sup> 411-C50, the fluorescence emission maximum of phenoxazone 660 blue-shifts from 617 nm to 597 nm during cure, as shown in Figure 3.4. In Figure 3.5, the time evolution of the intensity ratio  $I_{597}/I_{617}$  is illustrated for this system during polymerization. The sample emission at 597 nm and 617 nm were recorded every five seconds for this data set. It is easy to distinguish between the uncured system with  $I_{597}/I_{617} \approx 0.8$  and the cured system with  $I_{597}/I_{617} = 1.3$ . Only the first 60 minutes of the

exp

per

the em

st

in

C

t

t

•

р

ch.

the

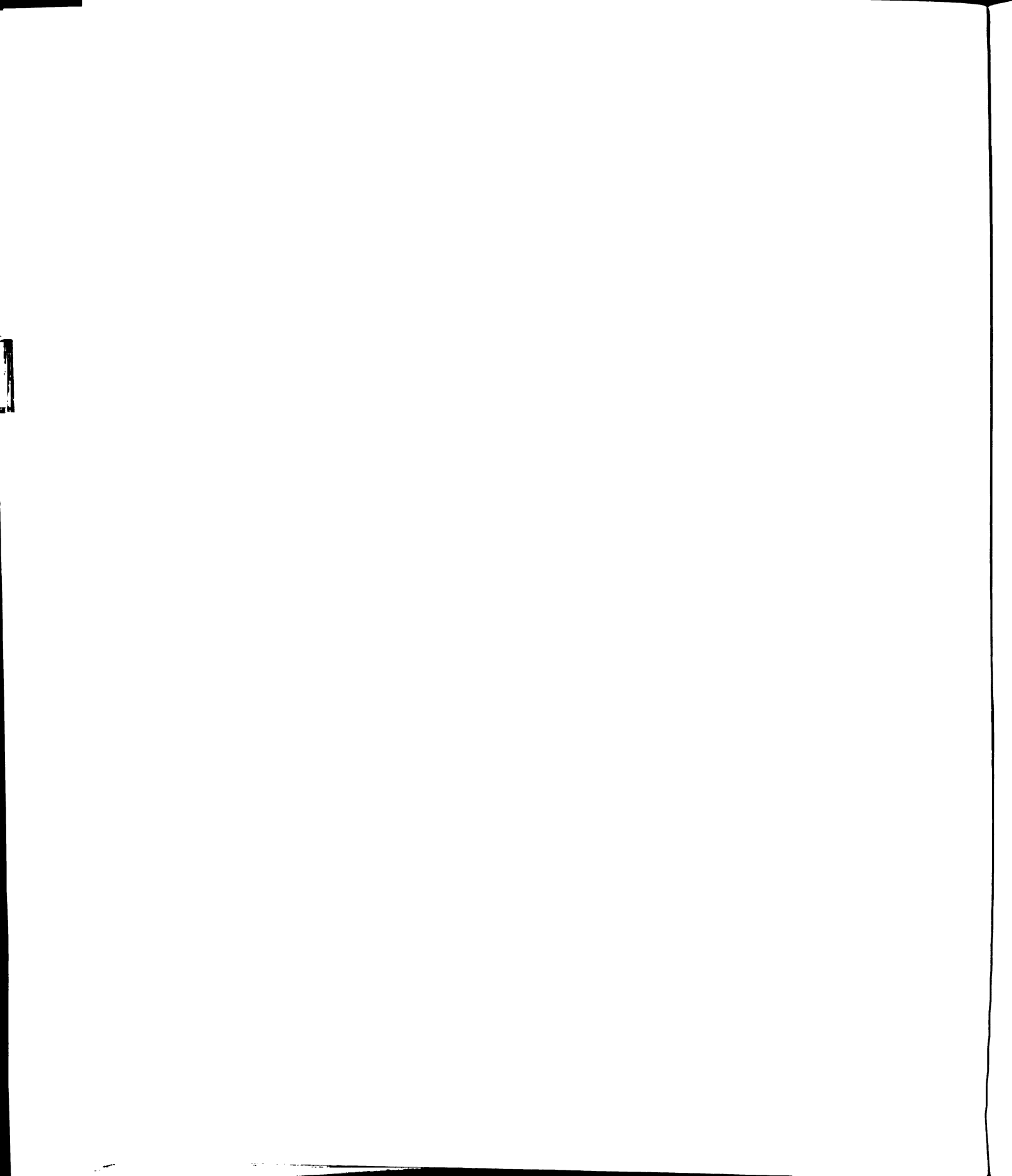
experiment are shown in Figure 3.5; however, the cured system ratio remained constant throughout the remaing 90 minues of the data run. Experiments have also been performed with up to 50-wt.% loading of chopped glass fibers, and the results show that the intensity ratio method is useful in composite structures as well, although the absolute emission intensities are diminished due to scattering by the fibers.

Similarly, the fluorescence emission maximum of phenoxazone 660 in the curing styrene system blue-shifts from 590 nm (monomer) to 570 nm (cured polymer). In this instance, the ratio  $I_{570}/I_{590}$  plateaus at a value of 1.30 when the system has attained complete cure, up from an initial value of 0.98 before cure has begun.

MMA cure characteristics were also examined using pyrene as the probe molecule. The fluorescence spectrum of pyrene does not shift with polarity, but exhibits a variation in the peak intensity ratio for two features within the emission band (see Figure 3.6). These two features, designated bands I (378 nm) and III (389 nm), change with the extent of cure in the MMA system. The ratio of peak I intensity to peak III intensity, I<sub>I</sub>/I<sub>III</sub>, is 0.93 prior to cure and subsequent to cure becomes 1.12 (Figure 3.7). However, the most dramatic indication of complete cure is found in taking a rolling time ratio:

$$ratio = \frac{I_t}{I_{t-1}}$$
 (3.1)

where I<sub>t</sub> is the intensity of band I or III at time t and I<sub>t-1</sub> is the intensity of that band at the pervious instance in time, as is shown in Figure 3.8 (the ratio is shown for 378 nm; however, the plot is the same for 389 nm). One explanation for this absolute intensity change is that the emission spectrum of pyrene is very sensitive to oxygen quenching and the diffusion rate of oxygen in the polymer system is directly related to viscosity. A more



detailed investigation of this effect, which will be discussed in a subsequent section, has shown that not all of the intensity change on matrix curing can be accounted for by oxygen availability. Some of this intensity change is the result of cure-dependent changes in the interactions between the pyrene molecule and its immediate surroundings.

### 3.3.3. Thermocouple measurements

To confirm that the phenoxazone probe molecules were indeed sensitive to the degree of cure in the Derakane<sup>®</sup> resin, temperature data were collected simultaneously with the fluorescence data. In these experiments, the heat of polymerization leads to a significant temperature rise since heat transfer from the 1 cm × 1 cm cuvette is inefficient. Therefore, a large temperature rise in a short period of time indicates a high polymerization rate. The experimental results, shown in Figure 3.9, show that the resin undergoes autoacceleration during the polymerization and that the probe molecules do indeed follow the curing process accurately. Similar results were obtained in the MMA/V-70 system when the pyrene data and thermocouple data were compared.

### 3.3.4. Sensitivity and interpretation of fluorescence response

## 3.3.4.1. Effect of temperature on fluorescence response

To determine the effect of temperature upon the probe molecule fluorescence emission, the probes were dissolved in non-reactive solvents and the fluorescence spectra as a function of temperature was monitored in the AB2 spectrometer. The samples were stirred continuously, and their temperatures were monitored with a thermocouple. The fluorescence emission was recorded for a series of temperatures starting at 30°C, ramping up to 85°C or 90°C in 5°C increments, and then returning to 30°C.

Ethylene glycol with  $10^{-3}$  wt.% phenoxazone 660 was excited at 550 nm. As the tempearture was increased from 30°C to 90°C, the wavelength of maximum peak emission shifted from 653  $\pm$  1 nm to 648  $\pm$  1 nm. This relatively small effect was reversible as well. Clearly, the 20-nm permanent shift does not occur from temperature.

Tri(ethylene glycol) divinyl ether with 10<sup>-3</sup> wt.% pyrene was excited at 330 nm. The ratio of peak I (378 nm) intensity to peak III (389 nm) intensity, I<sub>2</sub>/I<sub>III</sub>, is shown as a function of temperature in Figure 3.10; the noise magnitude due to the spectrometer detector would introduce a 3% error in the intensity ratio. As the temperature is increased between 30°C and 50°C, the intensity ratio decreases slightly; however, for temperatures greater than 50°C, the ratio is fairly constant. (When the sample is placed under a nitrogen blanket, the temperature effect is even more negligible.) In addition, the effect at low temperatures is in the opposite direction than that observed during cure, where the intensity ratio increases dramatically. Here, as with phenoxazone 660, any temperature effect upon the pyrene fluorescence response is reversible.

## 3.3.4.2. Comparison of probe responses during polymerization

The cure monitoring response of 10<sup>-4</sup> wt.% pyrene in a solution of Derakane<sup>®</sup> 470-45 and 0.75 wt.% AIBN was compared to the cure montioring response of 10<sup>-4</sup> wt.% phenoxazone 660 in the same Derakane<sup>®</sup> system. For both probe molecule systems, samples were placed in the AB2 spectrometer at 70°C for 75 minutes. The sample with pyrene was excited at 383 nm, and fluorescence emission data were collected every 30 seconds at 406 nm and 415 nm (corresponding to bands I and III, respectively). The sample with phenoxazone 660 was excited at 540 nm, and fluorescence emission data were collected at 609 nm and 629 nm (corresponding to the peak emission wavelengths

for cured and uncured samples, respectively). As shown in Figure 3.11, the correlation between the two probes in the Derakane<sup>®</sup> system confirms that they measure the same variable. Similar results were obtained with samples containing pyrene and phenoxazone 660 concentrations of 10<sup>-2</sup>, 10<sup>-3</sup> and 10<sup>-5</sup> wt.%.

# 3.3.4.3. Effect of polarity on fluorescence response of phenoxazone 660

In order to determine the solvatochromic origin(s) of the observed spectral shift, the emission spectra of phenoxazone 660 were recorded in a series of solvents spanning a range of polarity. For each solvent (Table 3.1), the wavelength of the phenoxazone 660 emission maximum is listed along with the values of  $E_T(30)$  (one measure of solvent polarity),  $\varepsilon_0$  (dielectric constant),  $\pi^*$  (a second measure of solvent polarity), and  $\mu$  (dipole moment), which are available in the literature.<sup>11</sup> The data in Table 3.1 shows that the best correlation is between emission maximum and solvent  $\pi^*$  value, as reflected by the  $R^2$  value of 0.93. These studies suggest that the shift in the phenoxazone 660 emission arises from alteration of the local polarity-polarizability during cure.

**Table 3.1.** Comparison of solvent polarity and phenoxazone 660 emission maximum.

Solvent	Emission maximum	E <sub>T</sub> (30)	εο	μ (Debye)	π
THF	595 nm	37.4	7.6	1.63	0.58
Acetone	612 nm	42.2	20.7	2.88	0.68
Acetonitrile	617 nm	46.0	37.5	3.92	0.86
DMF	623 nm	43.8	36.7	3.82	0.88
DMSO	633 nm	45.0	4.7	3.96	1.00

# 3.3.4.4. Effect of oxygen on fluorescence response of pyrene

Before implementing this cure monitoring technique in a fiber optic system, it was desired to observe the response of the fluorescence ratio to changes in process variables.

For example, in the case of free radical polymerizations, many process lines are run in oxygen-free environments to prevent oxygen from scavenging the free radicals that initiate the polymerization. Thus, it was of interest to investigate the effect of oxygen upon the ratio.

A sample of MMA and 1 wt.% V-70 with 10<sup>-3</sup> wt.% pyrene was degassed by cycling through three freeze-pump-thaw stages. The sample was placed in the AB2 spectrometer and cured at 40°C. The fluorescence emission was collected every five minutes for 150 minutes with an excitation wavelength of 334 nm. The ratio of peak I (378 nm) intensity to peak III (389 nm) intensity, I<sub>1</sub>/I<sub>III</sub>, is 0.93 prior to cure and subsequent to cure becomes 1.08 (Figure 3.12), which is typical for the MMA system. However, the fluorescence emission in the cured sample is approximately two to five times more intense than that which is observed when oxygen is present in this particular system: MMA with V-70 initiator (shown for 378 nm in Figure 3.13, top). The increased emission does not affect the rolling time ratio, which reaches a value between 6.0 and 9.0 upon cure completion regardless of sample oxygen content (see Figure 3.13, bottom).

# 3.3.4.5. Effect of temperature and initiator concentration on intensity ratio of phenoxazone 660

Two other variables of interest include temperature and initiation concentration. In order to investigate the effect of these variables upon the probe molecule fluorescence response, a matrix was constructed. Styrene samples with 0.78, 2, 4, and 5 wt.% AIBN and  $10^{-3}$  wt.% phenoxazone 660 were cured in the AB2 spectrometer at 70, 80 and 90°C, recording the sample emission at 570 nm and 590 nm every ten seconds with excitation at 510 nm. In Table 3.2, the time to cure completion and the final cure ratio,  $I_{570}/I_{590}$ , are

shown as a function of temperature and initiator concentration. There are no values for the 90°C and 4 or 5 wt.% AIBN because the bubbles produced by the release of nitrogen gas as the radical initator was formed became trapped in the polymer matrix, making it impossible to obtain an emission spectrum. As can be seen, the final ratio values are independent of cure temperature. However, the final ratio value does decrease with increasing initiator concentration, possibly due to the increased presence of chain ends. As expected, the results with the fluorescent probe molecule indicate that the polymerization rate increases (*i.e.*, polymerization time decreases) with increasing temperature and initiator concentration.

Table 3.2. Effects of temperature and initiator concentration upon the time to polymerization and final intensity ratio plateau for phenoxazone 660 in styrene with AIBN.

	0.78	wt.%	2 w	t.%	4 w	t.%	5 w	t.%
T (°C)	t (min)	Ratio						
70	445	1.30	275	1.28	200	1.22	185	1.20
80	225	1.31	125	1.27	80	1.21	85	1.20
90	145	1.30	65	1.26				

# 3.3.4.6. Effect of phenoxazone 660 concentration on intensity ratio

Finally, it was desired to ascertain the effect of the probe molecule concentration itself upon the cure monitoring ratio. Derakane® 470-45 samples with 0.75 wt.% AIBN and 10<sup>-2</sup>, 10<sup>-3</sup>, 10<sup>-4</sup> and 10<sup>-5</sup> wt.% phenoxazone 660 were cured in the AB2 spectrometer at 70°C, recording the sample emission spectrum every 45 seconds with excitation at 540 nm. In Table 3.3, the results show that probe concentration does not affect the peak emission wavelengths or the cure monitoring ratio when present in quantities of 10<sup>-4</sup> wt.% or less. Furthermore, at these low concentrations, the characteristic pink coloration is not

noticeable in the sample, which may make the probe molecule even more appealing in an industrial setting.

Table 3.3. Dependence of fluorescence peak emission wavelength and final cure monitoring ratio of phenoxazone 660 in Derakane® 470-45 with 0.75 wt.% AIBN upon probe concentration.

Wt.% Probe	Peak λ <sub>em</sub> (nm), Uncured	Peak λ <sub>em</sub> (nm), Cured	Cured Ratio
10-2	651	641	1.08±0.05
10-3	633	614	1.21±0.01
10-4	629	604	1.29±0.02
10-5	629	604	1.32±0.04

### 3.3.5. Equipment design

A fiber optic fluorescence sensor has been designed and assembled (Figure 3.14). In order to design and operate a practical monitoring system, special emphasis needs to be placed on the simplicity of the measurement scheme and the robust nature of the equipment used. The wavelength of the light source is necessarily determined by both the absorption profile of the probe molecule and any photochemistry that the incident light might initiate. For most practical applications of optical monitoring, the latter constraint is negligible due to the low light intensities used. A laser is the light source of choice for such measurements because of its inherent spectroscopic selectivity and the favorable properties of the output beam, thereby requiring a minimum of conditioning optics. Routing the excitation light to the process of interest should involve few, if any, adjustable optical components such as mirrors or lenses. Fiber optics can be used to route the excitation light to the analyte and then collect emission from the analyte and send it to the detection system. Optical fibers are available that can transmit UV and visible light with comparatively low optical loss and thus are ideally suited to this type of application.

For phenoxazone 660, inexpensive optical detection components optimized for pre-determined wavelengths have been chosen and incorporated into a fiber optic-based remote sensing system. Optical notch filters are used to separate 625 nm ( $\lambda_1$ ) and 605 nm ( $\lambda_2$ ) from 540 nm ( $\lambda_{exc}$ ), and sensitive solid state detectors are used for each monitoring wavelength. Measurement of the ratio of the output from the two detectors is accomplished using a simple comparator/differential amplifier.

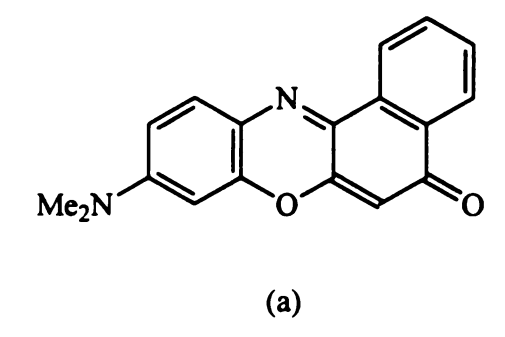
The output of such a system is proportional to the difference in intensity measured at 625 nm and 605 nm. Calibration of the system is accomplished using two standards: one where no curing occurs and the other where the system is cured completely. Construction of the spectrometer is straightforward and has been accomplished using inexpensive commercial components.

Experimental tests that utilize the *in-situ* cure monitoring device have successfully been performed with the Derakane® 411-C50 system. Phenoxazone-doped resin with AIBN was placed in the bottom of a watch glass on a hot plate. The samples were illuminated by a 200 W Hg(Xe) lamp (Oriel Corporation, Stratford, CT) with a 540-nm interference filter for four minutes. A fiber optic was positioned at a 45° to the sample to collect the fluorescence emission from the excited probe molecules. Fluorescence information was then routed to an Ocean Optic SD1000 fiber optic spectrometer (Dunedin, FL), and the spectrum was monitored between 500 nm and 800 nm, with spectra being taken every six seconds. Figure 3.15 shows an example of the results from the intensity ratio measurements taken during these experiments. The results show that the plateau is reached when cure is complete at I<sub>605</sub>/I<sub>625</sub> = 1.1, thus agreeing nicely with the experiments performed in the AB2 spectrometer.

#### 3.4. CONCLUSIONS

Two probe molecules for fluorescence monitoring of cure in polymer systems have been examined. The first probe, phenoxazone 660, exhibits a solvatochromic shift in fluorescence wavelength with increasing cure. For example, during the cure of a common vinvl ester resin (Derakane® 411-C50), this probe exhibits a shift in the wavelength of maximum fluorescence intensity from 617 nm in the uncured system to 597 nm in the fully cured system. This shift was found to correlate with the local polarity as characterized by the empirical quantity  $\pi^{\bullet}$ . The intensity ratio of these two peaks provides a measure of the degree of cure that is insensitive to background interferences and does not lose sensitivity after the gel point. The second probe, pyrene, exhibits a change in relative intensities for bands I and III (378 nm and 389 nm in MMA), as well as an overall increase in absolute fluorescence emission. Fluorescence cure monitoring strategies based upon these probes can be implemented using optical fibers to route both the excitation light to the sample and the fluorescence emission from the sample; therefore, these methods are amenable to in-situ and on-line monitoring of cure in polymerization systems.

Figure 3.1. General chemical structure of the Derakane® vinyl ester resins.



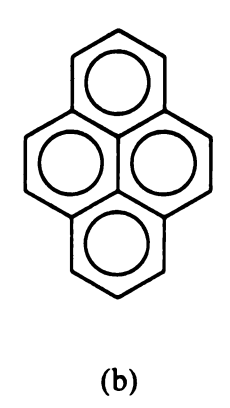


Figure 3.2. Chemical structures of phenoxazone 660 (a) and pyrene (b).

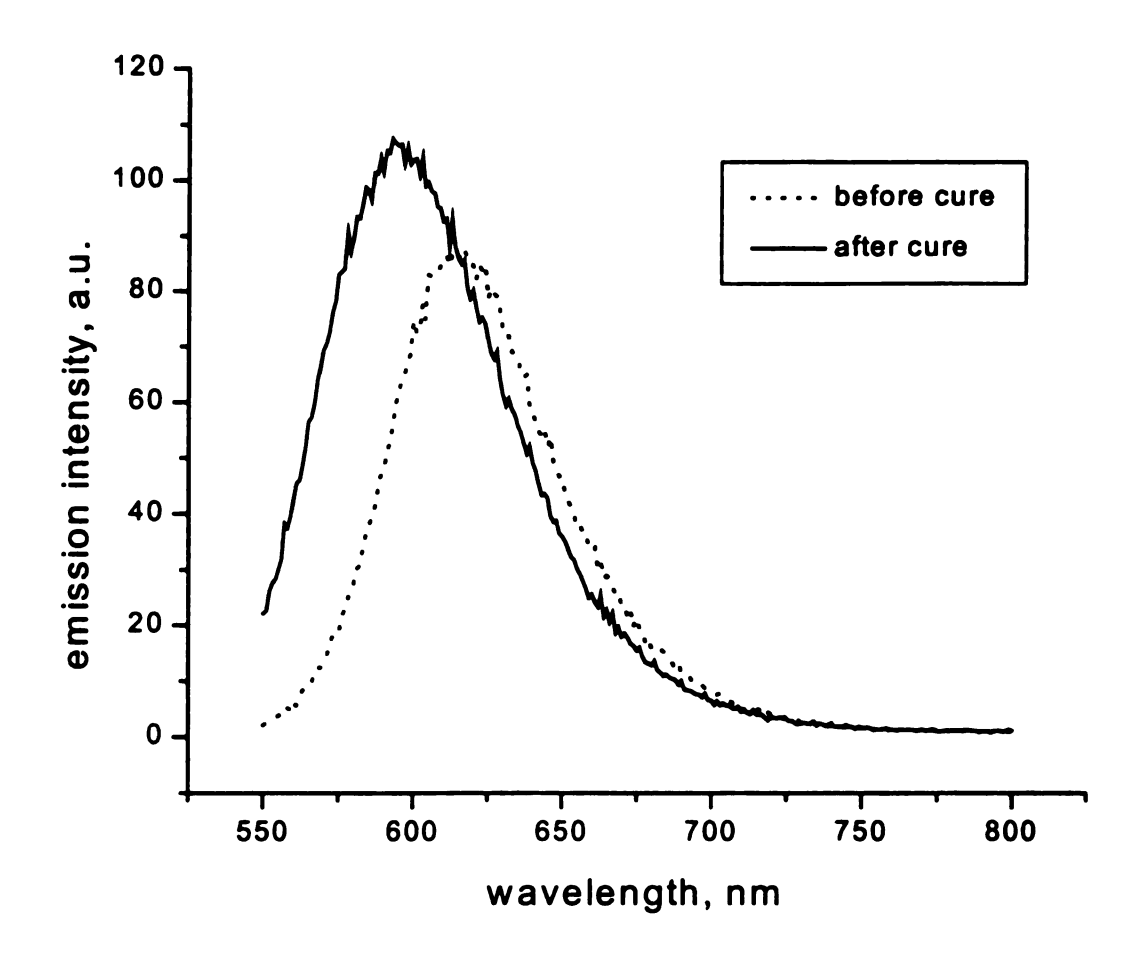


Figure 3.3. Spectral shift of phenoxazone 660 associated with curing Derakane® 411-C50 (with AIBN as initiator).

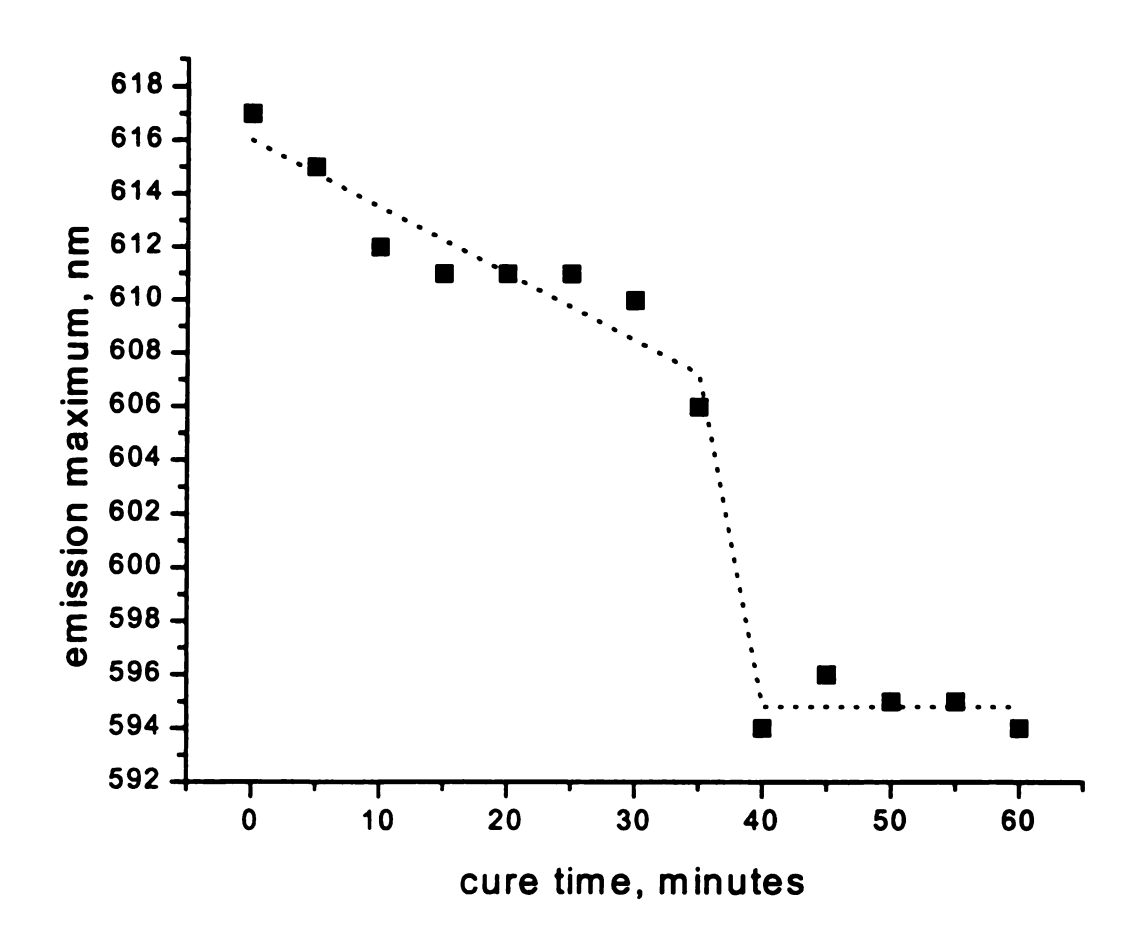


Figure 3.4. Blue-shift in phenoxazone 660 peak emission as the cure of Derakane<sup>®</sup> 411-C50 (with AIBN as initiator) progresses.

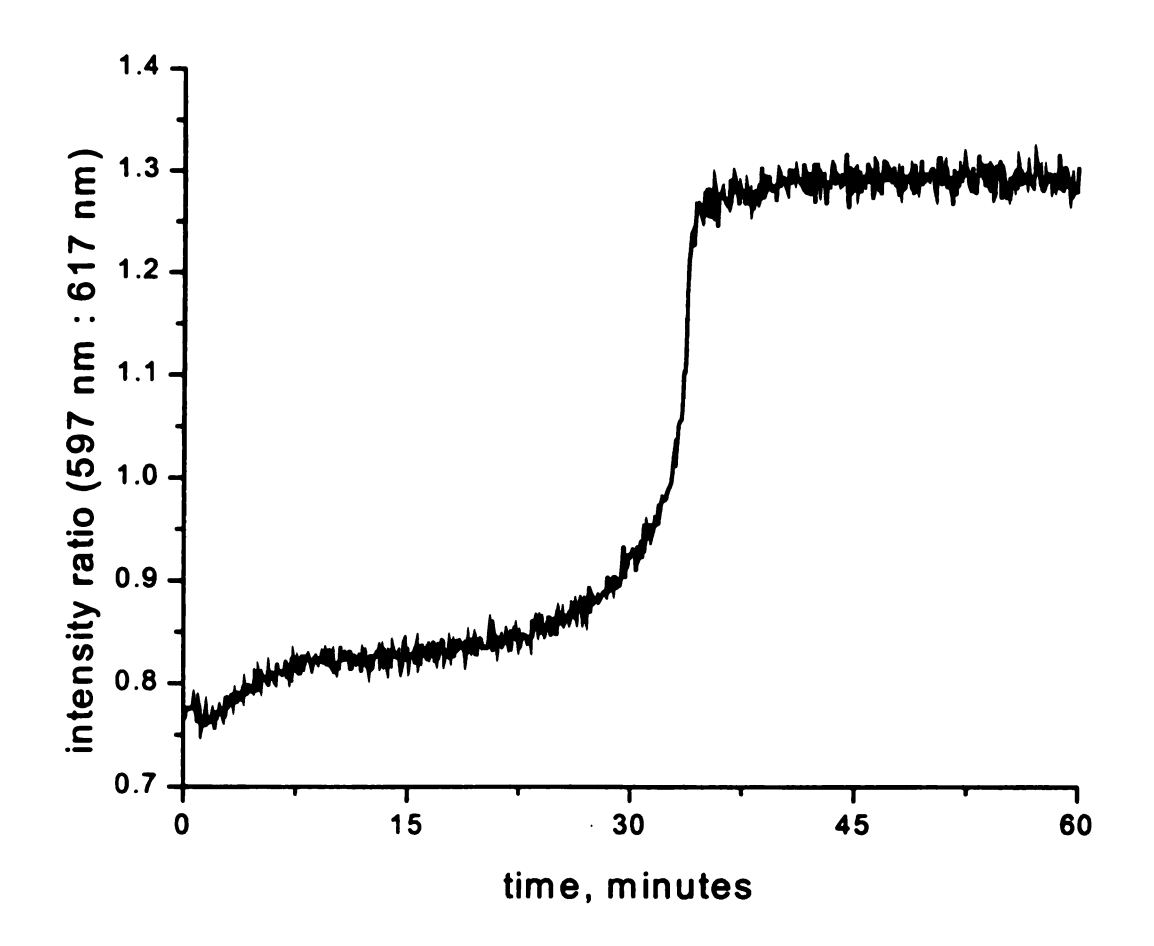


Figure 3.5. Change in phenoxazone 660 fluorescence intensity ratio in curing Derakane® 411-C50 with AIBN as initiator.

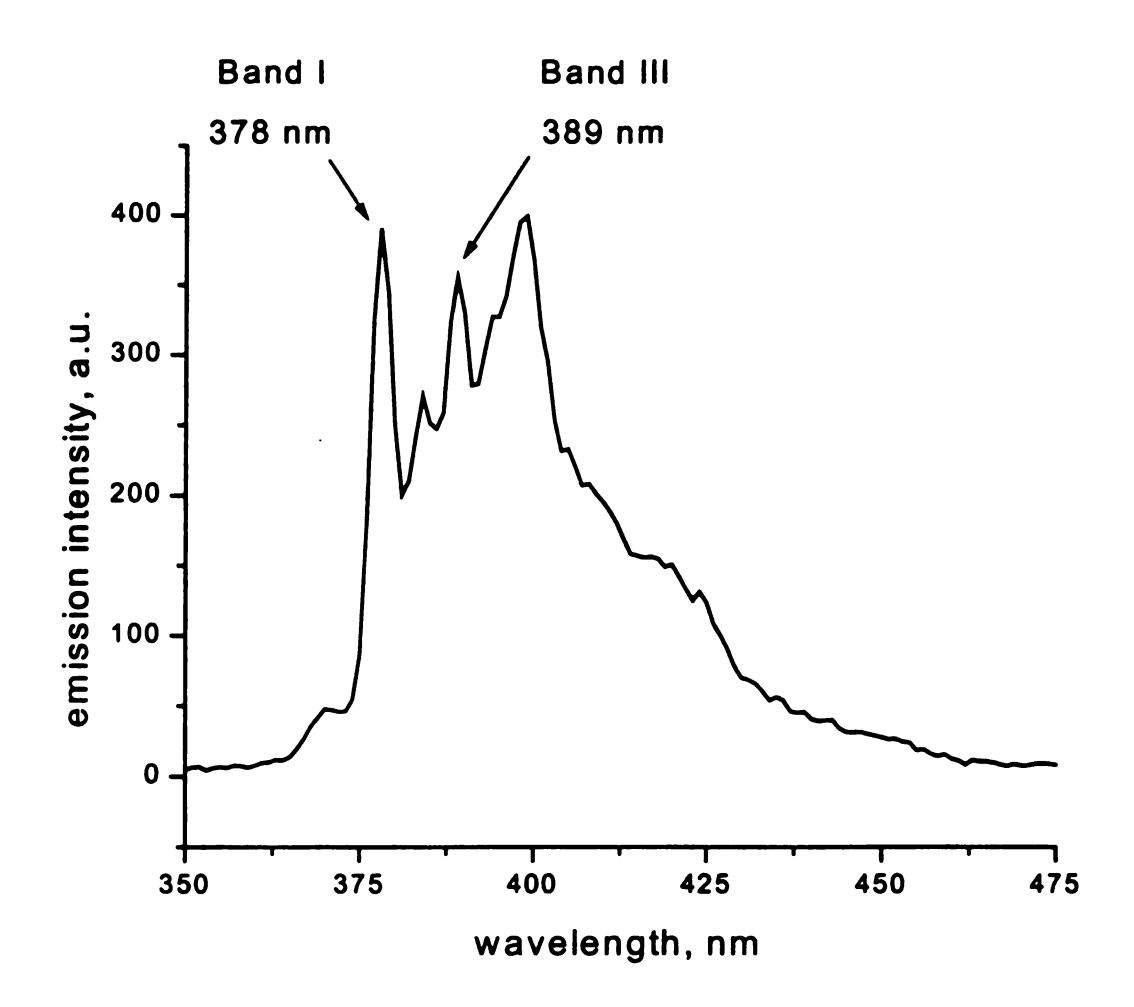


Figure 3.6. Fluorescence response of pyrene in MMA with AIBN as initiator.

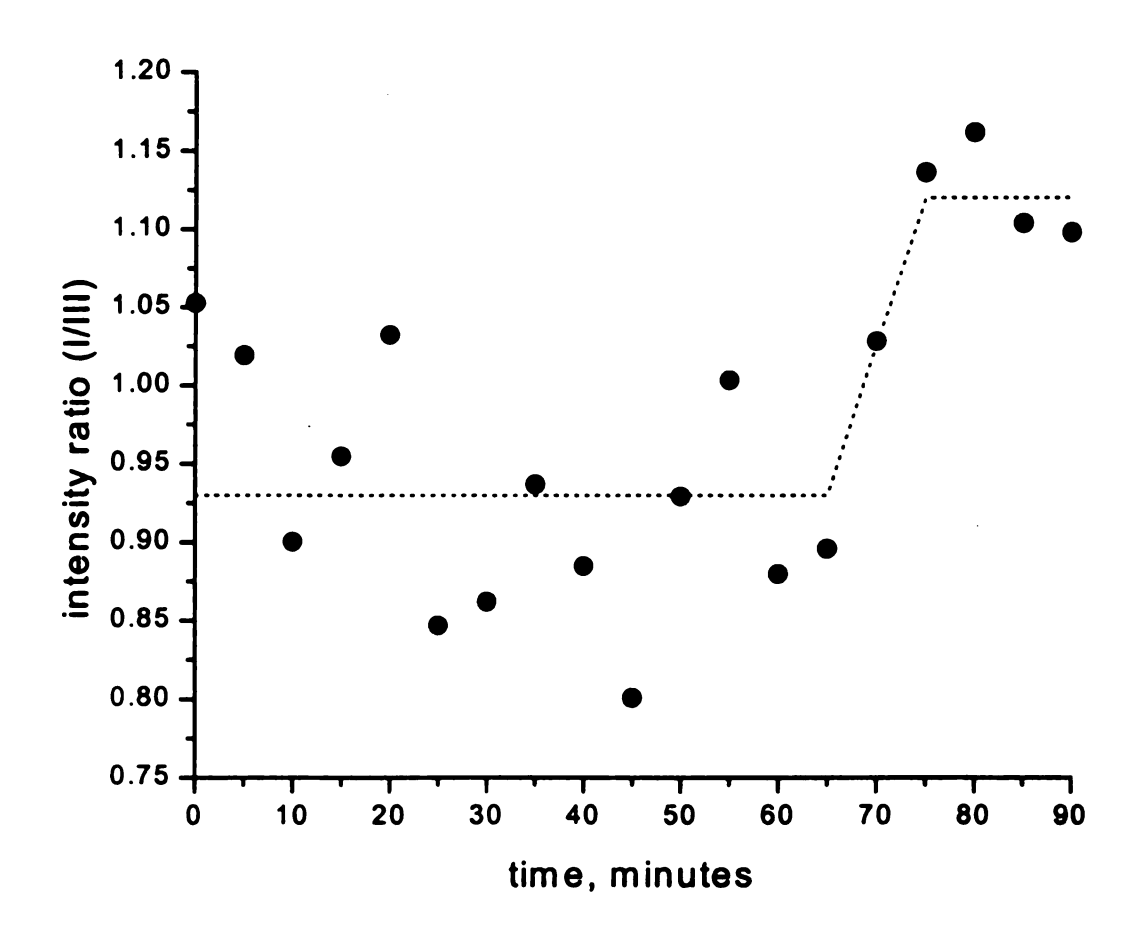


Figure 3.7. Change in pyrene fluorescence intensity ratio in curing MMA with AIBN as initiator.

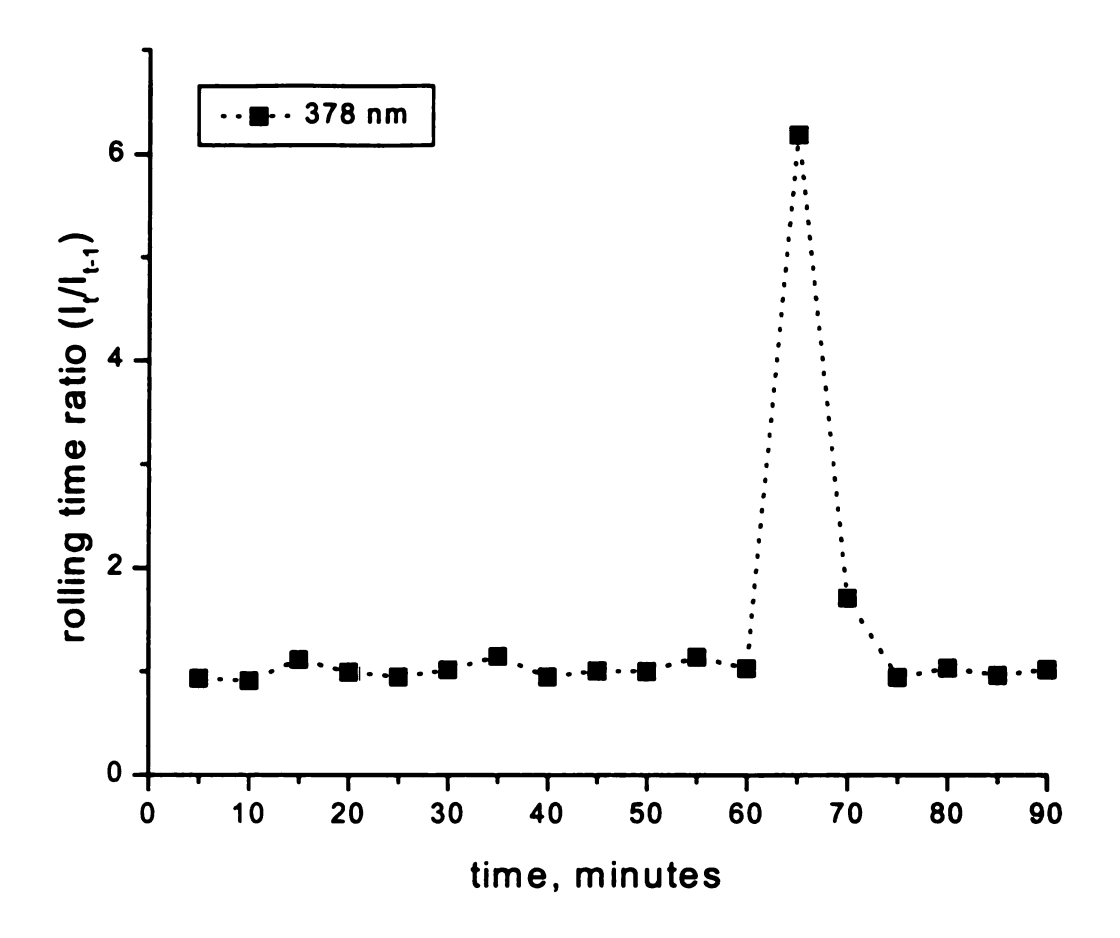


Figure 3.8. Change in pyrene fluorescence rolling time ratio at 378 nm in curing MMA with AIBN as initiator.

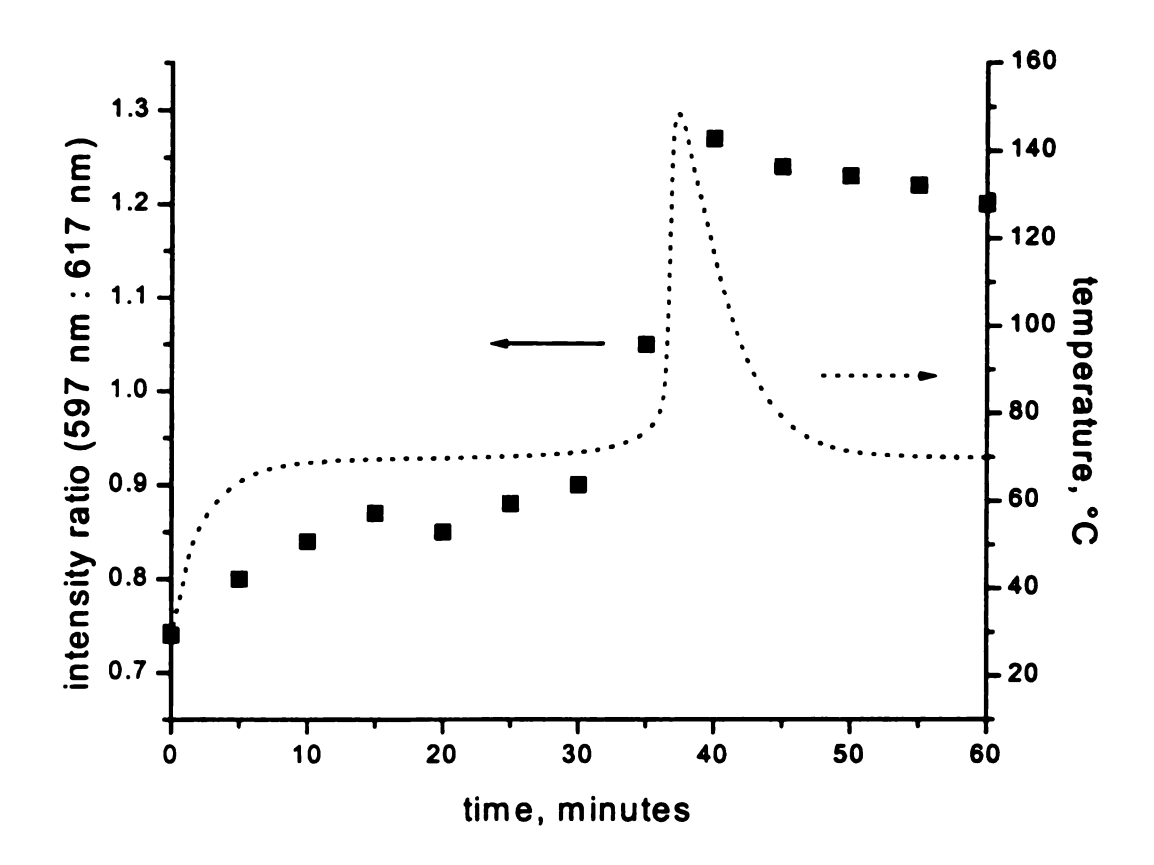


Figure 3.9. Comparison between thermocouple (...) and phenoxazone 660 intensity ratio (**a**) data in curing Derakane 411-C50 with AIBN as initiator.

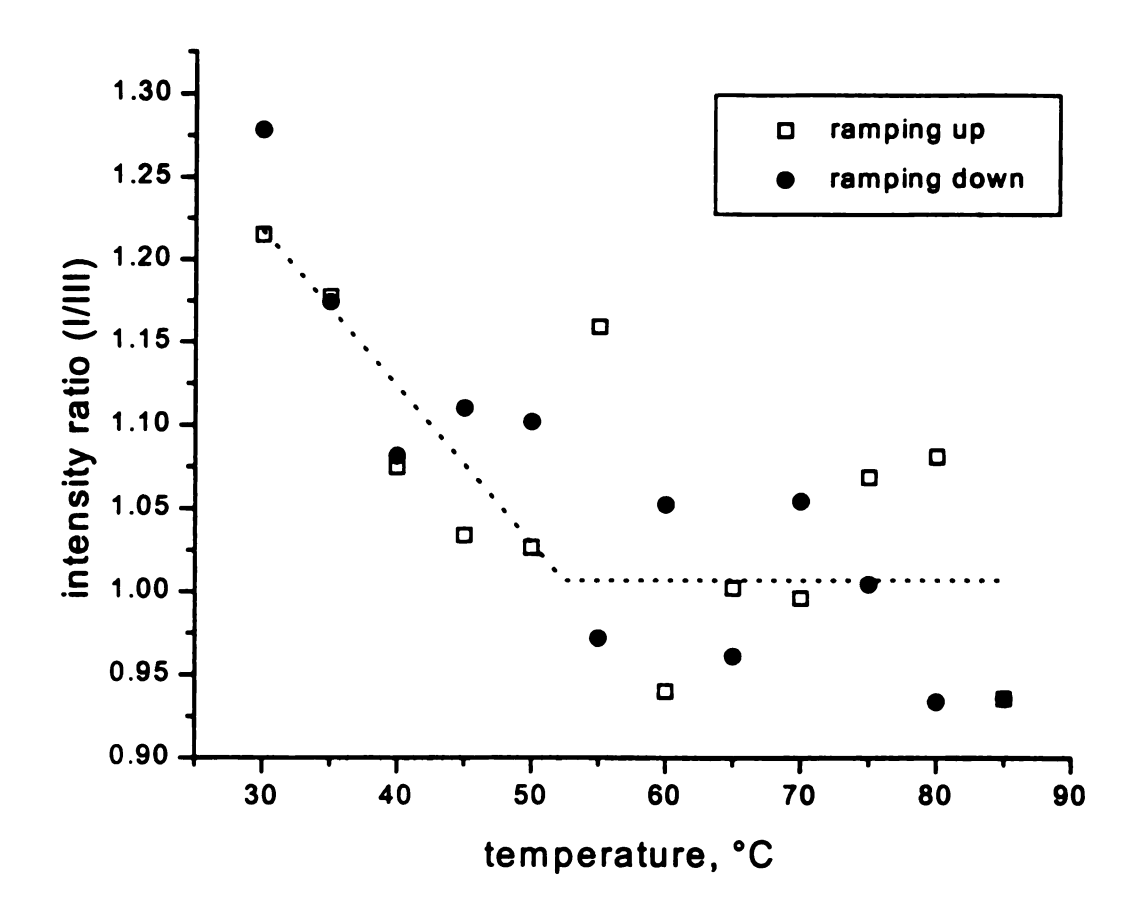


Figure 3.10. Change in pyrene fluorescence intensity ratio in tri(ethylene glycol) divinyl ether with increasing (□) and decreasing (●) temperature.

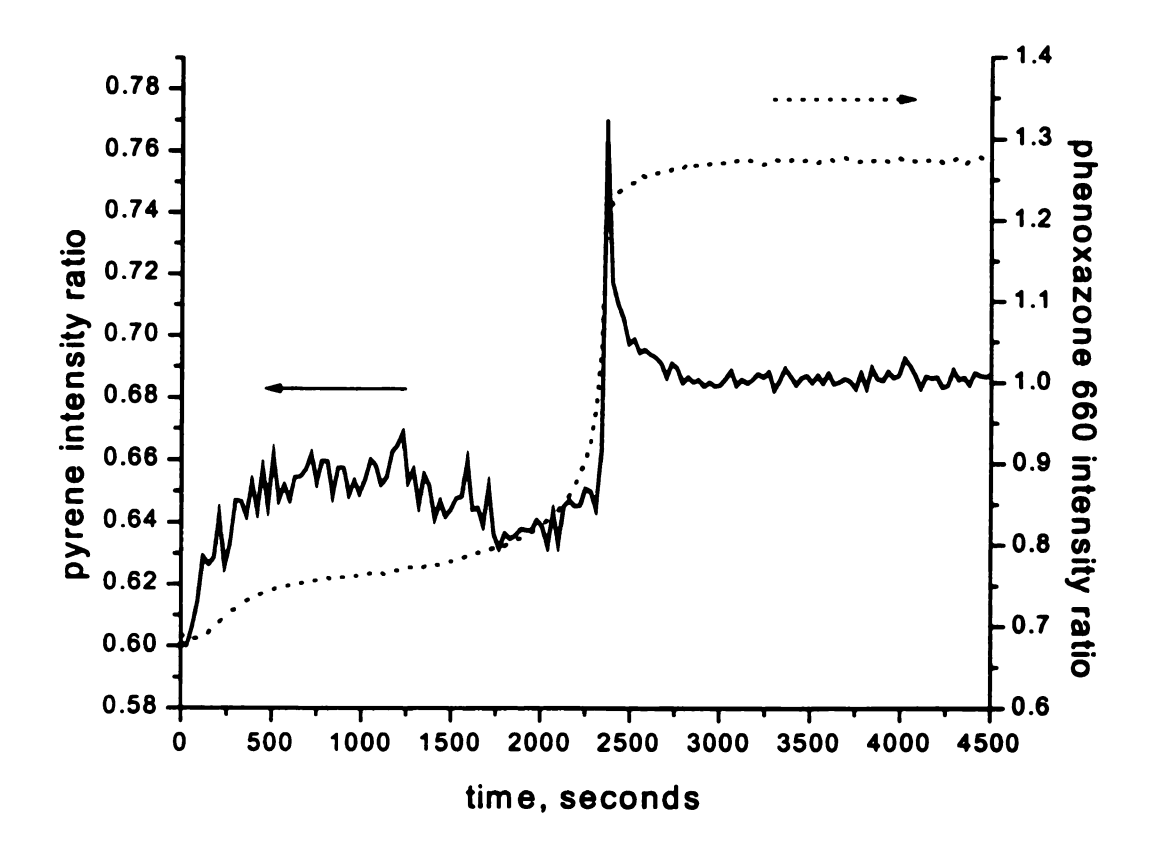


Figure 3.11. Change in pyrene fluorescence intensity ratio (—) and phenoxazone 660 fluorescence intensity ratio (…) in curing Derakane® 470-45 with AIBN as initiator.

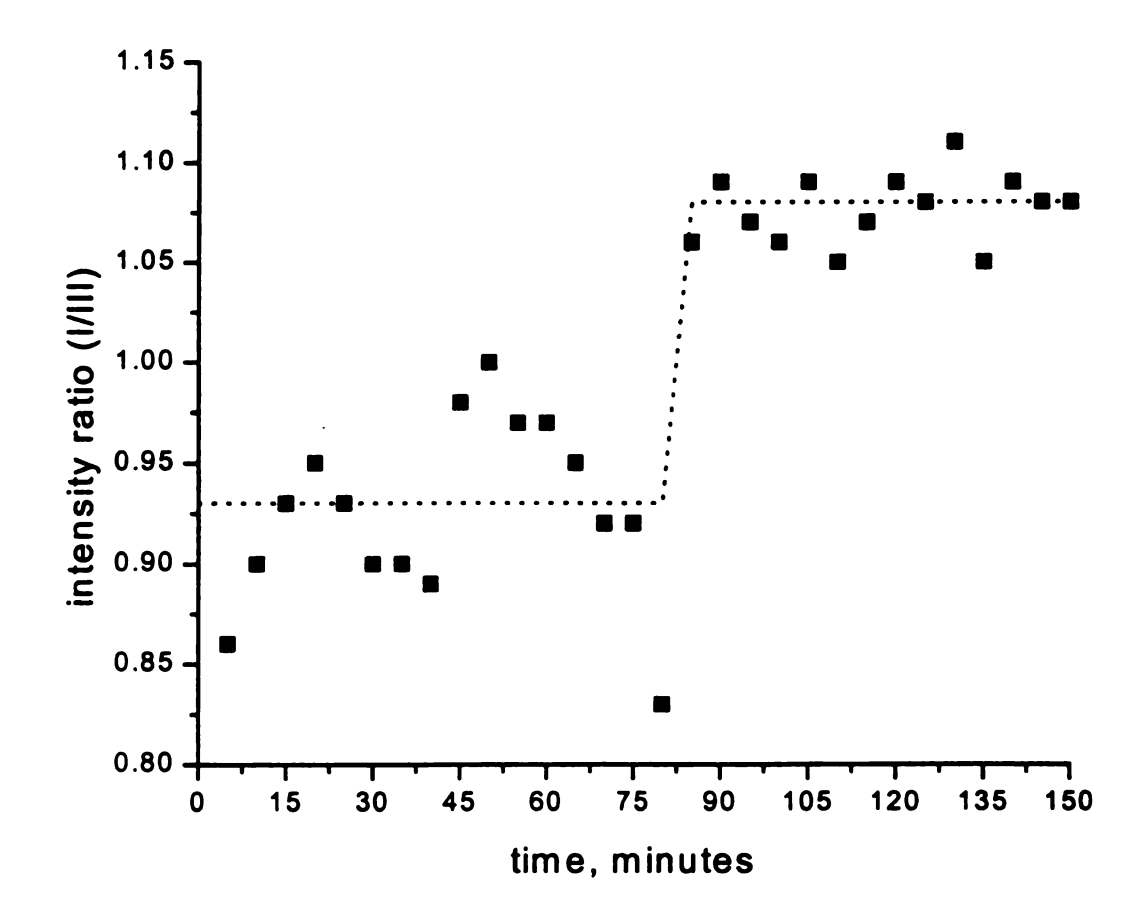
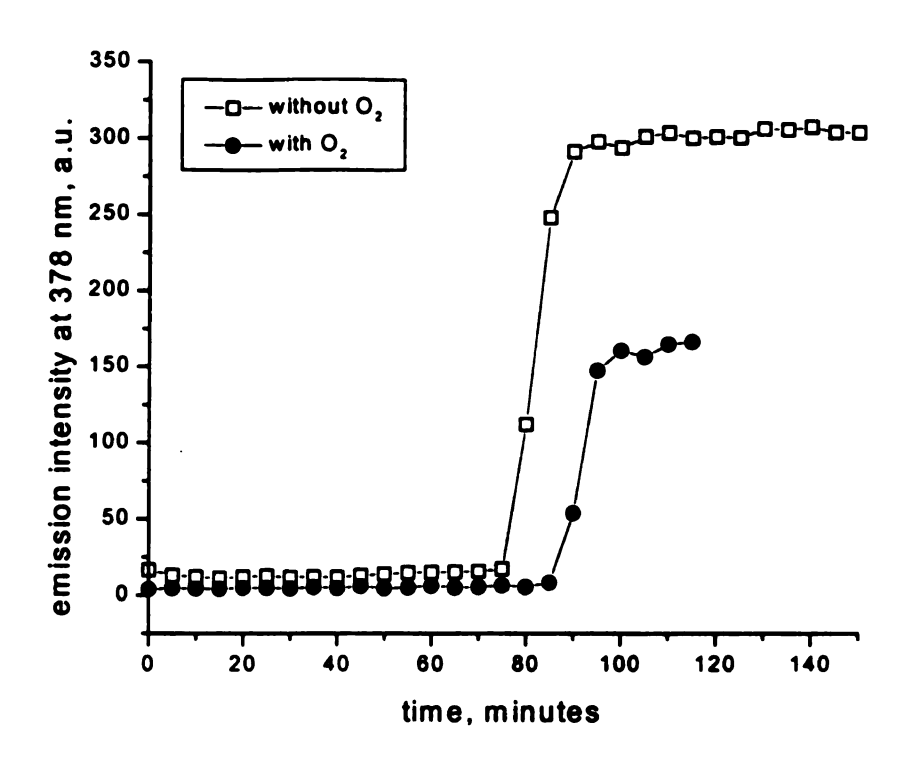


Figure 3.12. Change in pyrene fluorescence intensity ratio in curing MMA with V-70 as initiator: without oxygen.



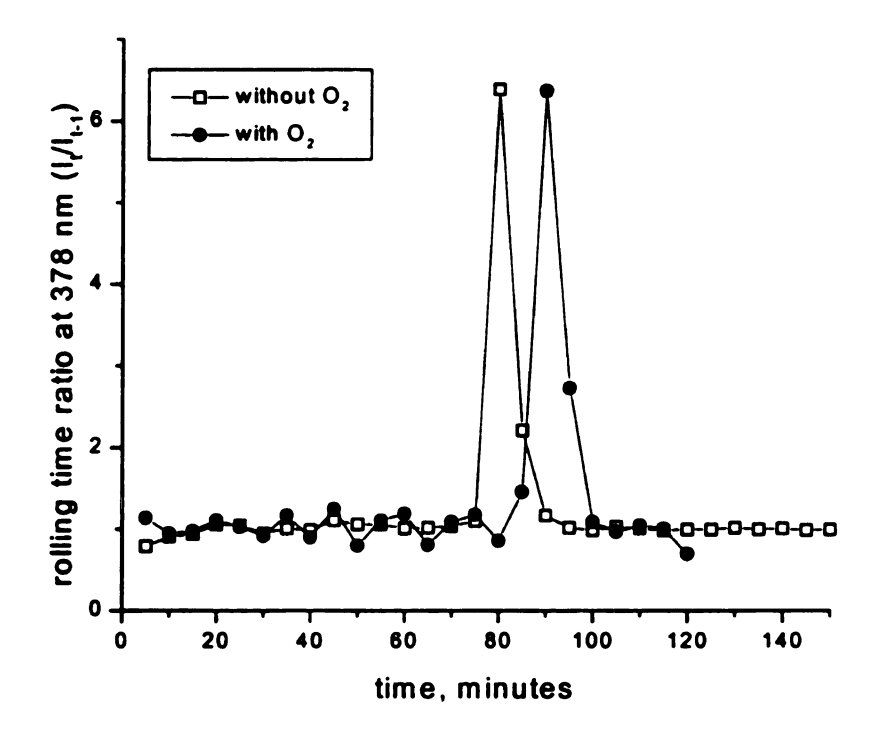


Figure 3.13. Change in pyrene fluorescence intensity (top) and rolling time ratio (bottom) at 378 nm in curing MMA with V-70 as initiator: without oxygen (□) and with oxygen (●).

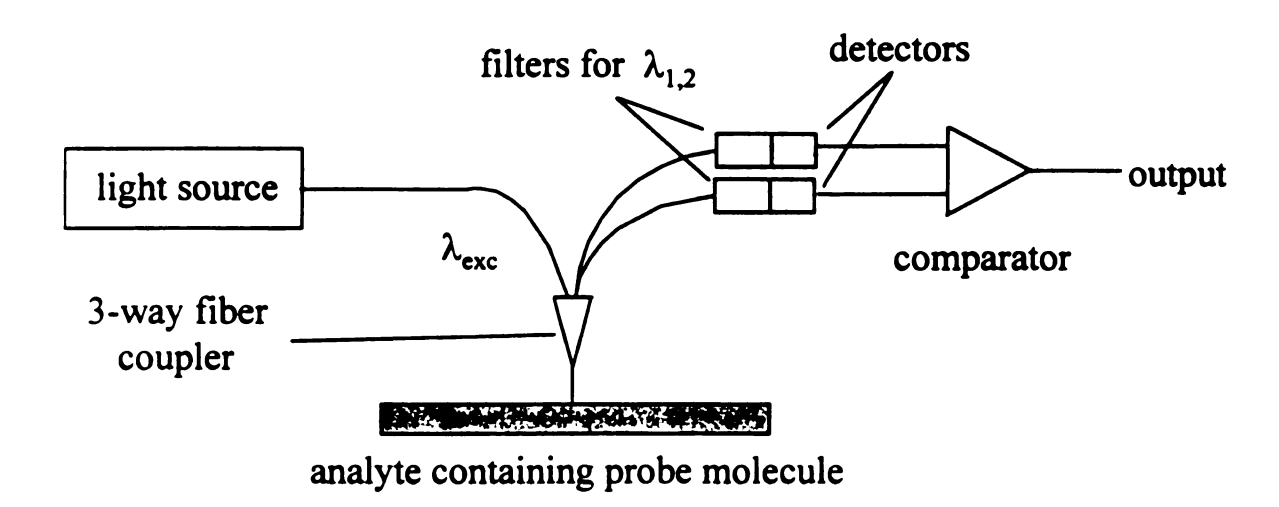


Figure 3.14. Diagram of in-situ monitoring instrument.

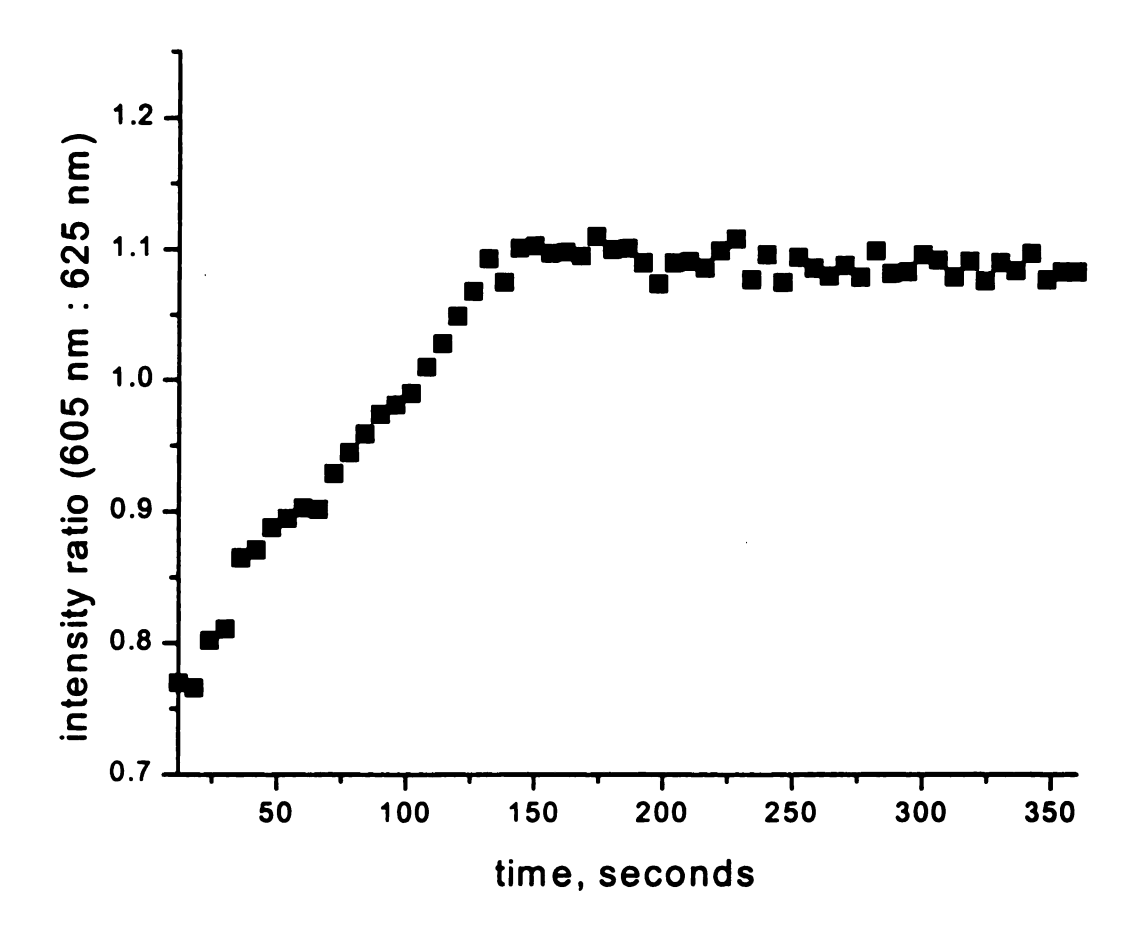


Figure 3.15. Change in intensity ratio of phenoxazone 660 emission in curing Derakane<sup>®</sup> 411-C50 with AIBN as initiator monitored by *in-situ* apparatus.

#### 3.5. REFERENCES

- 1. "Process Monitoring Sensors for Polymer Composites," U.S. Department of Commerce, NISTIR Report #4514, 1991.
- 2. R.L. Levy and S.D. Schwab, "Monitoring the Composite Curing Process With a Fluorescence-based Fiber-Optic Sensor," *Polymer Composites*, 12(2), 96 (1991).
- 3. F.W. Wang, R.E. Lowry, W.J. Pummer, B.M. Fanconi, and E.S. Wu, "Fluorescence Monitoring of Viscosity and Chemical Changes During Polymerization," *Photophysics of Polymers*, edited by C.E. Hoyle and J.M. Torkelson, ACS Symposium Series 358, American Chemical Society, Washington, DC, 454 (1987).
- 4. A. Stroeks, M. Shorhun, A.M. Jamieson, and R. Simha, "Cure monitoring of epoxy resins by excimer fluorescence," *Polymer*, 29, 467 (1988).
- 5. O. Valdes-Aguilera, C.P. Pathak and D.C. Neckers, "Pyrene as a Fluorescent Probe for Monitoring Polymerization Rates," *Macromolecules*, 23, 689 (1990).
- 6. S.F. Scarlata and J.A. Ors, "Fluorescence polarization: A method to monitor polymer cure," *Polymer Comm.*, 27, 41 (1986).
- 7. D. Basting, D. Ouw and F.P. Schafer, "The phenoxazones: A new class of laser dyes," Optics Communications, 18(3), 260 (1976).
- 8. D.S. Karpovich and G.J. Blanchard, "Relating the Polarity-Dependent Fluorescence Response of Pyrene to Vibronic Coupling. Achieving a Fundamental Understanding of the py Polarity Scale," J. Phys. Chem., 99, 3951 (1995).
- 9. G.R. Holtom, ASTM Proceedings, 1204-01, 1 (1990).
- 10. W.H. Tan, Z.Y. Shi, S. Smith, D. Birnbaum, and R. Kopelman, "Submicrometer Intracellular Chemical Optical Fiber Sensors," *Science*, 258, 778 (1992).
- 11. P. Suppan and N. Ghoneim, Solvatochromism, The Royal Society of Chemistry, United Kingdom, 1997.

# Chapter 4

# IN-SITU MONITORING OF ACID CONCENTRATION IN CHEMICALLY AMPLIFIED PHOTORESISTS

#### 4.1. INTRODUCTION

With chemically amplified resists, the photoacid is key to circuit pattern development, and the introductory discussion in this dissertation illustrates that the deprotection reaction may not be limited to the illuminated areas since the photogenerated protons may diffuse outside this region. For this reason, it is important to understand the concentration profile and diffusional characteristics of the photoacid within the actual photoresist thin film. The two processing steps that have the greatest impact on the concentration and diffusional mobility of the photoacid are exposure and post exposure bake. The acid is generally produced by the photolysis of an onium salt photoacid generator (PAG). For a given PAG concentration, the exposure dose will dictate the amount of acid that is generated. The temperature and duration of the post exposure bake impact both the diffusional mobility of the acid and the rate of the deprotection reaction. The post exposure bake is the time in which the actual acid diffusion and deprotection reaction take place, and therefore the post exposure bake conditions have the greatest impact on the resulting linewidth. Since pattern development depends upon the regeneration and diffusion of each photoacid to effect hundreds of deprotection events, the loss of any photons during the post exposure bake, namely by neutralization with airborne bases or evaporation, can adversely affect this process.

## 4.1.1. Utility of molecular probes

Molecular probes that exhibit a change in an optical property in response to a change in the local environment can provide valuable *in situ* information about chemical and physical processes. For example, a probe molecule may manifest a shift in wavelength in an absorbance or fluorescence peak, or a change in excited state lifetime, in response to a change in the local polarity or viscosity. Other probes may exhibit an optical response that changes with changing acid concentration. Probes that exhibit a change in optical properties are particularly useful since the excitation light may be easily generated using a wide variety of sources and the excitation and/or emitted light may be easily routed using optical fibers. In addition, the inherent timescale for the underlying photochemical events (absorption or fluorescence) are very short (on the order of femtoseconds to nanoseconds), providing excellent time resolution. Finally, it is usually possible to identify probes that possess high quantum yields and large optical responses such that reliable signals can be obtained using trace quantities of the probe.

There are a number of molecules whose optical response is sensitive to the pH of the local environment.<sup>1</sup> Typically, these compounds possess two or more different protolytic forms, each with a unique absorption and/or fluorescence spectrum. Examples of such probe molecules include xanthene dyes, aromatic azines and coumarin dyes. These probes have been used in various biological and medical applications to detect or quantify acid concentration in a system.<sup>2</sup> Recently, acid-sensitive dyes have been used to investigate photoacid generation in microlithographic systems. For example, Pohlers et al. have reported the use of such dyes to characterize the efficiency of photoacid generators.<sup>3</sup> These authors observed a shift in the absorbance spectrum of these dyes

upon protonation from the neutral state to the singly-charged state. In prior work, Pohler et al. observed shifts in the absorbance spectra and large changes in fluorescence intensity upon protonation of aromatic monoazines.<sup>4</sup> Dentinger et al. evaluated several xanthene dyes for monitoring and imaging photoacid production.<sup>5</sup> Finally, Okoroanyanwu et al. reported the use of an aromatic monoazine to monitor photoacid generation in films and solutions.<sup>6</sup>

#### 4.1.2. Studies of acid concentration in CARs

In this chapter, spectroscopic techniques are described that enable the characterization of acid concentration in chemically amplified resists during the exposure and post exposure bake steps. To measure the photoacid generation during exposure, steady-state fluorescence of fluorescein is used. Unlike some of the previous studies reported in the literature, these measurements on the absolute fluorescence intensity, but rather used the relative intensities of two interdependent acid sensitive peaks. Secondly, the steady-state absorption of crystal violet is used to characterize the acid concentration in the photoresist during post exposure bake. Since the absorption spectrum of crystal violet exhibits three bands, each corresponding to a different protonated form, the acid concentration can be quantified over a broad range.

#### 4.2. EXPERIMENTAL

## 4.2.1. Materials

These studies were performed using a commercial photoresist, Apex-E 2408 DUV photoresist (Shipley Company, Marlborough, MA). The acid-sensitive fluorescent probe fluorescein 548 (Exciton, Inc., Dayton, OH) was used in steady-state fluorescence studies to determine photoacid generation during exposure. The dye crystal violet

(Sigma Chemical Company, St. Louis, MO) exhibits a sensitivity to acid concentration in its absorption spectrum and was used to determine acid concentration during PEB using steady-state absorption. All chemicals were used as received.

#### 4.2.2. Methods

#### 4.2.2.1. Absorption and fluorescence measurements

Absorption spectra of the photoresist and probe molecules in the photoresist were obtained using a Hewlett Packard 8452A diode array spectrophotometer. A special sample holder was manufactured for the spectrophotometer to hold quartz slides for film studies. Fluorescence spectra of the materials were obtained using an Aminco-Bowman Series 2 Luminescence Spectrometer. Fluorescence data were taken using the maximum peak excitation and the maximum peak emission. Bulk solution samples were placed in quartz cuvettes; one-micron film samples on quartz slides were obtained using a PWM32 spinner from Headway Research, Inc. (Garland, TX).

# 4.2.2.2. Steady-state fluorescence measurements with photoresist films during exposure

Samples for the photoacid generation experiments were prepared by first dissolving 0.01 wt.% fluorescein in the commercial photoresist. The resist was spin coated at 1550 rpm onto quartz crystal disks. The fluorescein dye was excited at 457.9 nm with a Coherent Innova 70 argon ion laser. The fluorescence signal was collected with a Spex 1877 Triplemate monochromator with a subtractive dispersive filter stage and a second spectrograph stage. A gated EG&G Princeton Applied Research Model 1530 C/CUV CCD, cooled to -120°C to reduce dark current, was used to detect the signal. Simultaneously, the sample was illuminated with an Oriel 6035 mercury(argon)

pencil style lamp, fitted with a filter to select the UV lines, to induce dissociation of the photoinitiator into the photoacid. This experimental setup is depicted in Figure 4.1.

# 4.2.2.3. Steady-state absorption measurements with photoresist films during processing

These experiments were performed using crystal violet as the molecular probe. The absorption spectrum of crystal violet exhibits three bands, each corresponding to a different protonated form. To better understand this effect, and how it might relate to the choice of the pump and probe laser wavelengths, the steady state absorption spectra of crystal violet were recorded with 1 nm resolution as a function of pH using a Hitachi U-4001 spectrometer. A constant crystal violet concentration (6×10<sup>-6</sup> M) was maintained for all absorption measurements by dilution from a single stock solution. The pH of the solutions was controlled using a series of 0.2 M potassium chloride/0.2 M hydrochloric acid buffer systems. Outside the buffering range of this system, concentrated hydrochloric acid or 0.2 M potassium chloride was used to maintain the pH. A Fisher Scientific Accumet pH meter and combination electrode with automatic temperature correction was used for all pH determinations. The pH of the solutions ranged from 0.26 to 5.12, which was measured after the addition of the crystal violet. The ionic strength of the solutions was not controlled, as it does not give rise to significant error in our system.

#### 4.3. RESULTS AND DISCUSSION

#### 4.3.1. Probe molecule selection

As has been discussed above, fluorescence monitoring of chemical and biological systems has been widely used to gain a greater insight into the micro-environment about carefully selected probe molecules. This *in-situ* technique offers high sensitivity on fast time scales with minimal changes in the system under investigation since most probe

molecules need only be present in minute amounts for adequate signal detection.<sup>2</sup> Numerous dyes and chromophores are available for fluorescence monitoring and have been used successfully to detect such properties as polarity, viscosity, ion concentration, diffusion coefficients, etc. A literature survey of research accomplished with fluorescent probe molecules yielded a list of possible candidates that could be used in this study. From this list, likely candidates were chosen with several requirements in mind. First of all, the probes, which are typically large aromatic molecules, must be soluble in the resist mixture, which is composed of long, organic polymer chains. Secondly, the optical response of the probes should be distinguishable from the optical response of the resist mixture itself. For example, the Apex-E 2408 DUV photoresist absorbs strongly below 310 nm and possesses a weak fluorescence, as shown in Figure 4.2, so the optical response of the probe molecules should be in the near-UV or visible regions of the spectrum. In the case of fluorescence, it is also important that it be possible to induce this fluorescence emission using available laser lines. Finally, the probes must not significantly alter the kinetics of the system. If this criterion cannot be strictly met, then it should be possible to extrapolate what the measurements would have been in the absence of the probe. For example, probes which trap acids in order to measure the concentration could adversely affect the photoresist system (if one photoacid molecule is taken from the system, it would decrease the number of deprotection events drastically). Finally, the fluorescence probe or series of probes should be sensitive throughout the entire photoresist process, from prebake to illumination to postbake.

# 4.3.2. Acid-sensitivity of fluorescein

Fluorescein (shown in Figure 4.3) was chosen as a molecular probe to study photoacid generation in the resist during exposure because it exhibits a large fluorescence response that is well-characterized and dependent upon acid concentration. Figure 4.4 shows the absorption and emission spectra of 0.01 wt.% fluorescein in Apex-E 2408 DUV photoresist. From these spectra, it is evident that the optical response of fluorescein is not hampered by the photoresist itself and excitation of the probe is possible using one or more lines from an argon laser.

In order to verify the acid-sensitive fluorescence of fluorescein, preliminary studies were first done in bulk solution. The emission spectrum of 0.01 wt.% fluorescein in the photoresist was collected using an excitation wavelength of 460 nm. Two microliters of sulfuric acid were then added to the cuvette, which was stirred *in situ*. The emission spectrum of the acidic solutions was collected after waiting ten minutes and compared to the original formulation.

Figure 4.5 shows that the acid-sensitive response is characterized by a blue-shift in the fluorescence emission and by a change in the relative intensities of two interdependent peaks characterizing that emission.

# 4.3.3. Study of photoacid generation during exposure in photoresist films using steady-state fluorescence

Similar studies, in which small amounts of a mineral acid were added to the resist solution before spinning films, further demonstrated that the acid-sensitive response is characterized by the relative intensities of these two interdependent peaks. Therefore, we monitored photoacid generation during exposure by ratioing the intensity of the fluorescein fluorescence emission at these two wavelengths. By using this ratioing

method, rather than absolute intensities, the measurements are no longer dependent upon fluorescein concentration, detector settings, or scattered and background light.

A representative fluorescence profile obtained via *in-situ*, real-time experiments during exposure is shown in Figure 4.6. This plot shows the relative change in peak intensities at 525 nm and 560 nm as a function of photoacid generation during exposure. When the intensity ratio of 525 nm to 560 nm is taken for the duration of the monitoring, Figure 4.7 is obtained. In this experiment the build-up in the photoacid concentration occurs over a relatively long timescale since a low intensity mercury-argon pen lamp was used to induce the acid production, rather than the excimer laser common used in industrial photoresist processing. The photoacid generation in this system can be characterized as a first order response to a step-change perturbation from equilibrium (in this case the perturbation corresponds to the sudden illumination and the response is the dissociation of the photoacid generator):

$$[H^+] = [H^+]_{SS}(1 - e^{-\frac{t}{\tau}})$$
 (4.1)

where  $[H^+]$  is the acid concentration at time t,  $[H^+]_{SS}$  is the steady-state acid concentration in the film after exposure,  $\tau$  is the time constant associated with a specific lamp intensity ( $\tau$  will decrease as the intensity is increased), and t is the time of exposure. By calibrating the fluorescence response of the probe molecule with standard solutions, it will be possible to measure the concentration of photoacid present in the film as a function of time or exposure dose.

## 4.3.4. Acid-sensitivity of crystal violet

Crystal violet is a triphenylmethane dye that has been used widely as an indicator in acid/base titrations, especially in nonaqueous solvent systems.<sup>10</sup> The native form of crystal violet (CV<sup>+</sup>) is violet in color. Monoprotonation to produce HCV<sup>2+</sup> yields a green solution and further protonation to H<sub>2</sub>CV<sup>3+</sup> produces a yellow solution. The protonation of the amine groups on the phenyl rings is thought by Tuthill *et al.* to be responsible for the changes in the steady-state absorption spectroscopy of this molecule.<sup>7</sup> The three protonated forms of crystal violet and their equilibria are shown in Figure 4.8. The endpoints and transition points of crystal violet are difficult to differentiate, because of the similarity of the K<sub>2</sub> values for the different forms, which are discussed below.

Figure 4.9 shows the absorption spectrum of 1 wt.% crystal violet in Apex-E 2408 DUV photoresist spin coated onto a glass slide. The fluorescence emission of this sample was not detectable using the Aminco-Bowman spectrometer; however, it was possible to collect this information using an Ocean Optics SD2000 fiber optic spectrometer (Dunedin, FL). The sample was excited using all lines from an air-cooled argon ion laser (Omnichrome, Chino, CA), and the fluorescence emission spectrum was obtained via a fiber optic positioned at a 45° angle to the sample. This fluorescence information was then routed to the Ocean Optic spectrometer and is also displayed in Figure 4.9. From these spectra, it is evident that the optical response of crystal violet is in the spectral window not occupied by the photoresist itself.

In order to verify the acid-sensitive fluorescence of crystal violet, preliminary studies were first done in bulk solution. The emission spectra of crystal violet in acidic and basic water were collected using the Ocean Optic spectrometer. Figure 4.10 shows

that the acid-sensitive response is characterized by a blue-shift in the absorption and fluorescence emission.

# 4.3.5. Study of photoacid concentration during processing in photoresist films using steady-state absorption

The various forms of crystal violet in solution were characterized through the use of buffered pH systems, ranging from pH~5 to pH~0 (corresponding to an acid concentration range of ~10<sup>-5</sup> M to ~1 M). The changes in the absorption spectra as a function of acid concentration are presented in Figure 4.11, and these results are applicable to the resist films as well. The native, deprotonated, form of CV<sup>+</sup> absorbs strongly at 590 nm. As the pH decreases, the onset of a new absorption band centered near 630 nm, simultaneous with the decrease in absorbance at 590 nm, is observed. This spectral change is the result of protonation to form HCV<sup>2+</sup>. Additional protonation produces an absorption band at ~430 nm at the expense of the 630 nm and 590 nm bands. The equilibria among these three species of crystal violet may be described as:

$$H_2CV^{3+} \leftarrow \stackrel{K_1}{\longleftarrow} HCV^{2+} + H^+ \leftarrow \stackrel{K_2}{\longleftarrow} CV^+ + H^+$$
 (4.2)

resulting in the following expressions for the two equilibrium constants:

$$K_1 = \frac{[HCV^{2+}][H^+]}{[H_2CV^{3+}]}$$
 (4.3)

$$K_2 = \frac{[CV^+][H^+]}{[HCV^{2+}]}$$
 (4.4)

From these data, the constants for the protonation/deprotonation equilibria can be determined by applying Beer's law to the solutions and reduction of the data through a series of simultaneous equations for each pH. The molar absorptivities at each

wavelength for each species are available in the literature.<sup>11</sup> At a given pH, solution absorption was determined at 430 nm, 590 nm and 630 nm, leading to the concentrations of each form (see section A.1 in the Appendix for the derivation). The species concentrations were then used to calculate values for the equilibrium constants  $K_1$  and  $K_2$ .  $K_1$  was determined to be  $(2.5 \pm 1.5) \times 10^{-2}$  moles/L, and  $K_2$  was determined to be  $(6.7 \pm 2.5) \times 10^{-3}$  moles/L. These values correspond to pK<sub>1</sub> = 1.67 ± 0.29 and pK<sub>2</sub> = 2.20 ± 0.19. The first pK<sub>4</sub> for another triphenylmethane dye, malachite green, which differs from crystal violet by the absence of one dimethylamino group from a phenyl ring, was determined to be  $\sim 1.3$ , <sup>10</sup> in reasonable agreement with the data. These equilibria constants were then used to calculate alpha values for each crystal violet species, which in turn enable the determination of the acid concentration in the photoresist given an absorption spectrum of crystal violet in that medium (see section A.2 in the Appendix for the derivation).

The changes in the steady state absorption response of crystal violet doped in a polymer film were examined as a function of processing, and these data are presented in Figure 4.12. An absorption spectrum taken just after spin coating shows the native, deprotonated form of crystal violet with an absorption maximum at 590 nm. After exposure of the film and subsequent post exposure bake, a decrease in absorption at 590 nm and an increase in the intensities of the 630-nm and 430-nm bands were observed. This change is due to the protonation of crystal violet to both the monoprotonated and diprotonated forms in response to the photo-generated acid. Re-examination of the film several hours after post-exposure bake shows a change in the crystal violet absorption spectrum. The 430-nm band (H<sub>2</sub>CV<sup>3+</sup>) has decreased, and the 630-nm band (HCV<sup>2+</sup>) has

increased, indicative of a decrease in the extent of crystal violet protonation due to photoacid diffusion and/or consumption in the film. One possible mechanism for proton loss is long-term exposure of the film to air-borne amines. <sup>12,13</sup> Thus, steady-state absorption spectroscopy provides a facile means to quantify the photoacid production and consumption as a function of processing.

# 4.3.6. Effect of probe presence on photoacid concentration during processing in photoresist films using steady-state absorption

One of the concerns initially listed for the probe molecules was to be able to account for the effect of its presence upon the reaction occurring in the resist. One way to ascertain the effect of the probe upon deprotection efficiency is to monitor the steady-state absorption of the photoresist film during processing.

The absorption spectrum of Apex-E 2408 DUV photoresist is shown in Figure 4.2. There are two features of note: one peak between 200 and 250 nm and another between 250 and 300 nm. The first peak is characteristic of propylene glycol methyl ether acetate (PGMEA), used as the solvent in the resist formulation; the second peak is characteristic of poly(p-t-butoxycarbonyloxystyrene)-co-poly(vinyl phenol). It is this second peak that exhibits a change in intensity with deprotection. As the acid diffuses through the film during postexposure bake, the intensity at 278 nm increases due to the cleavage of the pendant groups, which converts the t-butoxycarbonyl (TBOC) portions of the copolymer to vinyl phenol groups. When crystal violet is introduced into the resist formulation, some of the acid generated upon exposure is taken up by this dye to produce the spectral shift that monitors acid concentration. This reduces the number of deprotection events so that the increase in intensity at 278 nm is not as high as in the neat

resist. A comparison of the absorption spectra for the neat and doped photoresist as a function of film processing is shown in Figure 4.13.

A series of experiments was carried out to estimate the effect of crystal violet upon the extent of deprotection in the resist. Apex-E 2408 DUV photoresist was doped with 0.1, 0.2 and 0.3 wt.% crystal violet. Neat and doped samples were spin coated onto clean quartz slides at 3000 rpm to produce a thin film. An absorption spectrum of each sample was collected after spin coating using the Hewlett Packard 8452A diode array spectrophotometer. Then the samples underwent post-application bake (PAB) for 60 seconds at 90°C, exposure with a 200 W Hg(Xe) lamp (Oriel Corporation, Stratford, CT) for 30 seconds, and post-exposure bake (PEB) for 90 seconds at 90°C. An absorption spectrum of the samples was also taken after each of these processing steps.

The absorbance intensity at 278 nm for each sample after processing step was ratioed against the absorbance intensity at 278 nm for the respective sample taken after spin coating. This information is presented below in Table 4.1. No significant change attributed to the deprotection reaction was noted until after PEB. This is to be expected since the acid is generated by exposure but does not start diffusing and reacting significantly until the temperature is elevated during PEB. As the concentration of crystal violet increased, the deprotection reaction efficiency decreased as predicted. This efficiency was estimated as follows:

% efficiency = 
$$\frac{I_{\text{doped, PEB}} - I_{\text{doped, spin}}}{I_{\text{neat, PEB}} - I_{\text{neat, spin}}} \times 100\%$$
(4.5)

where I is the absorbance intensity ratio at 278 nm for the specified sample (neat or doped with crystal violet) at the specified processing step (after spin coating or after

PEB). This assumes that the neat samples are 100% deprotected, which is a good approximation in this case where the slides are "overexposed."

Table 4.1. Comparison of the absorbance ratio at 278 nm for the neat Apex-E 2408 DUV photoresist film to that of the crystal violet doped films during various stages of processing.

	Absorbance Ratio During Film Processing				
Photoresist Sample	After PAB	After exposure	After PEB	% efficiency deprotection	
Neat	0.969±0.009	0.986±0.011	1.137±0.013	100	
0.1 wt.% CV	0.976±0.007	0.991±0.007	1.108±0.008	78	
0.2 wt.% CV	0.973±0.001	0.989±0.001	1.037±0.006	27	
0.3 wt.% CV	0.971±0.003	0.983±0.003	0.986±0.004	0	

Thus, it is important to avoid too high a concentration of crystal violet in the photoresist, else the entire population of photoacid will be sampled by the probe molecule such that none will be left for the deprotection events. A concentration of 0.1 wt.% crystal violet in the photoresist film is an acceptable compromise for the major monitoring concerns. Over 75% of the photoacid continues deprotecting during PEB, and the sensitivity of the probe molecule is not compromised (*i.e.*, the absorption spectra of the crystal violet registers the same acid sensitivity as seen in the 0.3 wt.% crystal violet case) or lost below the detection limits of the spectrometer.

#### 4.4. CONCLUSION

Spectroscopic techniques have been developed to characterize acid concentration and mobility in chemically amplified resists during the exposure and post exposure bake. Steady-state fluorescence of fluorescein is used to characterize the acid build-up during exposure *in situ*. The acid-sensitive response was characterized by ratioing the intensities of two interdependent peaks. By using this ratioing method, rather than absolute

intensities, the measurements are independent of detector settings, scattered and background light, or small changes in fluorescein concentration (such as that caused by photobleaching). Secondly, crystal violet is used to characterize the acid concentration in the photoresist during post exposure bake. The absorption spectrum of crystal violet exhibits three bands that each corresponds to a different protonated form. Therefore, the shape of the absorption spectrum depends upon the local acid concentration, and this dependence has been demonstrated both in aqueous solution and in polymer photoresist films. These data are consistent with relatively high local proton concentrations in the resist films subsequent to UV irradiation. The development of these experimental techniques can then be used for a systematic study of acid concentration in situ during the exposure and post exposure bake. For a given resist, a more thorough understanding of the factors that affect acid concentration (e.g., post exposure bake temperature and duration) can allow improved microlithographic pattern generation. In addition, this information could be used for the development and optimization of new CARs designed to control the mobility of the acid.

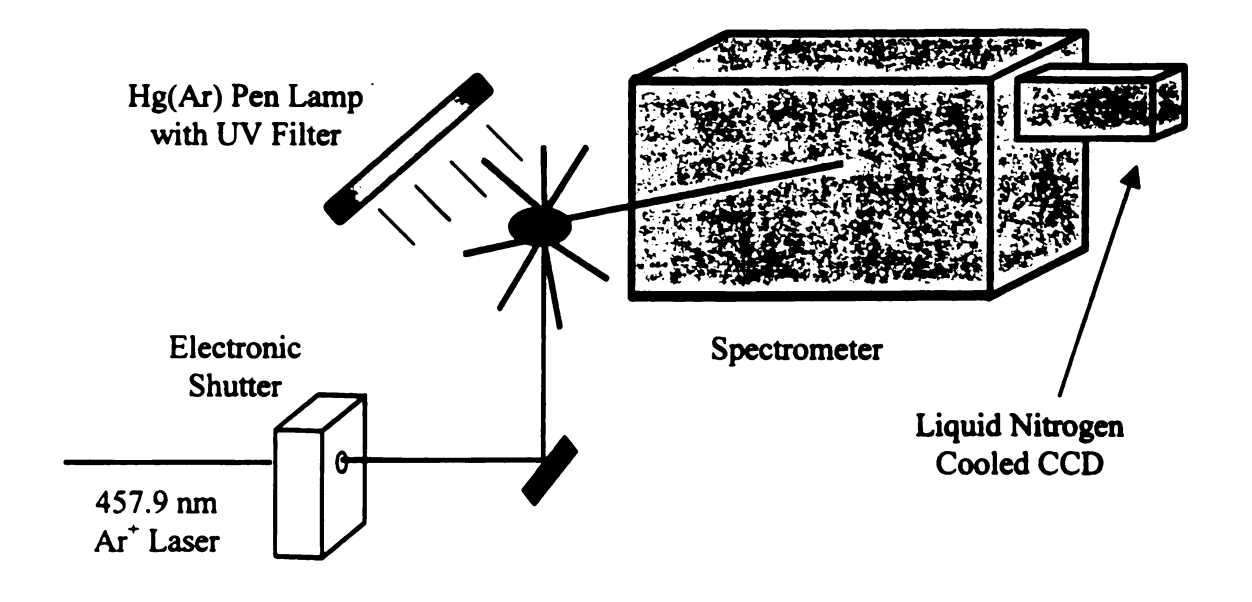


Figure 4.1. Experimental setup for *in-situ* fluorescence experiments to determine photoacid generation during exposure.

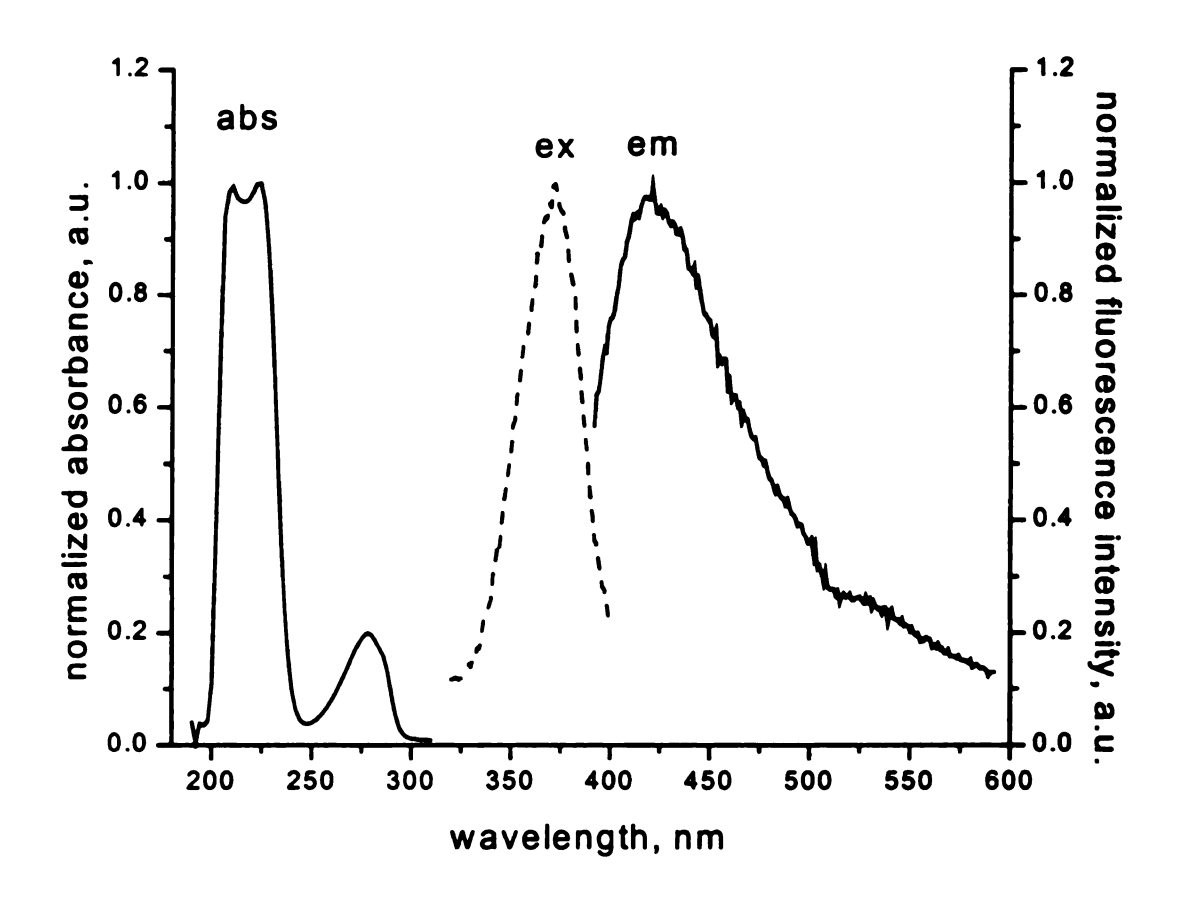


Figure 4.2. Absorption (abs), excitation (ex) and emission (em) characteristics of Apex-E 2408 DUV photoresist.

77

Figure 4.3. Molecular structure of fluorescein.

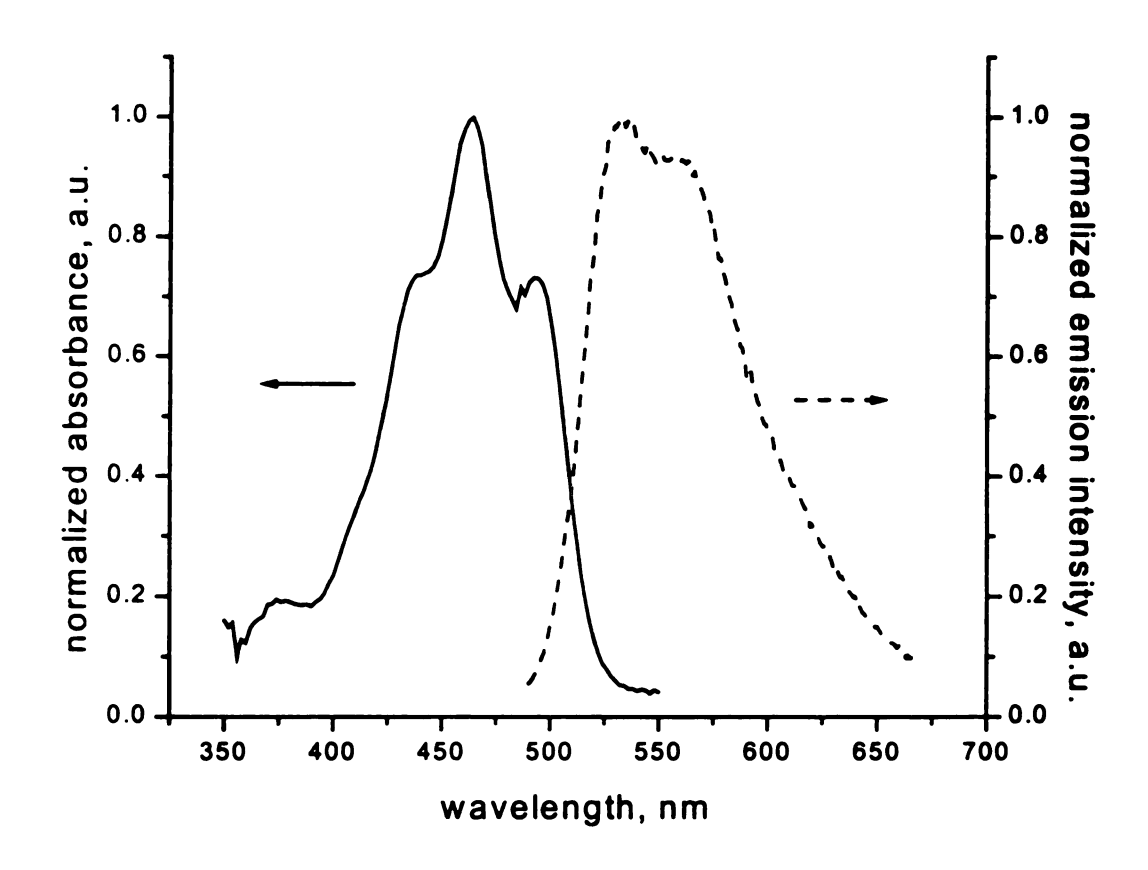


Figure 4.4. Absorption and emission characteristics of fluorescein in Apex-E 2408 DUV photoresist.

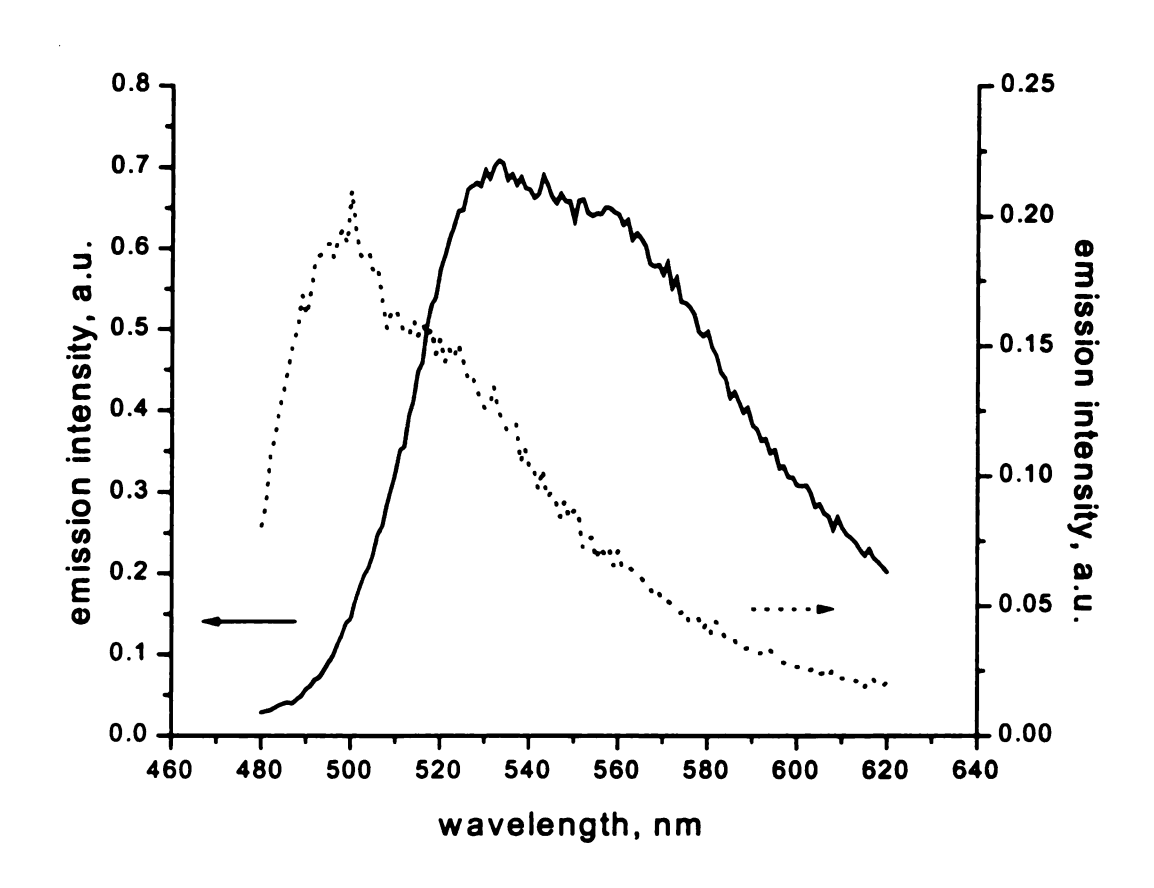


Figure 4.5. Change in fluorescein fluorescence emission in Apex-E 2408 DUV photoresist upon addition of sulfuric acid: before acid addition (—) and after acid addition (…).

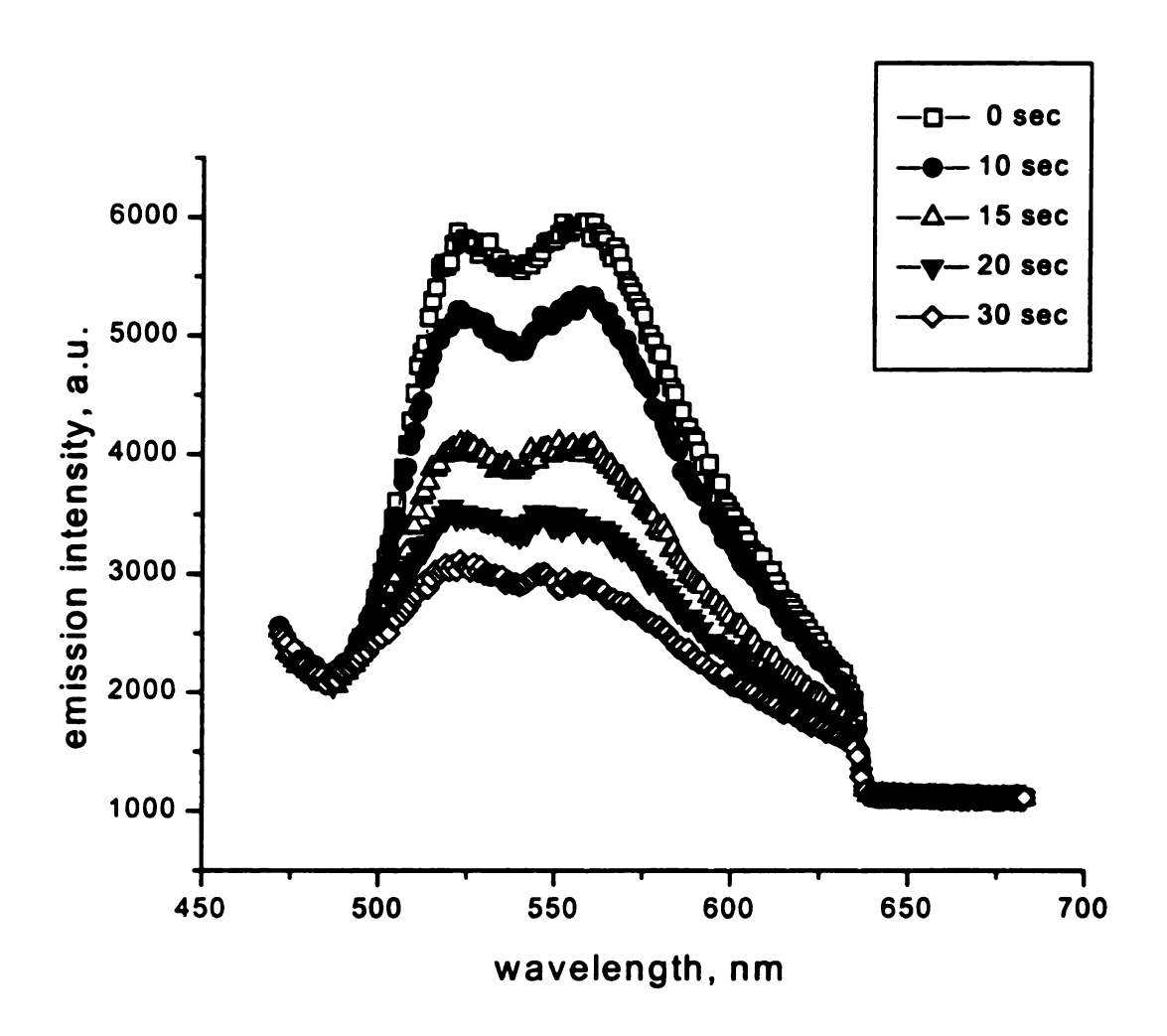


Figure 4.6. Fluorescence spectra of fluorescein in Apex-E 2408 DUV photoresist film as a function of increased exposure time.

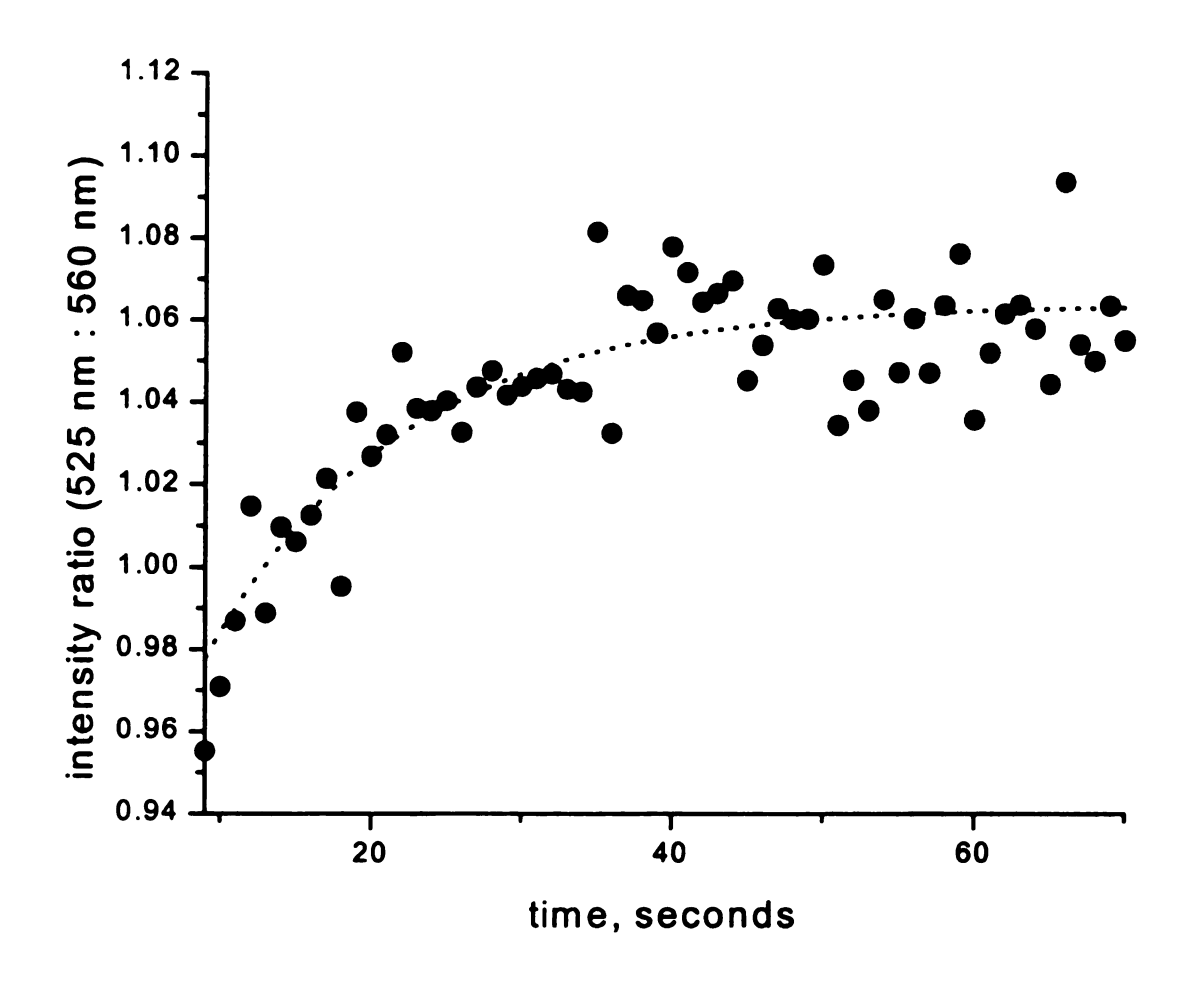


Figure 4.7. Intensity ratio at 525 nm and 560 nm of fluorescein in Apex-E 2408 DUV photoresist film as a function of increased exposure time.

Figure 4.8. Protonation/deprotonation equilibria for crystal violet. The corresponding spectra are shown in Figure 4.11.

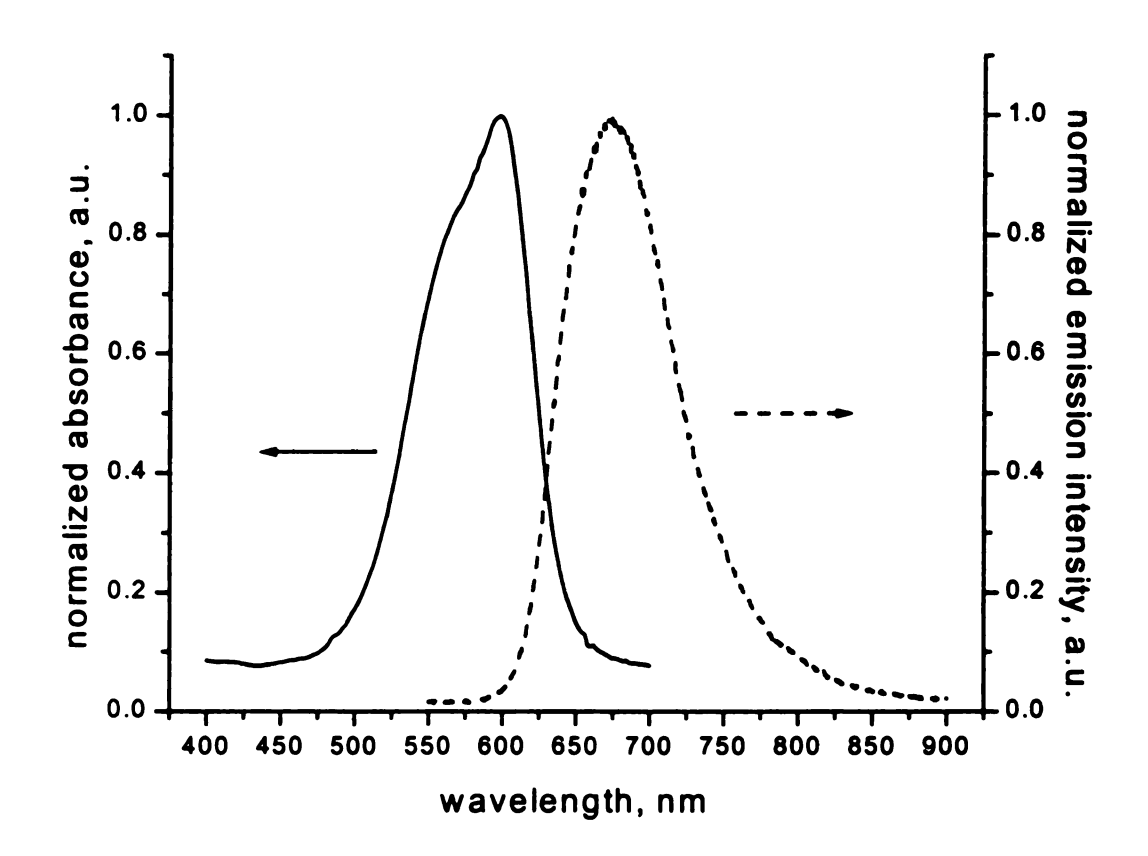
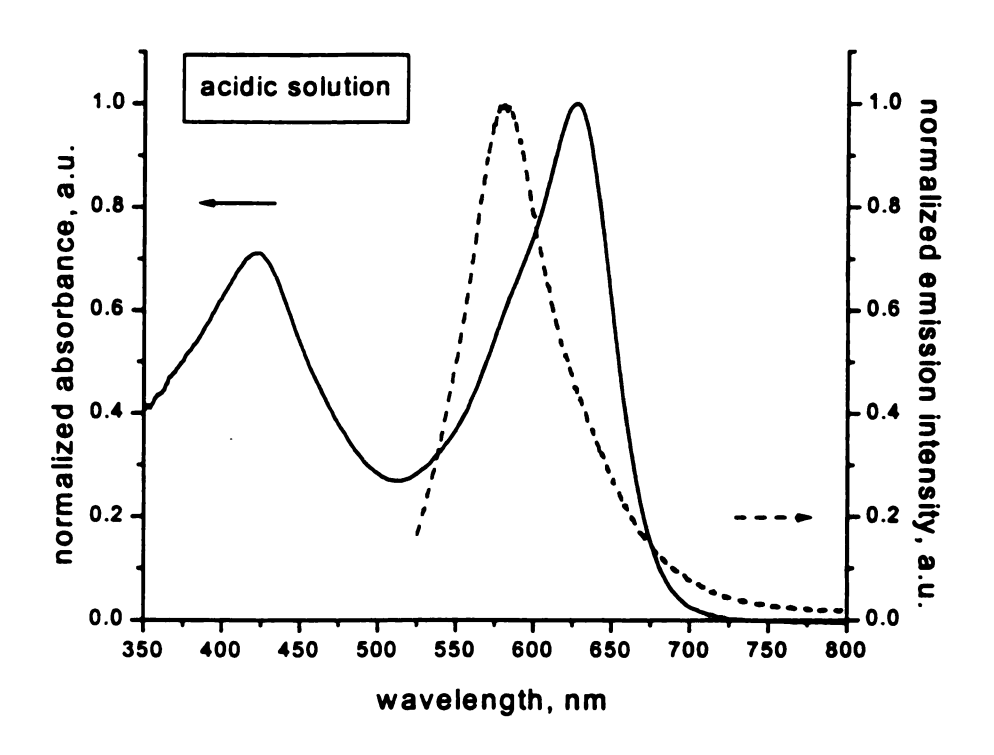


Figure 4.9. Absorption and emission characteristics of crystal violet in Apex-E 2408 DUV photoresist.



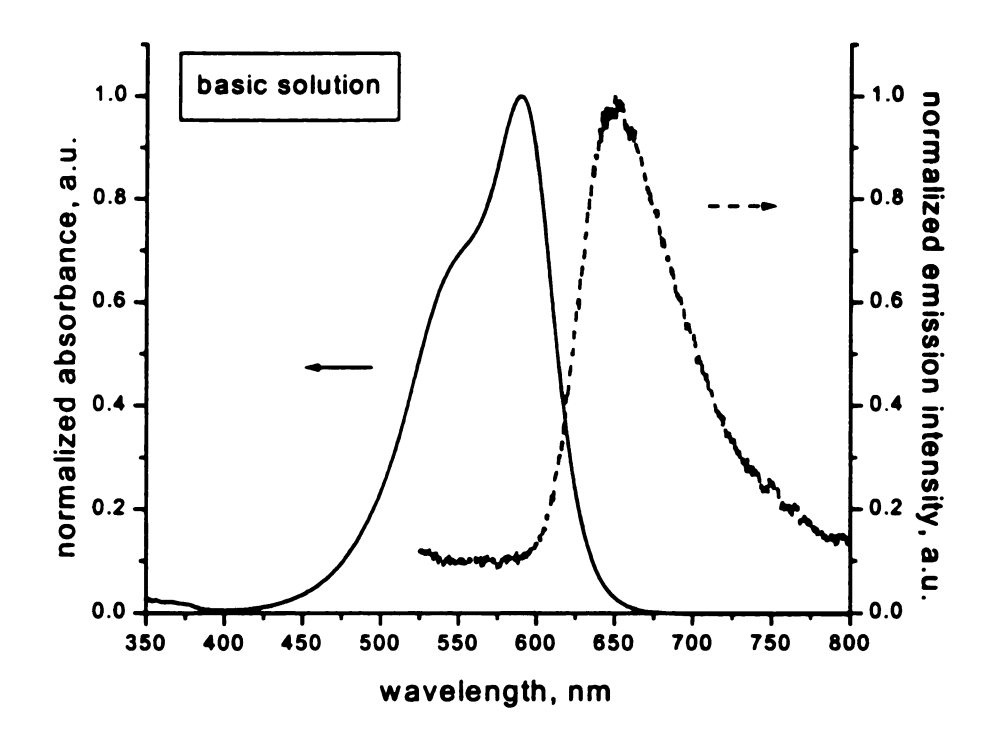


Figure 4.10. Absorption and emission characteristics of crystal violet in bulk acidic (top) and basic (bottom) solutions.

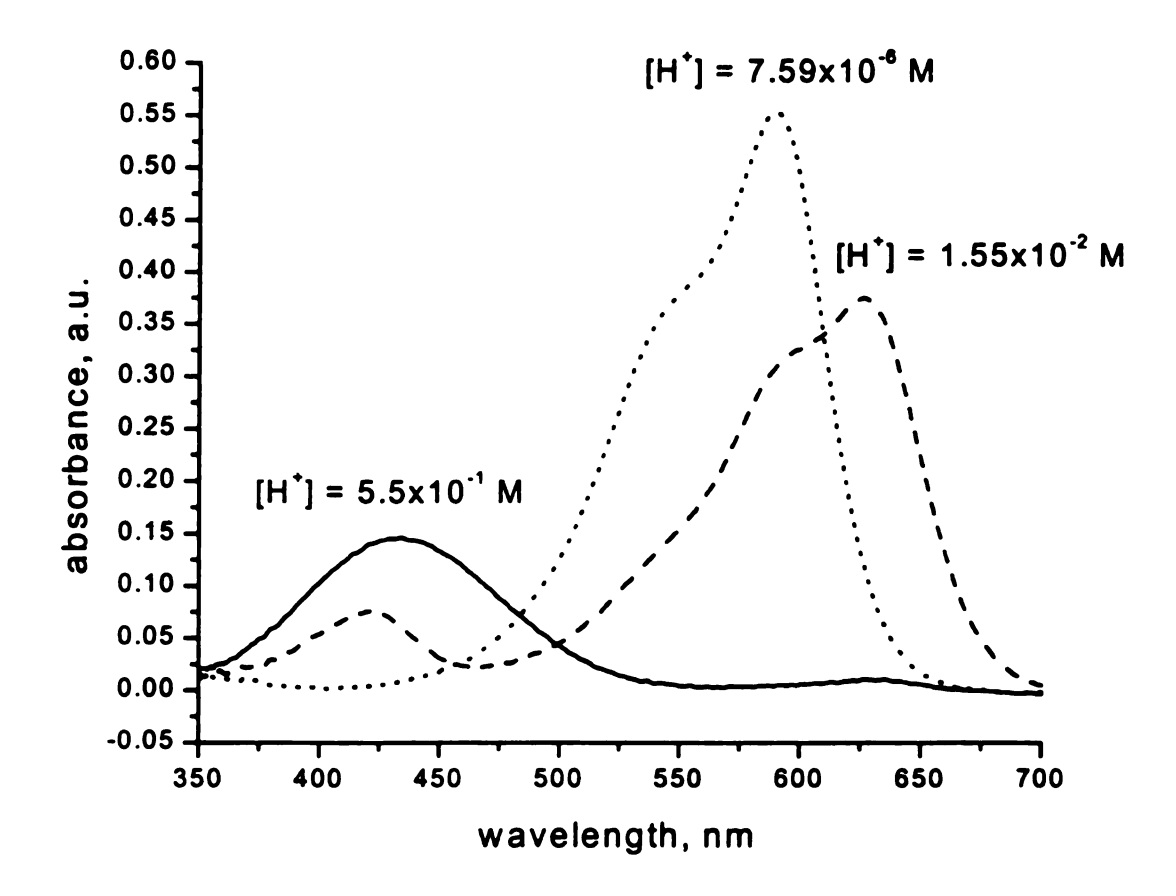


Figure 4.11. Absorption spectra of crystal violet in aqueous solution. [H<sup>+</sup>] for the solution spectra are indicated on the plot.

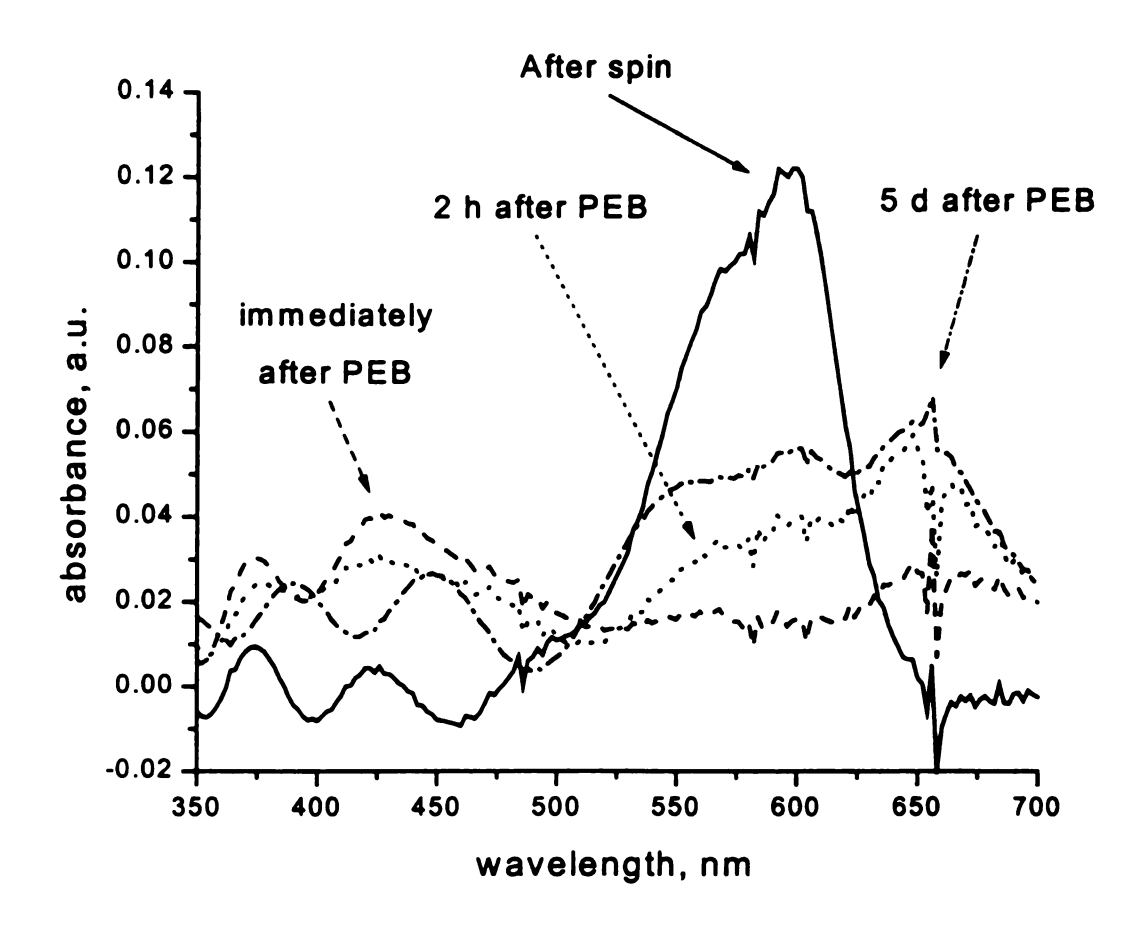
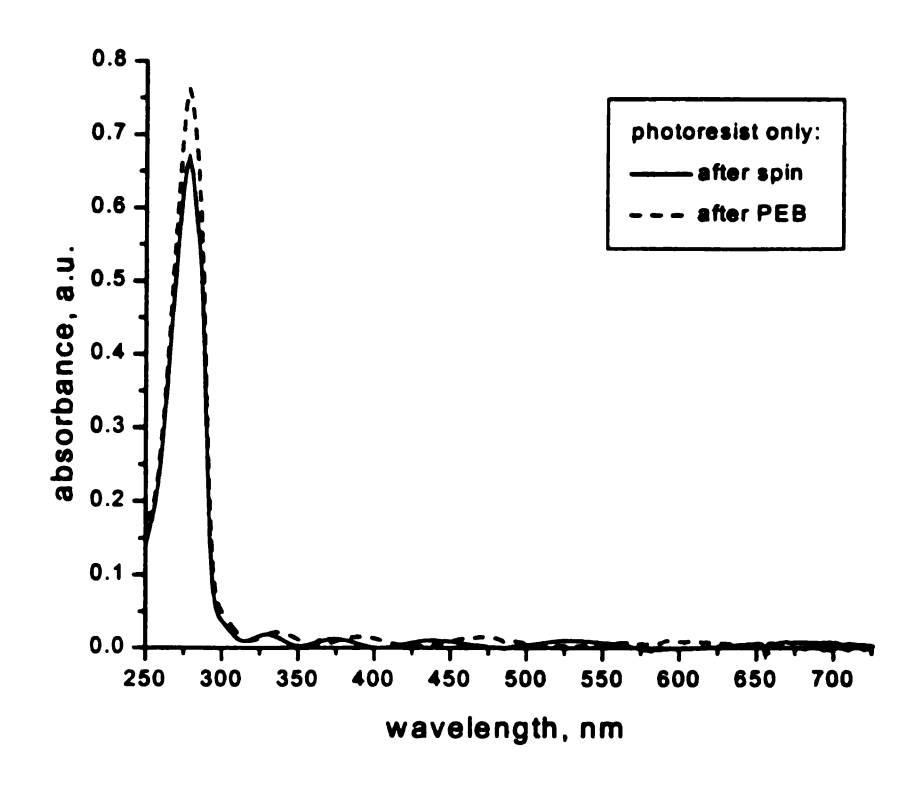


Figure 4.12. Absorption spectra of crystal violet in Apex-E 2408 DUV photoresist film during and after processing.



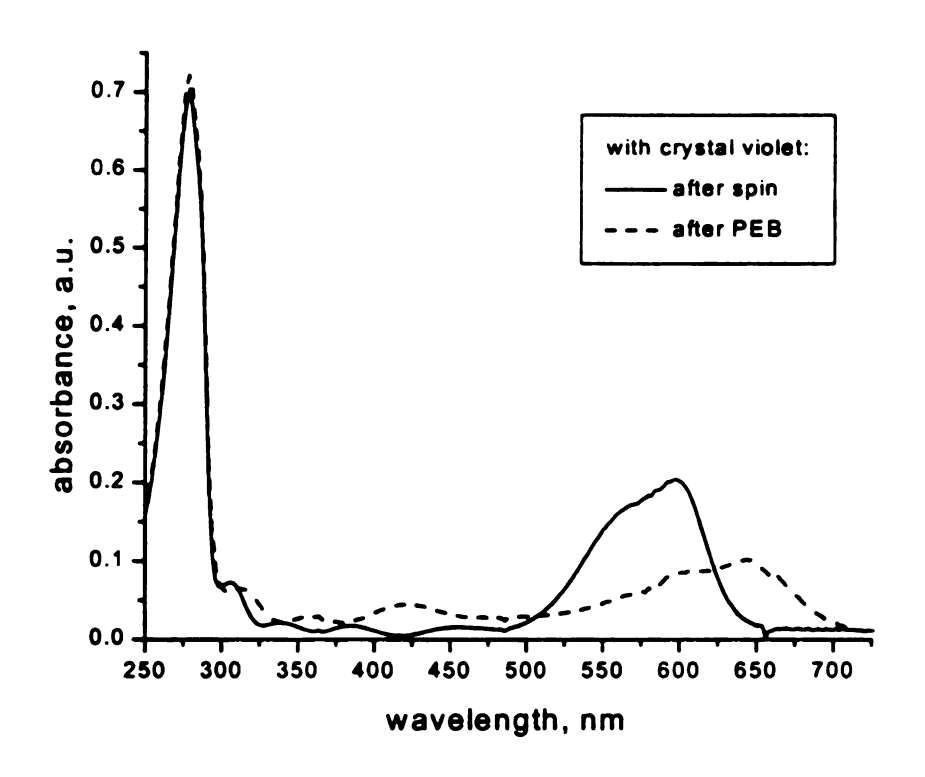


Figure 4.13. Effect of 0.3 wt.% crystal violet in Apex-E 2408 DUV photoresist film upon the absorbance spectrum before and after processing.

#### 4.5. REFERENCES

- 1. R.P. Haugland, *Handbook of Fluorescent Probes and Research Chemicals*, 6<sup>th</sup> ed., edited by M.T.Z. Spence and I.D. Johnson, Molecular Probes, Inc.: USA, 1996.
- 2. J. Slavik, Fluorescent Probes in Cellular and Molecular Biology, CRC Press, Inc.: Ann Arbor, 1994.
- 3. G. Pohlers, J.C. Scaiano, and R. Sinta, "A Novel Photometric Method for the Determination of Photoacid Generation Efficiencies Using Benzothiazole and Xanthene Dyes as Acid Sensors," *Chem. Mater.*, 9, 3222 (1997).
- 4. G. Pohlers, S. Virdee, J.C. Scaiano, and R. Sinta, "Aromatic Monoazines as Fluorescent Sensors for Photoacid Generation in Thin Polymer Films," *Chem. Mater.*, 8, 2654 (1996).
- 5. P.M. Dentinger, B. Lu, J.W. Taylor, S.J. Bukofsky, G.D. Feke, D. Hessman, and R.D. Grober, "On-wafer photoacid determination and imaging technique for chemically amplified photoresists," J. Vac. Sci. Technol. B, 16(6), 3767 (1998).
- 6. U. Okoroanyanwu, J.D. Byers, T. Cao, S.E. Webber, and C.G. Willson, "Deprotection Kinetics of Alicyclic Polymer Resist Systems Designed for ArF (193 nm) Lithography," *Micro and Nano-patterning Polymers*, edited by H. Ito, E. Reichmanis, O. Nalamasu, and Y. Ueno, American Chemical Society, Washington, D.C., 1998.
- 7. S. M., Tuthill, O. W. Kolling, K. H. Roberts, "Photometric and visual titration of certain alkaloids in glacial acetic acid using malachite green as indicator," *Anal. Chem.*, 32, 1678 (1960).
- 8. M.M. Martin and L. Lindqvist, "The pH Dependence of Fluorescein Fluorescence," J. Luminescence, 10, 381 (1975).
- 9. H. Leonhardt, L. Gordon, and R. Livingston, "Acid-Base Equilibria of Fluorescein and 2',7'-Dichlorofluorescein in Their Ground and Fluorescent States," J. Phys. Chem., 75(2), 245 (1971).
- 10. E. Bishop, "Indicators for Non-Aqueous Acid-Base Titrations," *Indicators*, edited by E. Bishop, Pergamon, New York, 1972.
- 11. J. B. Conant, T. H. Werner, "The determination of the strength of weak bases and pseudo bases in glacial acetic acid solutions," J. Am. Chem. Soc., 52, 4436 (1930).

- 12. C.A. Mack, "Lithographic Effects of Acid Diffusion in Chemically Amplified Resists," *Microelectronics Technology: Polymers for Advanced Imaging and Packaging*, edited by E. Reischmanis, C.K. Ober, S.A. MacDonald, T. Iwayanagi, and T. Nishikubo, American Chemical Society, Washington, D.C., 1995.
- 13. L.F. Thompson, "Resist Processing," *Introduction to Microlithography*, 2<sup>nd</sup> ed., edited by L.F. Thompson, C.G. Wilson, M.J. Bowden, American Chemical Society, Washington, D.C., 1994.

# Chapter 5

## FREE VOLUME IN CHEMICALLY AMPLIFIED PHOTORESISTS

#### 5.1. INTRODUCTION

As discussed in Chapter 1, in order to predict adequately the behavior of chemically amplified photoresist, it is crucial to understand and characterize the mobility of the photo-induced acid that provides the sensitivity to pattern development on semiconductor substrates. A portion of this task is being able to quantify the acid concentration during processing, which was addressed in the previous chapter. The other portion is to determine the effect or impact of available free volume upon the diffusional mobility of the photoacid during post exposure bake. First of all, free volume increases with the higher temperature of the bake, thus increasing the diffusivity of the photoacid according to the following relationship:

$$D(T) = D_0 \exp\left(\frac{-E_d}{RT}\right)$$
 (5.1)

where D is the diffusivity,  $D_0$  is a reference diffusivity,  $E_d$  is the activation energy for diffusion, R is the gas constant, and T is the absolute temperature. In addition, there is "chemically produced" free volume arising from the deprotection reaction, which liberates carbon dioxide and isobutylene. These small molecules diffuse out of the film relatively rapidly (the characteristic time for diffusion through the one micron film is on the order of a second), creating free volume that is transient in nature. This "transient" free volume is eliminated by the relaxation of the polymer chains, leading to a decrease in the thickness of the film. In general, free volume provides the acid greater mobility and

freedom to attack the next available pendant TBOC group. Thus, diffusion of the photoacid should be greater as the number of deprotection reactions increases. Recently, Jakatdar *et al.* have developed a model to correlate the deprotection-induced thickness loss of the photoresist film as a function of post exposure bake; however, no research has been undertaken to understand the correlation between the free volume in the photoresist films and the photoacid diffusional mobility.

## 5.1.1. Utility of molecular probes

In addition to measuring the concentration of acid as discussed in the previous chapter, fluorescence can be used to probe the local environment of the system. There are a number of probe molecules that exhibit an increase in the fluorescence signal and excited-state lifetime as the local viscosity is increased. As the molecular rotations become hindered, non-radiative pathways for energy transfer are less efficient; therefore, more of the excited state energy must be dispelled through radiative (fluorescent) pathways. Other free volume sensitive probes are based upon photoisomerization and intramolecular excimer formation. With a small amount of a viscosity-sensitive molecule, the micro-viscosity or free volume of the system can be measured. Many researchers have exploited this technique to gather such information in polymer systems. For example, Francis Wang et al. have used 1,3-bis-(1-pyrene) (BPP) to monitor the polymerization of methyl methacrylate in situ.<sup>3</sup> Moorjani and coworkers further demonstrated the utility of fluorescence monitoring when dealing with diffusioncontrolled reactions in media of different viscosity. Victor and Torkelson have also used molecular probes to measure the free volume available in polymer structures.<sup>5</sup>

### 5.2.1. Studies of free volume evolution in CARs

In this chapter, spectroscopic techniques are identified that may be used to characterize acid mobility in chemically amplified resists during the post exposure bake steps. To measure the free volume changes during post exposure bake, ground-state recovery measurements were used to characterize the excited-state lifetime of crystal violet. As is shown below, the lifetimes of the excited state for this triphenylmethane "propeller" molecule increase as the local free volume decreases, and molecular rotation is hindered. In addition, the effects of the post exposure bake time upon the overall film thickness and macroscopic free volume were investigated using dynamic film thickness measurements.

#### 5.2. EXPERIMENTAL

#### 5.2.1. Materials

These studies were performed using a commercial photoresist, Apex-E 2408 DUV (Shipley Company, Marlborough, MA). The dye crystal violet (Sigma Chemical Company, St. Louis, MO) exhibits a sensitivity to free volume in its excited state lifetime. It was used to determine free volume generation during PEB using ground state recovery measurements. All chemicals were used as received.

#### 5.2.2. Methods

# 5.2.2.1. Ground-state recovery measurements with photoresist films during processing

The picosecond pump-probe laser spectrometer<sup>6</sup> used for the ground-state recovery measurements is shown in Figure 5.1. In these experiments, a mode-locked CW Nd:YAG laser (Coherent Antares 76-S) produces 30 W of average power (1064 nm, 100 ps pulses, 76 MHz repetition rate). The output of this laser is frequency-doubled to

produce ~2.1 W of average power at 532 nm. The second harmonic light is used to excite two cavity-dumped dye lasers synchronously (Coherent 702-3). Both lasers operate with Rhodamine 6G laser dye (Kodak). The output of each laser is ~100 mW average power at 8 MHz repetition rate with a pulse that produces a 7 ps FWHM autocorrelation trace using a three plate birefringent filter. The pump laser wavelength was set to 589.5 nm, coincident with the absorption maximum of the first singlet transition of crystal violet. The probe wavelength was chosen to lie within the absorption band of crystal violet. The probe beam was polarized at 54.7° with respect to the pump beam to eliminate molecular reorientation contributions to the signal. The time resolution of this system, ~10 ps, is determined by the cross-correlation between the pump and probe laser pulse trains. Detection of the transient signals was accomplished using a radio and audio frequency triple-modulation scheme, with synchronous demodulation detection. The probe time constant is the average of at least five individual determinations that are themselves the average of seven to ten time-scans.

Samples for these experiments were prepared in the following manner. Resist solution with 0.1 wt.% crystal violet was spin coated at 2000 rpm onto quartz slides and processed according to standard procedures. One set of samples experienced no processing subsequent to spin coating, while a second set of samples was processed through the post-exposure bake. The samples were mounted in a manually driven translation stage and the two laser beams were co-focused on them. To minimize the effects of photobleaching and thermal degradation, the slide was translated as the sample was scanned, and neutral density filters were used to attenuate the incident light.

## 5.2.2.2. Multi-wavelength interferometry

Multi-wavelength interferometry was performed using the Inspector Model 800 (SC Technology, Fremont, CA). The instrument was used to observe changes in the macroscopic free volume of the photoresist as the deprotection reaction occurs. Multi-wavelength interferometry is used to determine film thickness in semi-transparent films by measuring the interference between reflections of incident light from the film top surface and from the film interface with the substrate, in this case the quartz slide. A generalized schematic of this method is shown in Figure 5.2. Thus, small changes in the film thickness due to the effects of the deprotection reaction can be recorded. In these experiments, the time-evolution of the free volume (averaged over the area illuminated by the optical fiber probe) was characterized by continuously monitoring the resist film thickness during the post exposure bake.

The instrument was calibrated in the reflectance mode using a clean quartz slide. Film thickness measurements were calculated using the Prolight data acquisition package with the LithoPak applications module, which accompanies the Inspector Model 800, and the Cauchy coefficients provided by the Shipley Company in the technical data sheet for the photoresist. Samples for these experiments were prepared by spin coating the neat photoresist at 3000 rpm onto quartz slides and by processing with a post application bake for 60 seconds at 100°C, an exposure time for 60 seconds under a 200 W Hg(Xe) lamp (Oriel Corporation, Stratford, CT), and a post exposure bake for 90 seconds at 100°C. A second set of samples were prepared as controls to which all processing steps, save exposure, were applied.

#### **5.3. RESULTS AND DISCUSSION**

# 5.3.1. Study of microscopic free volume changes in photoresist films using groundstate recovery

Crystal violet is a member of the triphenylmethane dye family, with three identical N,N-dimethylaniline rings bound to a central carbon atom. The structure of crystal violet is presented in Figure 5.3. The predominant conformation of crystal violet in solution is a propeller shape, having D<sub>3</sub> symmetry, with each of the three phenyl rings tilted slightly out of the molecular plane. The phenyl rings rotate around their bonds to the central carbon atom in what is believed to be a barrierless process. Ring rotation along the excited state potential energy surface provides access to efficient non-radiative decay channels. Studies have indicated a strong dependence of the excited state lifetime on solvent viscosity, which is indicative of essentially no intramolecular rotational barrier to ring rotation. Crystal violet was chosen as a probe of the local environment in the photoresist thin films under examination here because of its combined sensitivity to local acid concentration and viscosity.

The recovery time of the ground-state population of crystal violet is measured instead of its fluorescence lifetime because of the characteristically low fluorescence quantum yield of this family of molecules. The ground-state recovery measurement is equivalent to a fluorescence lifetime measurement for the triphenylmethanes. The ground state recovery measurement is accomplished by detecting the transient change in absorption of the probe pulse resulting from excitation by the pump laser pulse (Figure 5.4). The difference in arrival time at the sample between the pump pulse and the probe pulse is controlled mechanically.

An exponential decay of the ground-state recovery signal for the spin coated, doped resist film is observed, and these data are shown in Figure 5.5. A fit of the decay to a sum of two exponentials results in a 25-ps time component and a 120-ps time component. The behavior observed is similar to fluorescence decay experiments using malachite green, another triphenylmethane dye at similar temperatures in highly viscous systems. 12,13 A double exponential decay has also been observed for the ground state absorption recovery behavior of malachite green in a solid SiO<sub>2</sub>-ZrO<sub>2</sub> matrix<sup>14</sup> and in polymethyl methacrylate (PMMA) and polyvinyl alcohol (PVA) films. 15,16 Therefore, the observation of two exponential decay components for a triphenylmethane dye is not new, although there is an ongoing debate in the literature over its physical origin. Nonethe-less, there is a well-established relationship between the values of both decay time constants and the local viscosity of the medium, with the constants increasing with increasing microviscosity. The values of the two time constants observed here are similar to the time constants obtained by Ben-Amotz and Harris, 10 Canva et al. 14 and Ippen, Shank and Bergman.<sup>17</sup>

A linear calibration curve (quality of fit as reflected by the R<sup>2</sup> value was 0.98) was developed, shown in Figure 5.6, that relates the short time constant from the ground state recovery time of crystal violet in a series of viscous liquid to the matrix viscosity. The ground state recovery measurements were accomplished using the pump-probe laser configuration modified with a recirculating flow loop to accommodate the viscous liquid samples. The liquid was pumped through the coils of a temperature bath maintained at 300 K and into a 0.1-cm square flow cell. From the flow cell, the liquid entered a reservoir before repeating the pump cycle. The samples contained 0.1 wt.% crystal

violet. The viscosities of ethylene glycol and propylene glycol were acquired from the literature. <sup>18</sup> The viscosities for the remaining data points were measured using a Brookfield Model DV-I+ Viscometer (Brookfield Engineering Labs, Inc., Stoughton, MA). Due to the highly viscous nature of the liquids, it was necessary to use the small sample adapter with spindle #18 for the diols and spindle #34 for glycerol in order to obtain accurate readings.

The resist before exposure and post exposure bake exhibits free-volume characteristics similar to that of glycerol. A fit of the excited-state lifetime decay (a representative plot of which is shown in Figure 5.7) to a sum of two exponentials results in  $25 \pm 4$  ps for the short-time component ( $\tau_1$ ) and  $115 \pm 18$  ps for the long-time component ( $\tau_2$ ). Thus, the effective free volume of the photoresist in this stage of the processing is 141.0 cP. As free volume is created in the film during post exposure bake, a decrease in the ground-state recovery times of crystal violet due to the increased freedom available for its ring rotations is predicted. However, as that free volume collapses due to polymer relaxation, the time constants will increase as the ring rotations of the crystal violet embedded in the film are restricted.

### 5.3.2. Multi-wavelength interferometry

As mentioned at the start of this chapter, there is a change in film thickness associated with the post exposure bake. During the deprotection reaction, which mainly occurs during post exposure bake, two small molecules are created by the breakdown of the TBOC pendant group that is cleaved by the photoacid. These gas molecules, namely carbon dioxide and isobutylene, diffuse out of the film, thus creating free volume.

However, as the polymer chains relax, the film will collapse into itself and decrease the overall film thickness and the available microscopic free volume.

In order to differentiate between solvent volatilization and polymer relaxation, the film thickness behavior of the exposed photoresist samples was compared to those that had not undergone exposure. There is a definite difference in shape between the two thickness loss curves collected during the post (exposure) bake step, which confirms that the mechanism by which film reduction occurs is related to the deprotection reactions during post exposure bake. In the case of the control samples, which were not exposed, the film thickness reduction is best described by a linear fit (Figure 5.8, top). This profile is consistent with volatilization of solvent remaining in the film after the post application bake. In contrast, the film thickness reduction of the exposed samples is best described by a second-order exponential decay (Figure 5.8, bottom). This suggests that two mechanisms are occurring during post exposure bake: relaxation of the polymer chains facilitated by the evaporation of the gases produced during deprotection and volatilization of any remaining solvent.

This explanation for the decrease in film thickness during post exposure bake is further confirmed by examination of the diffusional properties for carbon dioxide and isobutylene. The diffusion coefficient of the small molecules in the thin film can be described using the Stokes-Einstein equation:<sup>19</sup>

$$D = \frac{kT}{6\pi nr}$$
 (5.2)

where k is the Boltzmann constant, T is the absolute temperature,  $\eta$  is the viscosity of the medium, and r is the radius of the diffusing molecule. For carbon dioxide, this radius is 0.165 nm; for isobutylene, this radius may be approximated using that of iso-butane,

which is 0.25 nm.<sup>20</sup> Thus, given a bake temperature of 100°C and an effective viscosity of 141 cP for the photoresist film initially, the diffusion coefficients for carbon dioxide and isobutylene are  $1.17 \times 10^{-7}$  cm<sup>2</sup>/s and  $7.8 \times 10^{-8}$  cm<sup>2</sup>/s, respectively. These diffusion coefficients can then be used to estimate a characteristic diffusion time ( $\tau$ ) using the following expression:

$$\tau = \frac{L^2}{D} \tag{5.3}$$

where L is the length for diffusion. In the case of the photoresist films, the longest vertical diffusion length is one micron. Therefore, the diffusion time for these small molecules is on the order of one second or less. With this time scale for diffusion, there is adequate time during the post exposure bake for the polymer chains to relax and fill the free volume created as the small molecules diffuse from the film.

In addition to the difference in film thickness loss profiles, there is a difference in the total thickness lost during the bake times for the two sample sets. With the unexposed samples, the thickness reduction observed was less than 1% of the total film thickness measured at the beginning of the bake time. For the exposed samples, the thickness reduction observed was greater than 3%. Thus, the greatest film thickness loss during post exposure bake is due to the polymer chain relaxation.

Similar studies, conducted at Advanced Micro Devices (Sunnyvale, CA), corroborate these results, as well as lend insight into the effect of bake time upon the thickness loss profile. Resist was spin coated onto silicon wafers, and each wafer was subdivided into a grid. Each grid section was exposed using a KrF excimer laser at a different dose. The wafers were then subjected to different post exposure bake times, and

the film thickness of each grid section was measured thereafter. In Figure 5.9, these data are shown for the Apex-E 2408 DUV photoresist at a bake temperature of 100°C. If the film does not undergo post exposure bake, the activation energy for deprotection is not realized; thus, no change in thickness is observed. At shorter post exposure bake times, less thickness loss occurs regardless of the exposure dose because there is not enough time for the photoacid to effect more deprotection events. As the post exposure bake time is increased, less energy expenditure is necessary to effect a higher number of deprotection reactions, as manifested by the steepness in the exponential curves. Similar trends are observed for a second Shipley resist, UV5-0.6 positive DUV photoresist, at a bake temperature of 130°C (Figure 5.10).

#### **5.4. CONCLUSIONS**

Spectroscopic techniques designed to characterize acid mobility in chemically amplified resists during post exposure bake have been developed. To measure the free volume changes during post exposure bake, ground-state recovery measurements using the triphenylmethane dye crystal violet as a molecular probe were used. The lifetimes of the excited state of crystal violet increase as the local free volume decreases and molecular rotation is hindered. Secondly, dynamic film thickness measurements were applied to understand the physical phenomena behind the thickness loss observed during post exposure bake. The results indicate that the majority of the thickness loss is due to the relaxation of polymer chains facilitated by the diffusion of gases out of the film after deprotection events take place and not due to volatilization of solvent. The further application of these experimental techniques will provide a systematic study of free volume evolution in situ during post exposure bake. For a given resist, a more thorough

understanding of the factors that affect free volume evolution and acid mobility (e.g., post exposure bake temperature and duration) can allow improved microlithographic pattern generation.

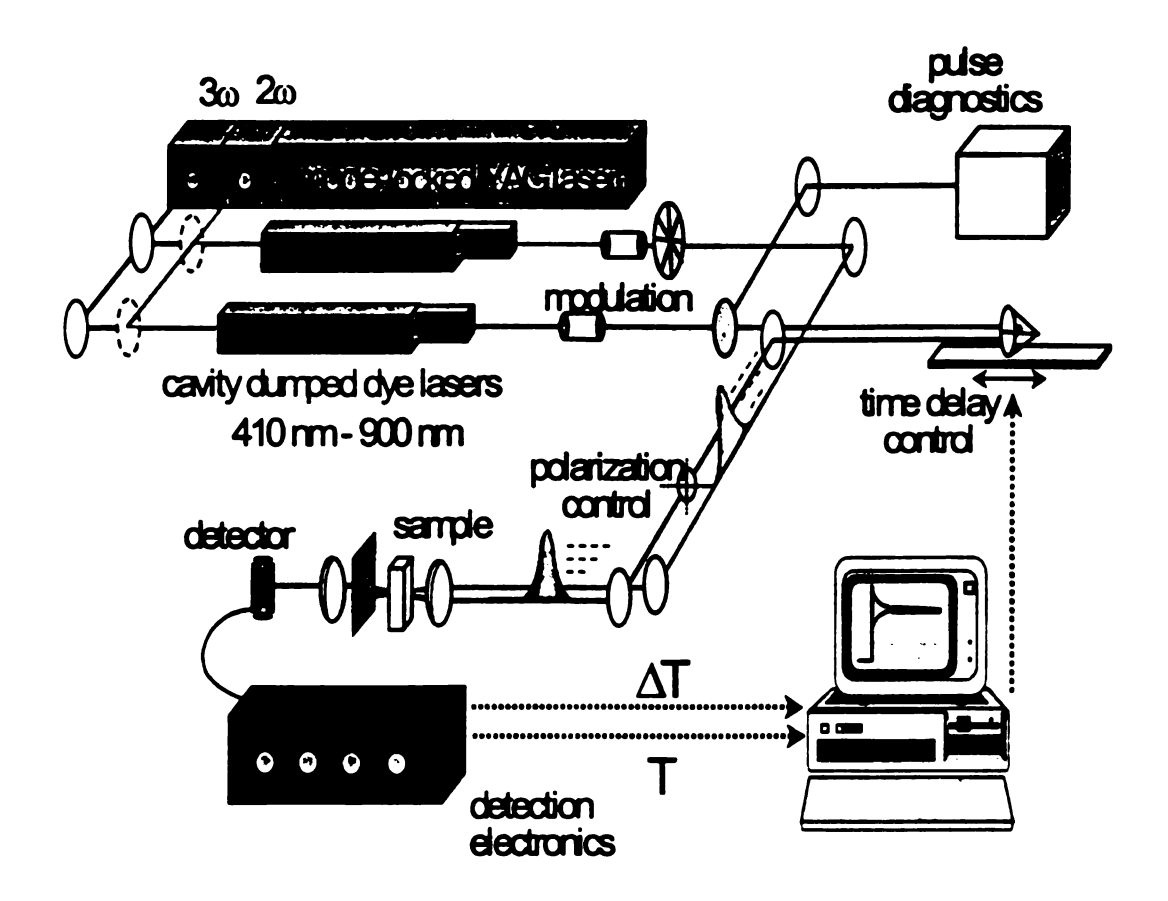


Figure 5.1. Experimental setup for ground state recovery experiments to determine microscopic free volume in the photoresist films.

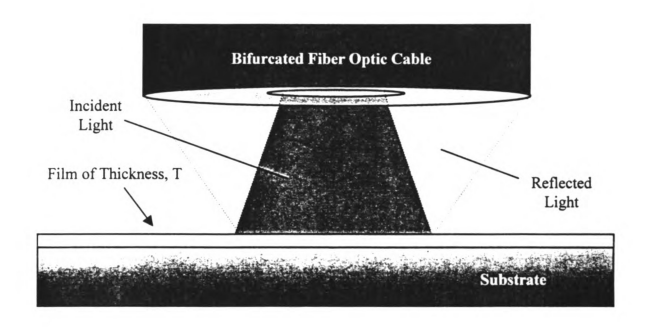


Figure 5.2. Experimental setup for dynamic film thickness measurements to observe macroscopic free volume evolution.

Figure 5.3. Molecular structure of crystal violet.

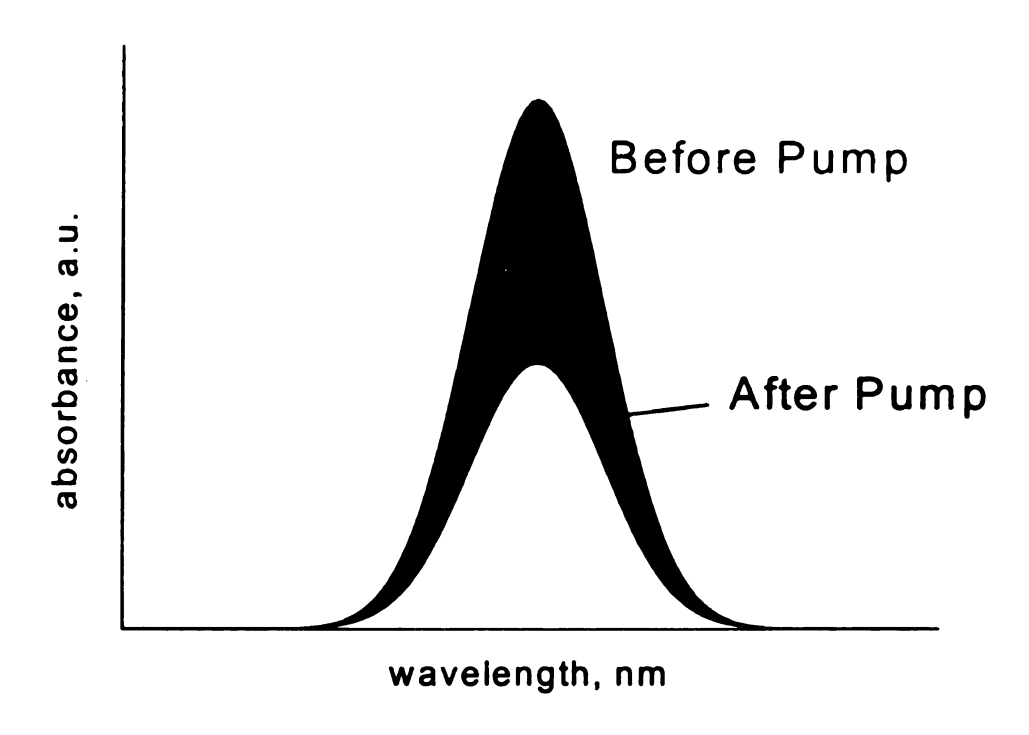


Figure 5.4. Schematic representation of the transient change in ground state absorption of crystal violet in response to excitation by a pump laser pulse.

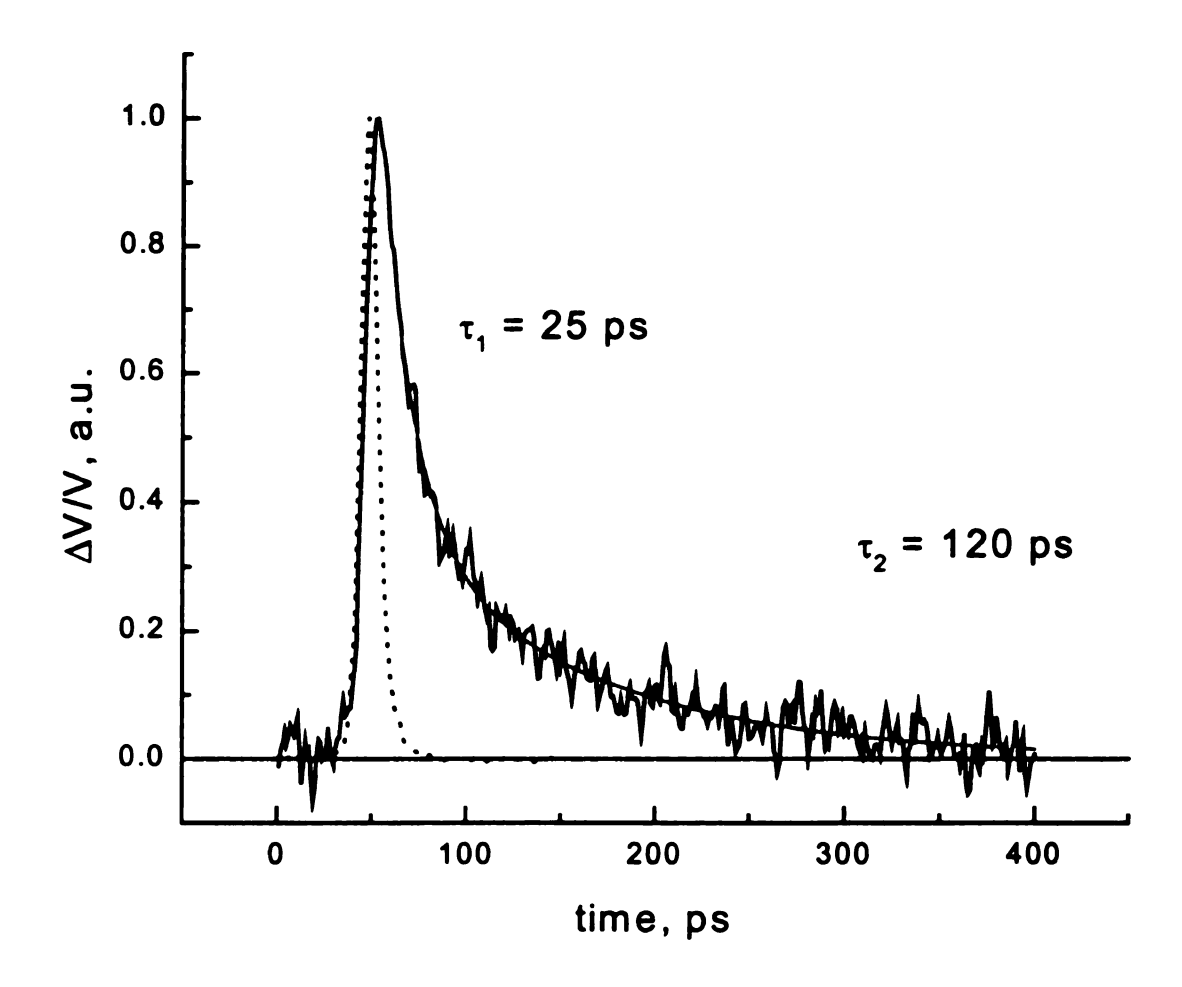


Figure 5.5. Instrumental response function (····) and experimental ground state recovery data (—) for crystal violet in the Apex-E 2408 DUV photoresist film.

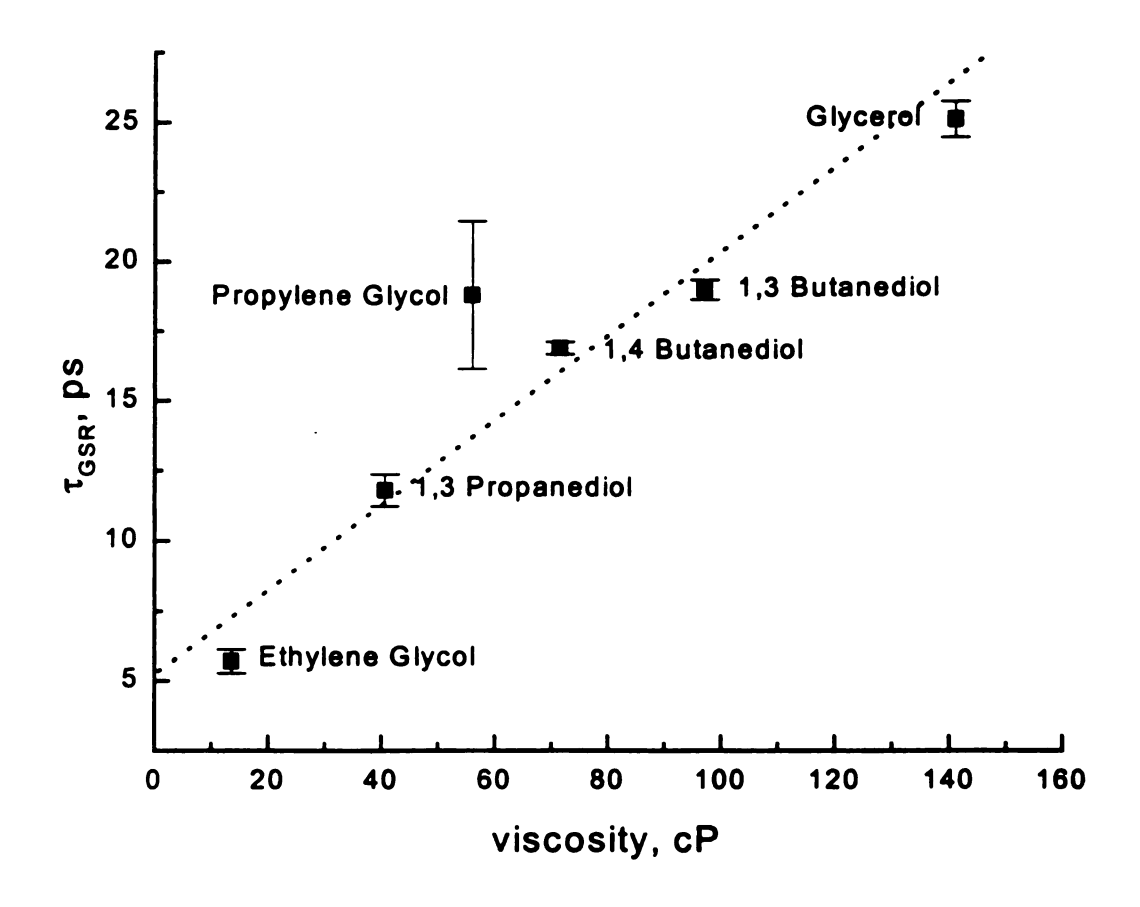


Figure 5.6. Linear calibration curve relating the short time constant,  $\tau_1$ , from the ground state recovery experiments of viscous liquids doped with 0.1 wt.% crystal violet to the matrix viscosity.

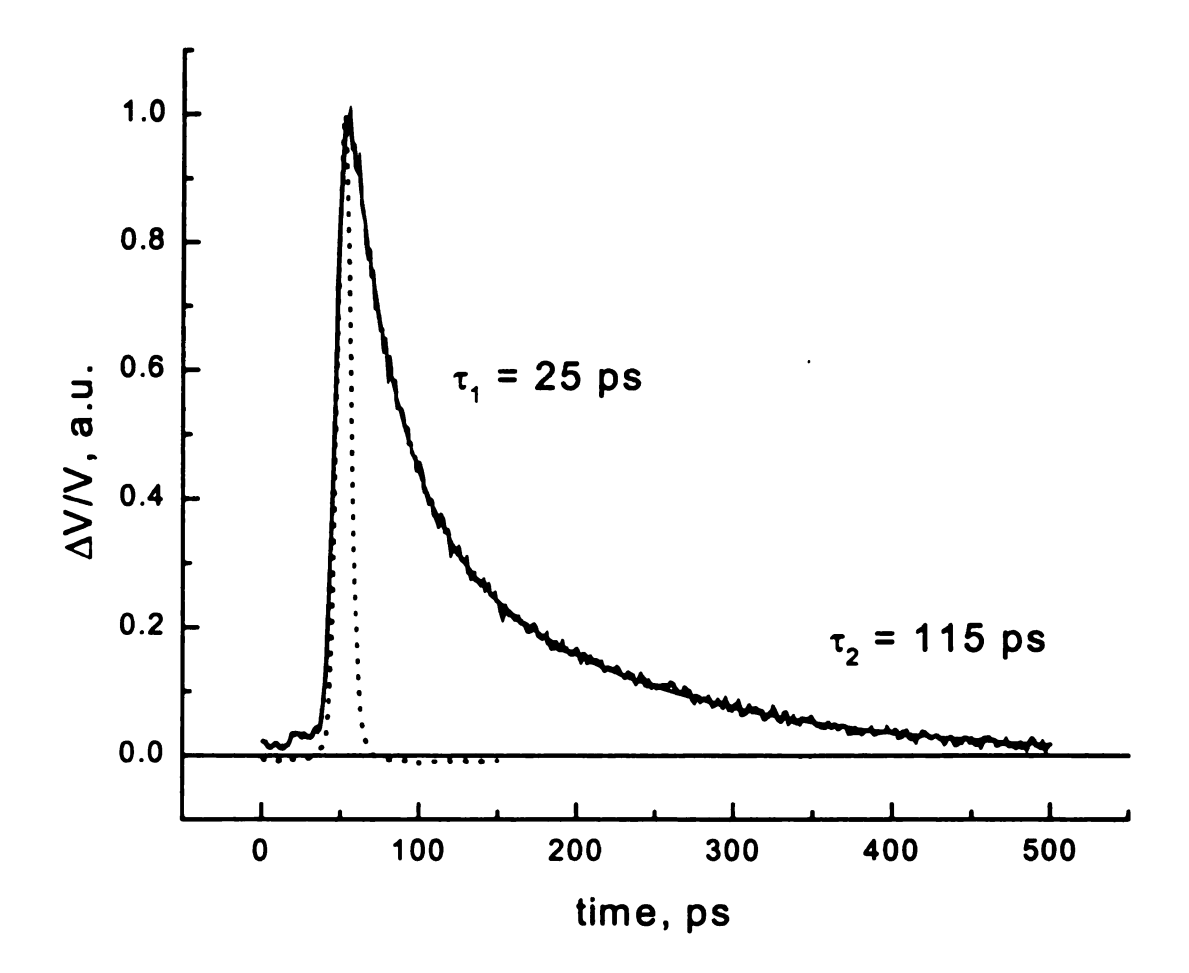
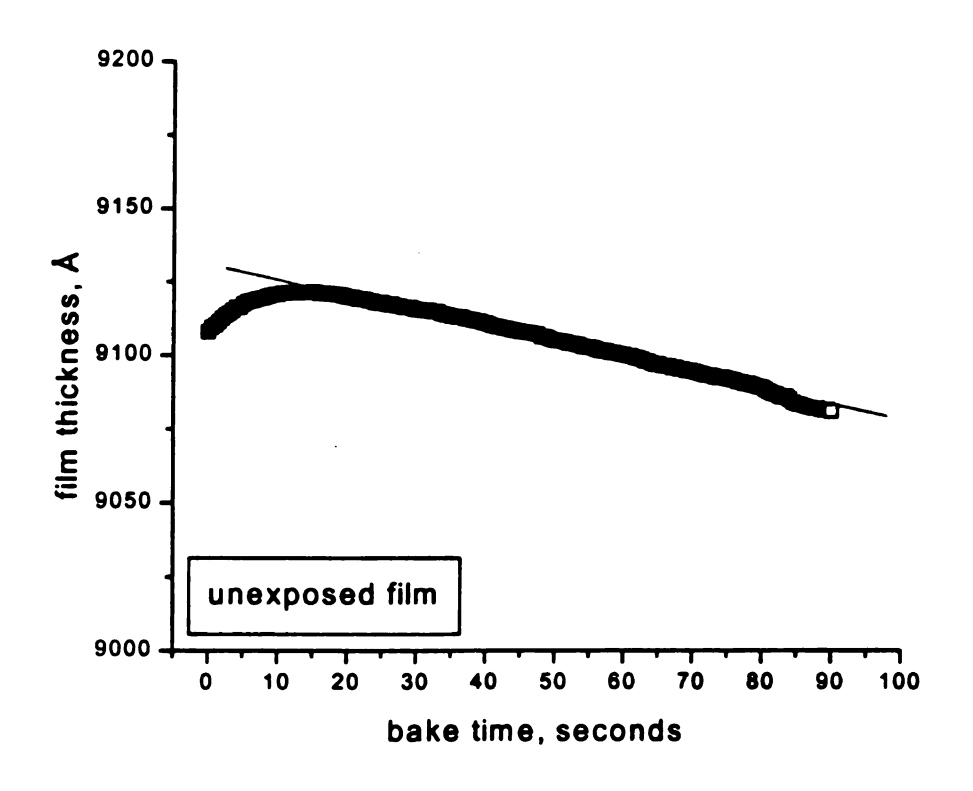


Figure 5.7. Instrumental response function (....) and experimental ground state recovery data (—) for crystal violet in glycerol.



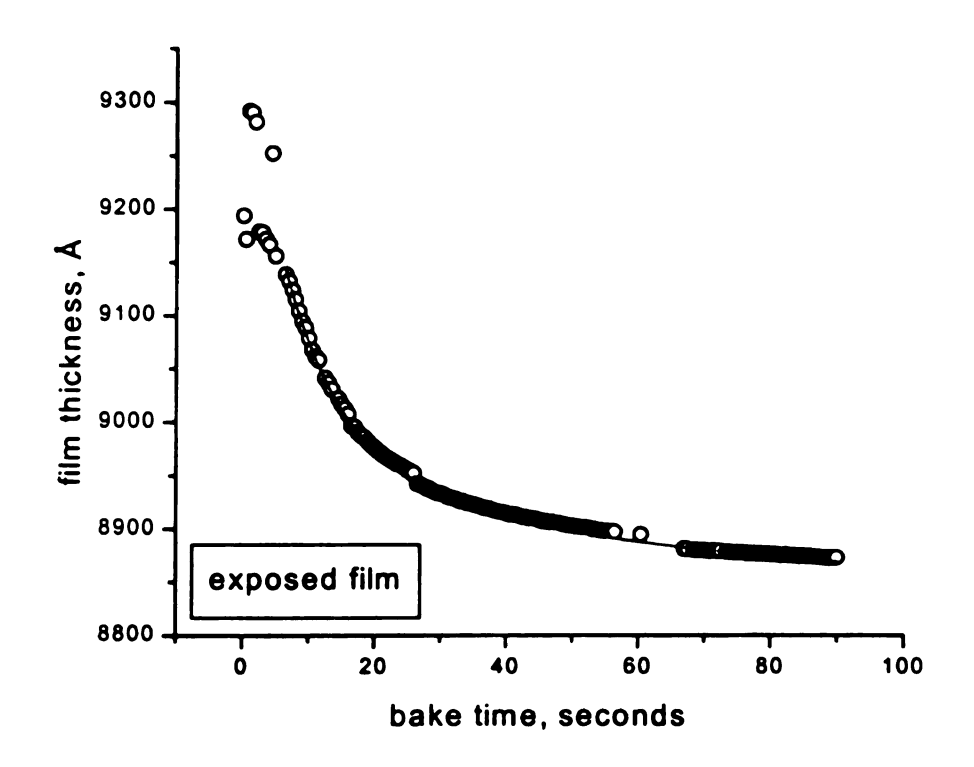


Figure 5.8. Change in Apex-E 2408 DUV photoresist film thickness as a function of bake time at 100°C for unexposed (top) and exposed (bottom) films.

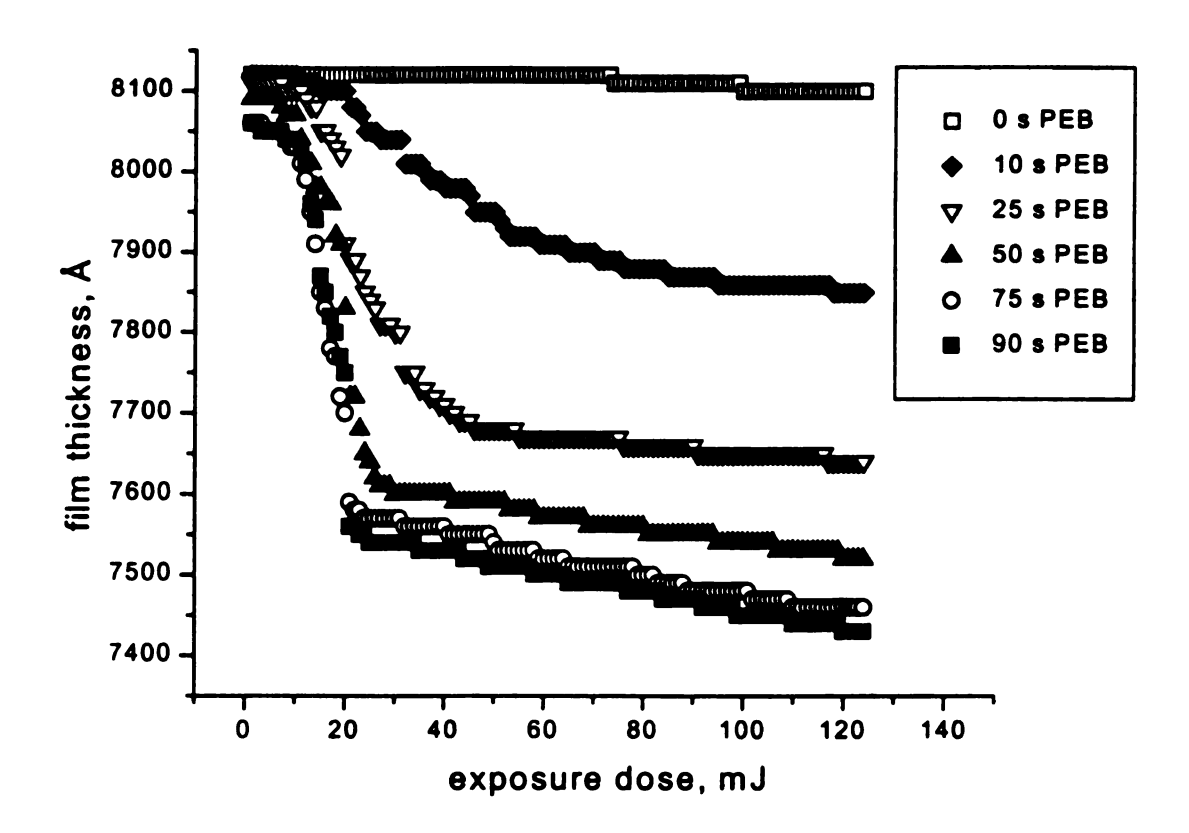


Figure 5.9. Change in thickness of Apex-E 2408 DUV photoresist film as a function of exposure dose and post exposure bake time.

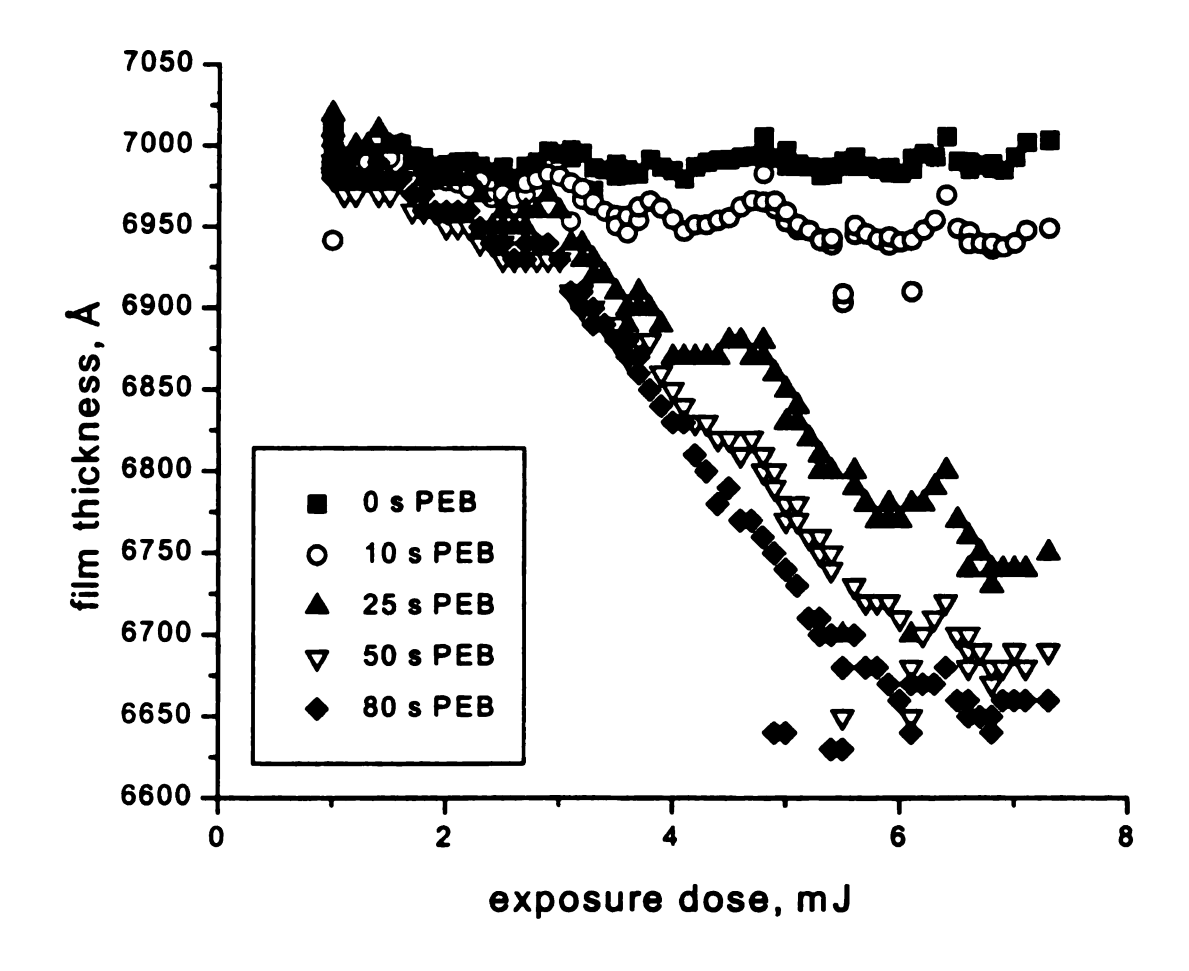


Figure 5.10. Change in thickness of UV5-0.6 positive DUV photoresist film as a function of exposure dose and post exposure bake time.

#### 5.5. REFERENCES

- 1. Z. Tadmor and C.G. Gogos, *Principles of Polymer Processing*, John Wiley & Sons, Inc., New York, 1979.
- 2. N.H. Jakatdar, J. Bao, C.J. Spanos, R. Subramanian, B. Rangarajan, "Physical modeling of deprotection-induced thickness loss," *Proceedings of SPIE*, **3678**, 275 (1999).
- 3. F.W. Wang, R.E. Lowry and W.H. Grant, "Novel excimer fluorescence method for monitoring polymerization: 1. Polymerization of methyl methacrylate," *Polymer*, 25(5), 690 (1984).
- 4. S.K. Moorjani, B. Rangarajan, and A.B. Scranton, "Effect of viscosity on the rate of photosensitization of diaryliodonium salts by anthracene," *Photopolymerization: Fundamentals and Applications*, edited by A.B. Scranton, C.N. Bowman, and R.W. Peiffer, American Chemical Society, Washington, D.C., 1997.
- 5. J.G. Victor and J.M. Torkelson, "On Measuring the Distribution of Local Free Volume in Glassy Polymers by Photochromic and Fluorescence Techniques," *Macromolecules*, **20**, 2241 (1987).
- 6. Y. Jiang, S. A. Hambir, G. J. Blanchard, "Synchronous pumping of two dye lasers using a single UV excitation source," Opt. Commun., 99, 216 (1993).
- 7. P. Bado, S. B. Wilson, K. R. Wilson, "Multiple modulation for optical pump-probe spectroscopy," *Rev. Sci. Instrum.*, 53, 706 (1982).
- 8. L. Andor, A. Lorincz, J. Siemion, D. D. Smith, S. A. Rice, "Shot-noise-limited detection scheme for two-beam laser spectroscopies," *Rev. Sci. Instrum.*, 55, 64 (1984).
- 9. G. J. Blanchard, M. J. Wirth, "Measurement of small absorbances by picosecond pump-probe spectrometry," *Anal. Chem.*, **56**, 532 (1986).
- 10. D. Ben-Amotz, C. B. Harris, "Torsional dynamics of molecules on barrierless potentials in liquids. I. Temperature and wavelength dependent picosecond studies of triphenylmethane dyes," J. Chem. Phys., 86(9), 4856 (1987).
- 11. D. Ben-Amotz, C. B. Harris, "Torsional dynamics of molecules on barrierless potentials in liquids. II. Test of theoretical models," *J. Chem. Phys.*, **86**(10), 5433 (1987).

- 12. J.Y. Ye, T. Hattori, H. Inouye, H. Ueta, H. Nakatsuka Y. Maruyama, M. Ishikawa, "Glass transition of associated solvents studied by fluorescence measurement of doped chromophores," *Phys. Rev. B*, **52**(13), 8349 (1996).
- 13. J. Y. Ye, T. Hattori, H. Nakatsuka, Y. Maruyama, M. Ishikawa, "Microscopic dynamics of the glass transition investigated by time-resolved fluorescence measurements of doped chromophores," *Phys. Rev. B.*, **56**(9), 5286 (1997).
- 14. M. Canva, G. Le Saux, P. Georges, A. Brun, F. Chaput, J.P Boilot "Time-resolved saturated absorption recovery in malachite green-doped xerogel," *Chem Phys. Lett.*, 176(5), 495 (1991).
- 15. K. M. Abedin, J. Y. Ye, H. Inouye, T. Hattori, H. Sumi, H. Nakatsuka, "Diffusive torsional dynamics of malachite green molecules in solid matrices probed by fluorescence decay," *J. Chem. Phys.*, 103(15), 6414 (1995).
- 16. K. M. Abedin, J. Y. Ye, H. Inouye, T. Hattori, H. Nakatsuka, "Local dynamics in solid matrices investigated by malachite green optical microprobes," *J. of Luminescence*, 64, 135 (1995).
- 17. E. P. Ippen, C. V. Shank, A. Bergman, "Picosecond recovery dynamics of malachite green," *Chem. Phys. Lett.*, 38(3), 611 (1976).
- 18. Lange's Handbook of Chemistry, 14th ed., edited by J.A. Dean, McGraw-Hill Book Company, New York, 1992.
- 19. J.E. Guillet, "Mass Diffusion in Solid Polymers," *Photophysical and Photochemical Tools in Polymer Science*, edited by M.A. Winnik, D. Reidel Publishing Company, Hingham, MA, 1986.
- 20. L.H. Sperling, *Introduction to Physical Polymer Science*, 2<sup>nd</sup> ed., John Wiley & Sons, Inc., New York, 1992.

# Chapter 6

# **CONCLUSIONS AND RECOMMENDATIONS**

#### **6.1. SUMMARY OF RESULTS**

In this body of research, spectroscopic methods have been developed to gain insitu and on-line information for two different polymer systems: thermoplastic polymer composites and chemically amplified resists. With these techniques, it is possible to conduct quality control and process optimization efforts during actual polymer processing. Spectroscopic techniques such as fluorescence and absorption are attractive for in-situ and on-line characterization because pertinent processing information can be gathered in a quick and timely manner.

## 6.1.1. Cure monitoring of polymer composites

First of all, a method was developed to monitor polymer cure based upon the fluorescence response of a specially chosen probe molecule. The use of an optical spectrometer to implement this method provides an inexpensive, non-intrusive, and portable means of cure monitoring. This method is based on the introduction of trace quantities of a solvatochromic probe into the system. These molecules do not lose sensitivity at the gel point and can be implemented easily using optical fibers. Two such molecules are phenoxazone 660 and pyrene, whose fluorescence spectra change in response to the conversion of double to single bonds during the polymerization. In the case of the phenoxazone 660, the emission spectra blue-shifts with increasing polymer conversion; in the case of pyrene, the relative intensities of two interdependent peaks in the emission spectra invert. The fluorescence cure monitoring scheme using these probe

molecules was successfully demonstrated in a variety of curing polymers, including methyl methacrylate, styrene and Derakane® vinyl ester resins.

# 6.1.2. Characterization of chemically amplified photoresists

Secondly, highly sensitive, time-resolved spectroscopic techniques were developed to address two basic, yet significant, questions for reaction-diffusion phenomenon in chemically amplified resists: (i) how much acid is in the system and (ii) where is the acid going. This was an extremely challenging task because the photoresist films are typically one-micron thick, making it difficult to detect optical signals during processing. These difficulties were in part overcome by carefully selecting probe molecules that would allow inquiry into the status of acid concentration and free volume.

To answer the first question, focus was placed on two stages in the resist processing: exposure and post exposure bake. Steady-state fluorescence of the acid-sensitive molecular probe fluorescein was used to measure the photoacid generation during exposure. With this technique, the concentration of acid was characterized as a first order exponential in response to illumination with 248-nm light. Steady-state absorption of a second acid-sensitive molecular probe, crystal violet, was used to measure proton concentration during post exposure bake. This technique allows the quantification of acid concentration throughout the deprotection reaction regime based on the alpha charts for three possible states of crystal violet.

In answering the second question, focus was placed on the development of free volume during the post exposure bake and its effect upon acid mobility; this was investigated on two different physical scales: macroscopic and microscopic. Dynamic film thickness measurements based on multi-wavelength interferometry confirm the

difference in thickness reduction mechanisms between solvent volatilization and polymer chain relaxation during post exposure bake. The major film thickness loss occurs as the polymer chains relax, causing the film to collapse into itself and decrease the overall free volume provided by the small molecules, created during the deprotection reaction, which quickly diffuse out of the film. The nature of the free volume evolution on a microscopic level was probed using ground state recovery experiments with the molecular probe crystal violet, which also exhibits a free volume-sensitive behavior in its transient response. This technique allows the correlation of the resist microenvironment to an effective viscosity. As this viscosity increases, the free volume available for acid diffusion decreases.

#### **6.2. SUGGESTIONS FOR FUTURE WORK**

With this foundation laid, further research is recommended in order to apply fully the techniques developed in this body of work. Specifically, quantitative correlation studies and industrial application strategies are suggested in furthering the work completed on cure monitoring of polymer composites. In the area of characterization of chemically amplified resists, the extension of the spectroscopic techniques to quantify acid loss and free volume evolution is recommended, as well as application of the techniques to forthcoming 193-nm resist technology.

## 6.2.1. Cure monitoring of polymer composites

Although the thermocouple studies show that the fluorescence emission of the probe molecules does indeed follow the polymerization reaction, it would be advisable to correlate the results with well-accepted, quantitative techniques such as differential scanning calorimetry and/or Raman spectroscopy. In differential scanning calorimetry,

the overall heat of reaction for the polymerization is measured at a constant temperature (see Figure 6.1, top). By integrating the area under the resulting curve (when the exothermic peak are pointed up), the conversion over time is obtained (see Figure 6.1, bottom). In order for this measurement to have quantitative significance, the heat of polymerization must be known for the polymer under investigation, a number of which are reported by Sawada.<sup>3</sup> However, the qualitative shape of the conversion curve is adequate to compare the fluorescence response of the molecular probe to the polymerization in the case of those monomers, such as the Derakane® resins, for which this information is not readily available. In order to accomplish these experiments, a special adapter for the Perkin-Elmer DSC7 (Norwalk, CT) must be constructed so that the fluorescence monitoring technique may be applied simultaneously. Basically, the adapter should consist of a quartz window with an SMA connection for an optical fiber, which would be placed over the sample pan. Using a bifurcated optical fiber, the excitation light can be directed onto the sample while the fluorescence emission is collected and sent to the spectrometer. Some considerations for the sample include: (i) a high concentration of the molecular probe (say, 10<sup>-3</sup> wt.%) to enhance the fluorescence signal, (ii) the largest sample size permitted in the pan (namely, 30 mg) to prevent the sample from concentrating around the edges of the pan out of the sampling area of the optical fiber set-up, and (iii) a less volatile monomer, such as one of the more viscous Derakane<sup>®</sup> resins, to discourage evaporation of the monomer during the experiment.

A second possible method of verification is Raman spectroscopy, which is based upon a frequency shift of inelastic scattered light. Thus, it is well suited to observe polymerization reactions in which there is a conversion from double to single bonds.<sup>4</sup>

This technique has been used to follow conversion of many polymer systems, including acrylates,<sup>5</sup> styrene,<sup>6,7</sup> vinyl ethers,<sup>8,9</sup> and epoxies.<sup>10</sup> Two sets of samples would be necessary for these experiments: one set containing only the monomer and thermal initiator for Raman spectroscopy and the other set with the molecular probe added for fluorescence spectroscopy. It is advisable to conduct the experiments in this manner, separating the real-time collection of Raman spectra from that of fluorescence spectra, because the fluorescence from the molecular probes may overwhelm the Raman signal. Finally, since preliminary studies have shown that the excitation laser beam may photodegrade the molecular probe, it is important that the intensity of the beam be reduced with neutral density filters to alleviate the problem.

In addition to comparing polymer conversion directly to the fluorescence intensity ratios, it is recommended that specific control strategies involving this technique be developed. Integration of this method into various industrial processing scenarios presents a special challenge. On the one hand, there is the high-speed web processing format in which thin films are applied and photopolymerized. This is in contrast to the traditional molding process in which thick parts of varying geometry are thermally cured. In the former case, algorithms must be developed to correlate the position of the sample with the signal obtained so that corrective action may be taken on the appropriate section of film. In the latter case, the concern is sampling port placement so that areas in which cure is problematic are monitored appropriately.

Finally, although this method is applicable with glass fiber-filled composites, no work has been done with carbon fiber-filled or pigmented systems. These are challenging systems in that the fibers and pigments may absorb or reflect the monitoring

signals. An investigative study in this area to tailor the monitoring method to these systems is suggested, since it would allow the technique to encompass a broader range of industrial processing situations.

# 6.2.2. Characterization of chemically amplified resists

#### 6.2.2.1. 248-nm resists

The ultimate goal of research in this area is to obtain accurate physical parameters for the reaction and diffusion in chemically amplified photoresists, which may be incorporated into a model in order to predict pattern mask outcomes. concentration calibration curves for crystal violet absorption allow a great flexibility in examining various aspects of the photoacid diffusional behavior. First of all, this technique can be applied to the systematic study of acid loss due to airborne bases and/or evaporation. This is accomplished by the reversibility of the protonated states of crystal violet. Secondly, the diffusion times of the acid can be determined via spatial resolution of this method. As a portion of the photoresist sample is exposed, a second portion a known distance away may be monitored for acid incursion. If the photoresist components are combined in the lab, rather than using a commercial formulation, then the effect of the acid counterion on acid diffusion may be assessed by varying the photoacid generator. Finally, as suggested by the fluorescence work in Chapter 4, a similar set of calibration curves may be developed for the fluorescence emission response of crystal violet in order to work with photoresist samples on silicon (rather than quartz) substrates.

The relationship between the viscosity extracted from ground state recovery data of crystal violet  $(\eta)$  and the translational diffusion coefficient of a diffusing moiety was first introduced in the previous chapter:

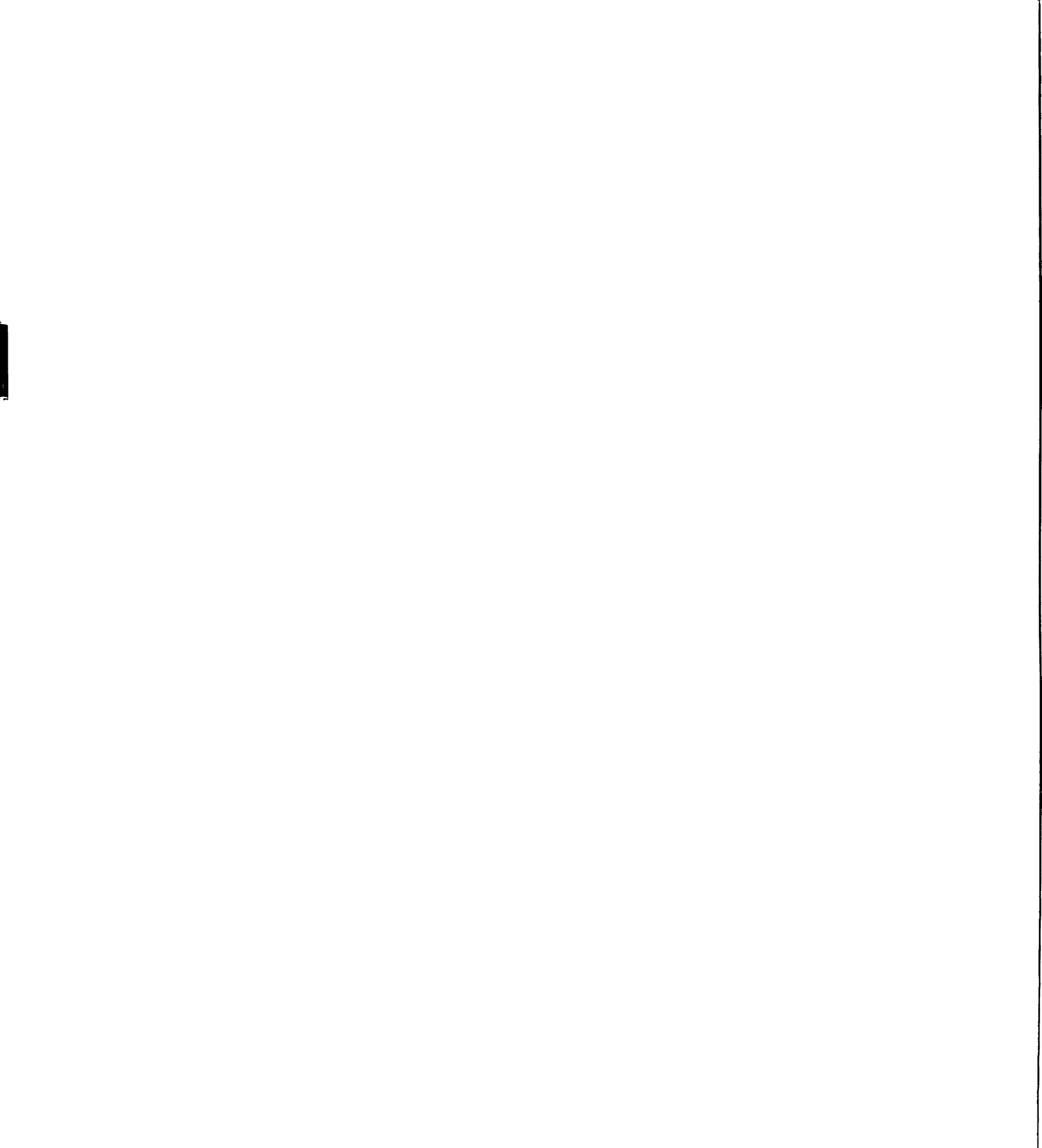
$$D = \frac{kT}{6\pi\eta r} \tag{5.2}$$

Here, the (spherical) diffusing entity under consideration is a proton with its associated counterion. The relationship between D and the free volume of the polymer matrix has been treated by Ganesh *et al.*<sup>11</sup> and is given below as Equation 6.2.

$$D_{1} = D_{01} \left\{ e^{-E/RT} \right\} \left\{ exp \left( -\frac{\gamma}{\hat{V}_{FH}} \left[ \overline{\omega}_{1} \hat{V}_{1J} + \zeta \overline{\omega}_{2} \hat{V}_{2J} \right] \right) \right\}$$
(6.2)

$$\zeta = \frac{\hat{\mathbf{V}}_{1J} \mathbf{M}_{1J}}{\hat{\mathbf{V}}_{2J} \mathbf{M}_{2J}} \tag{6.3}$$

 $\hat{V}_{FH}$  is the average hole free volume per gram of mixed polymer,  $\hat{V}_{iJ}$  is the specific critical hole free volume of species *i* required for diffusion to occur,  $\zeta$  (Equation 6.3) is the ratio of the critical molar volume of the proton in the polymer matrix,  $\gamma$  is the overlap factor which accounts for cooperative nature of the diffusing proton and the surrounding matrix,  $M_{IJ}$  is the molecular weight of the diffusing species,  $M_{2J}$  is the molecular weight of a polymer matrix segment that can occupy the same space as the diffusing moiety,  $\omega_1$  and  $\omega_2$  are the weight fractions of the diffusing species in the matrix and the matrix itself, E is the activation energy for diffusive motion, and  $D_{01}$  is an effective Arrhenius prefactor. Thus, through this analysis of the ground state recovery data, it is possible to correlate the microscopic evolution of free volume in the photoresist as a function of

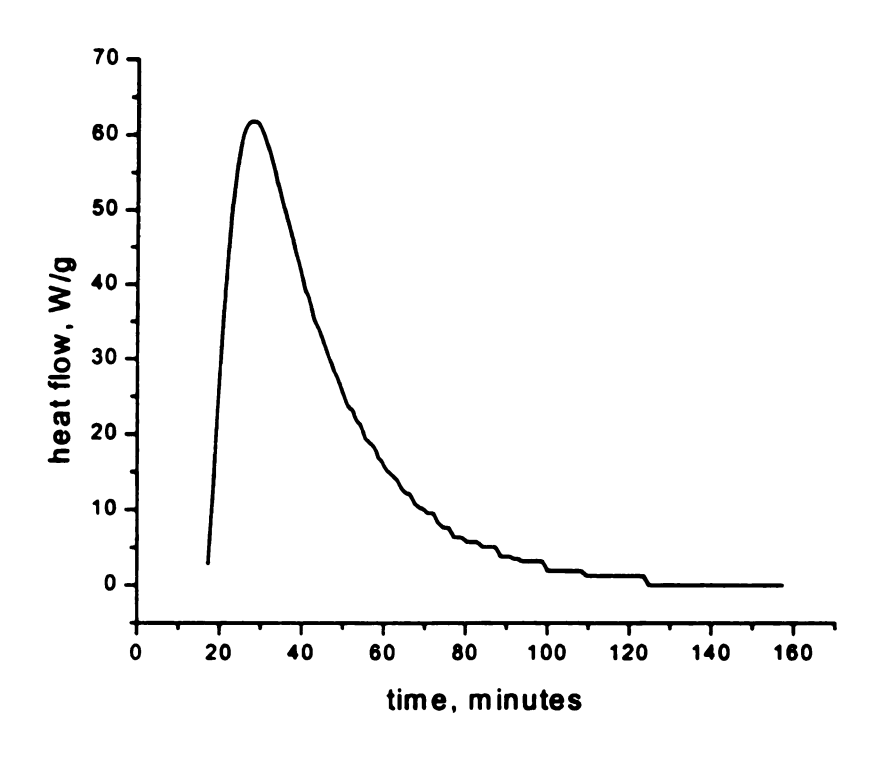


processing time, which in turn will allow insight into the diffusional cross-section available to the photoacid.

#### 6.2.2.2. 193-nm resists

With the recent advent of the 193-nm resist films on the commercial market, microelectronics companies are pressed to understand the correlation between acid diffusion in these photoresists and resulting line defects, such as line end shortening and iso-dense bias, before full-scale production begins in the next few years. These processing problems will be more prominent than in the 248-nm resists since the shorter exposure wavelength will enable smaller feature sizes and more compact devices. In addition, the resist formulation has been significantly altered to obtain a transparent spectral window at 193 nm by removing the benzene rings, yet retaining the high carbon to hydrogen ratio with unsaturated ring systems to obtain acceptable etch rates (see Figure 6.2). Thus, optical and kinetic characterization studies must be completed in order to optimize use in microlithographic processing.

In-situ and on-line characterization can be used to address these imminent concerns with the 193-nm photoresists. Absorption and FTIR spectroscopies can be adapted to determine the kinetics of chemical amplification in these photoresist films on the wafer. Fluorescence and absorption spectroscopies used in conjunction with judiciously chosen probe molecules can track photoacid concentration in the resist film during processing. Finally, ground-state recovery measurements can be applied to monitor the changes in film viscosity throughout the baking cycles and correlated to acid diffusion.



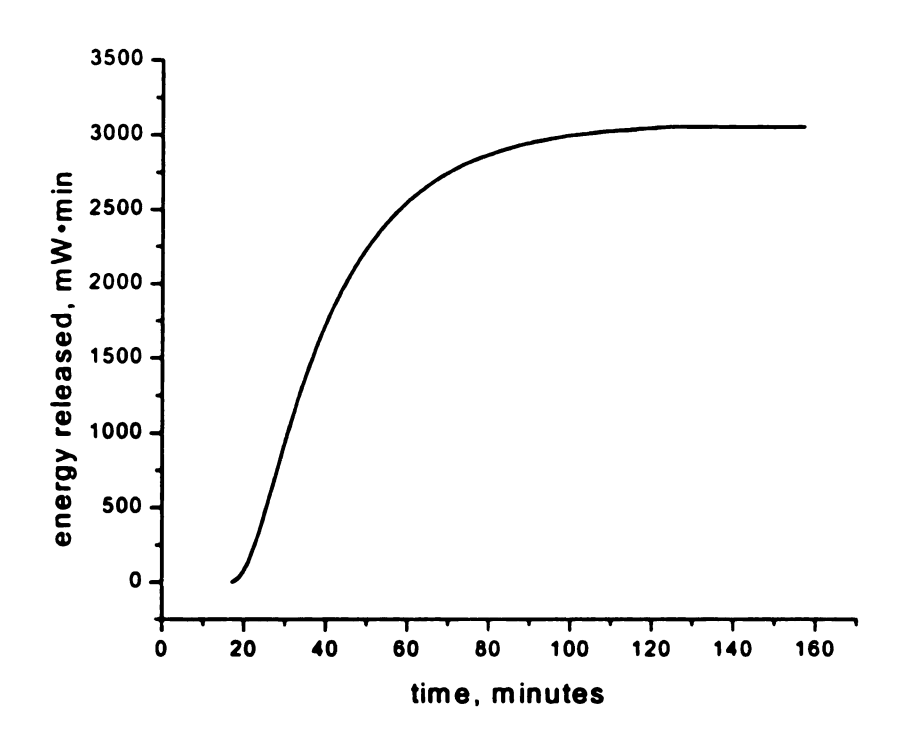


Figure 6.1. Differential scanning calorimetry plots for polymerization of Derakane® 411-C50 at 70°C: heat of reaction (top) and conversion (bottom).

Figure 6.2. Chemical structure of the latest 193-nm resist formulation.

#### 6.3. References

- 1. G.J. Blanchard, J.L. Jessop, A.B. Scranton, "Method and apparatus for in situ, non-invasive polymer cure determination," US Patent #5633313, May 27, 1997.
- 2. G.J. Blanchard, J.L. Jessop, A.B. Scranton, "Apparatus for in situ, non-invasive polymer cure determination," US Patent #5707587, January 13, 1998.
- 3. H. Sawada, "Thermodynamics of Polymerization. I," J. Macromol. Sci.—Revs. Macromol. Chem., C3(2), 313 (1969).
- 4. H.G.M. Edwards, A.F. Johnson and I.R. Lewis, "Applications of Raman Spectroscopy to the Study of Polymers and Polymerization Processes," *J. Raman Spectrosc.*, 49A, 475 (1993).
- 5. J. Clarkson, S.M. Mason and K.P.J. Williams, "Bulk radical homo-polymerisation studies of commercial acrylate monomers using near infrared Fourier transform Raman spectroscopy," *Spectrochimica Acta*, 47A, 1345 (1991).
- 6. E. Gulari, K. McKeigue and K.Y.S. Ng, "Raman and FTIR Spectroscopy of Polymerization: Bulk Polymerization of Methyl Methacrylate and Styrene," *Macromolecules*, 17, 1822 (1984).
- 7. B. Chu, G. Fytas and G. Zalczer, "Study of Thermal Polymerization of Styrene by Raman Scattering," *Macromolecules*, 14, 395 (1981).
- 8. E.W. Nelson and A.B. Scranton, "Kinetics of Cationic Photopolymerizations of Divinyl Ethers Characterized Using *In Situ* Raman Spectroscopy," *J. Polym. Sci.: Part A: Polym. Chem.*, 34, 403 (1996).
- 9. E.W. Nelson and A.B. Scranton, "In Situ Raman Spectroscopy for Cure Monitoring of Cationic Photopolymerizations of Divinyl Ethers," J. Raman Spectrosc., 27, 137 (1996).
- 10. K.E. Chike, M.L. Myrick, R.E. Lyon, S.M. Angel, "Raman and near-infrared studies of an epoxy resin," Appl. Spectrosc., 47(10), 1631 (1993).
- 11. K. Ganesh, R. Nagarajan and J.L. Duda, "Rate of Gas Transport in Glassy Polymers: A Free Volume Based Predictive Model," *Ind. Eng. Chem. Res.*, 31, 746 (1992).
- 12. C.G. Willson, *Resists for Deep UV Lithography*, SPIE's International Symposium on Microlithography, March 18, 1999.

# **APPENDIX**

# A.1. DETERMINATION OF EQUILIBRIUM CONSTANTS

In order to develop a calibration curve that can be used to determine the acid concentration in the photoresist thin films, the effect of acid concentration upon the absorption spectrum of crystal violet was obtained using a buffered solution series (see Figure A.1). From these spectral data, it was possible to calculate the concentration of the three crystal violet species ( $c_V = [CV^+]$ ,  $c_G = [HCV^{2+}]$  and  $c_Y = [H_2CV^{3+}]$ ) in solution using the application of Beer's Law to mixtures:<sup>1</sup>

$$A_{430} = \varepsilon_{V(430)}bc_{V} + \varepsilon_{G(430)}bc_{G} + \varepsilon_{Y(430)}bc_{Y}$$
(A.1)

$$A_{630} = \varepsilon_{V(630)}bc_{V} + \varepsilon_{G(630)}bc_{G} + \varepsilon_{V(630)}bc_{Y}$$
(A.2)

$$A_{590} = \varepsilon_{V(590)}bc_{V} + \varepsilon_{G(590)}bc_{G} + \varepsilon_{V(590)}bc_{Y}$$
(A.3)

where, for a given acid concentration (or pH),  $A_j$  is the absorption at wavelength j,  $\epsilon_{ij}$  is the extinction coefficient of species i at wavelength j, b is the pathlength, and  $c_i$  is the concentration of species i. The three wavelengths (430, 590 and 630 nm) were chosen because they represent the wavelengths of maximum peak absorption for the three species of crystal violet under consideration: yellow, violet and green, respectively. The extinction coefficients for these wavelengths and species were obtained from the literature.<sup>2</sup> Extinction coefficients for the violet and yellow forms at 430 nm were extrapolated from these data (see Figure A.2).

Equations A.1 - A.3 were written in matrix form, as shown below, and solved by Gauss reduction to obtain the three species concentrations at each acid concentration:

$$\begin{bmatrix} 7.14 \times 10^{2} & 0 & 2.83 \times 10^{4} \\ 1.62 \times 10^{4} & 1.12 \times 10^{5} & 0 \\ 9.32 \times 10^{4} & 5.6 \times 10^{4} & 2.8 \times 10^{1} \end{bmatrix} = \begin{bmatrix} A_{430} \\ A_{630} \\ A_{590} \end{bmatrix}$$
(A.4)

The equilibrium constants that relate the concentrations of the three crystal violet species were then determined using the equations described in Chapter 4 and the species concentrations calculated from above:

$$K_1 = \frac{[HCV^{2+}][H^+]}{[H_2CV^{3+}]}$$
(4.3)

$$K_2 = \frac{[CV^+][H^+]}{[HCV^{2+}]}$$
 (4.4)

The reported equilibrium constants are the average of these calculated values for the nine acid concentrations evaluated.

#### A.2. DETERMINATION OF ALPHA PLOTS

From these equilibria data, it is then possible to construct alpha plots, which enable the determination of acid concentration based on the concentration distribution of the three crystal violet species. The following set of equations was solved algebraically to obtain the alpha values ( $\alpha_0$ ,  $\alpha_1$  and  $\alpha_2$ ) for this system:<sup>1</sup>

$$K_1 = \frac{[HCV^{2+}][H^+]}{[H_2CV^{3+}]} = 0.025 \, \frac{\text{moles}}{L}$$
(4.3)

$$K_2 = \frac{[CV^+][H^+]}{[HCV^{2+}]} = 0.0067 \text{ moles/L}$$
 (4.4)

$$[CV]_{total} = [CV^+] + [HCV^{2+}] + [H_2CV^{3+}]$$
 (A.5)

$$\alpha_0 = \frac{[H_2CV^{3+}]}{[CV]_{total}} \tag{A.6}$$

$$\alpha_1 = \frac{[HCV^{2+}]}{[CV]_{total}} \tag{A.7}$$

$$\alpha_2 = \frac{[CV^+]}{[CV]_{total}}$$
 (A.8)

$$\alpha_0 + \alpha_1 + \alpha_2 = 1 \tag{A.9}$$

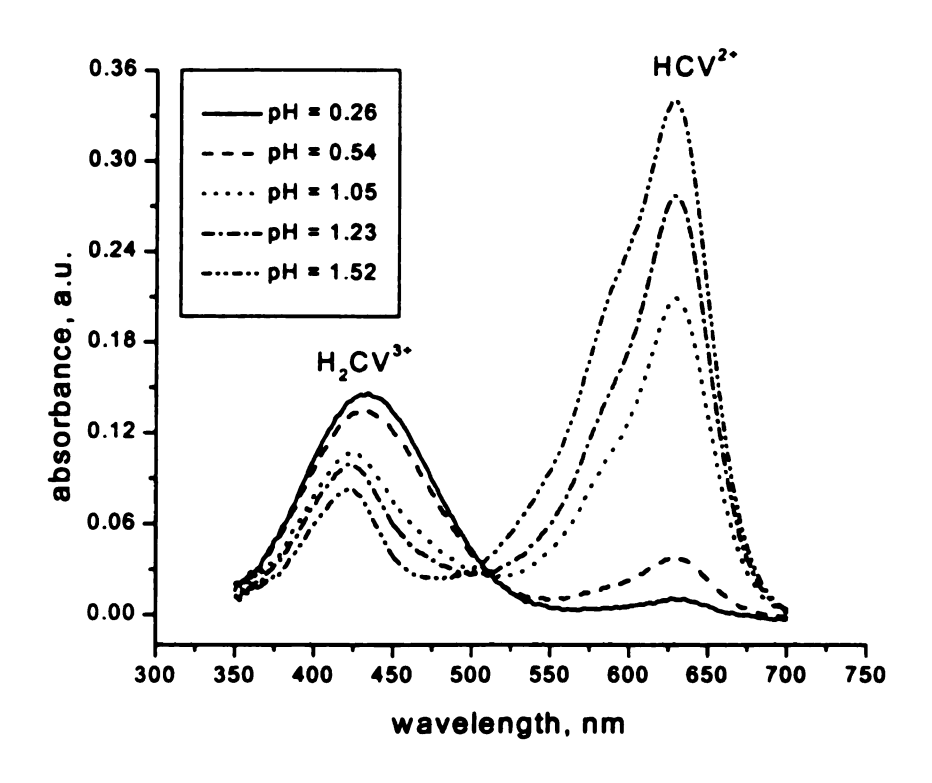
Substitution and rearrangement of the seven equations above yields the following expressions for the alpha values:

$$\alpha_1 = \frac{K_1[H^+]}{[H^+]^2 + K_1K_2 + K_1[H^+]}$$
(A.10)

$$\alpha_2 = \frac{K_1 K_2}{[H^+]^2 + K_1 K_2 + K_1 [H^+]}$$
(A.11)

$$\alpha_0 = 1 - \alpha_1 - \alpha_2 \tag{A.12}$$

Figure A.3 shows the relationship among the three species of crystal violet as a function of acid concentration based upon computation of the alpha values. Thus, with an absorption spectrum of crystal violet in the photoresist film, it is possible to calculate the individual concentrations of the three crystal violet species and determine the acid concentration in the film using the alpha plot.



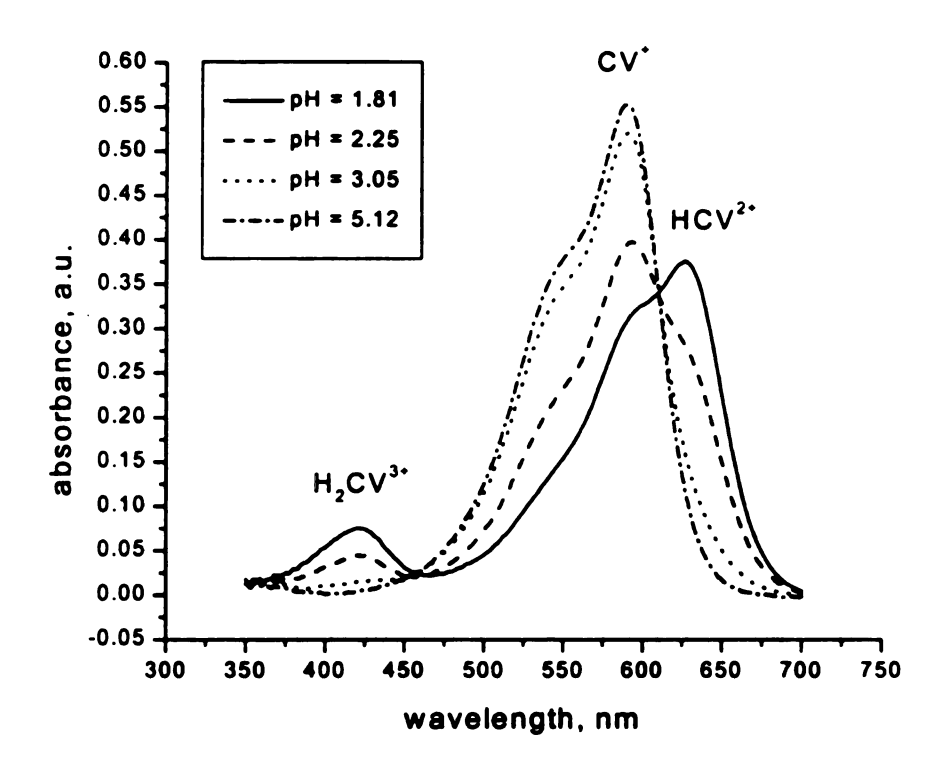
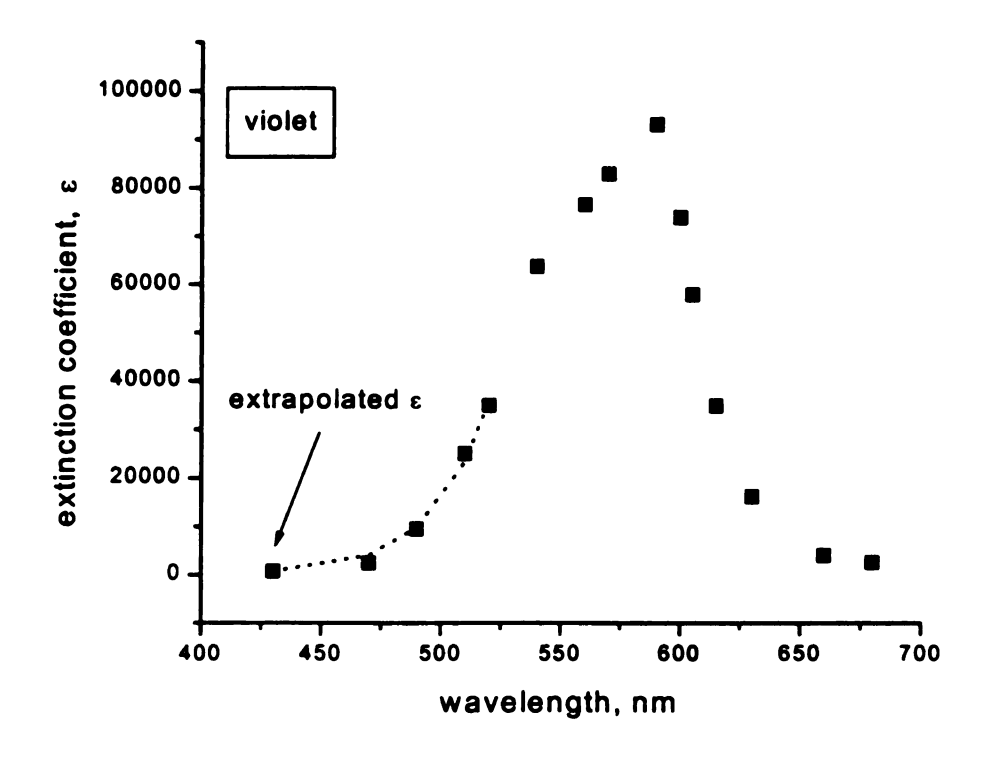


Figure A.1. Change in absorption spectrum of crystal violet with increasing acid concentration in buffered solution series.



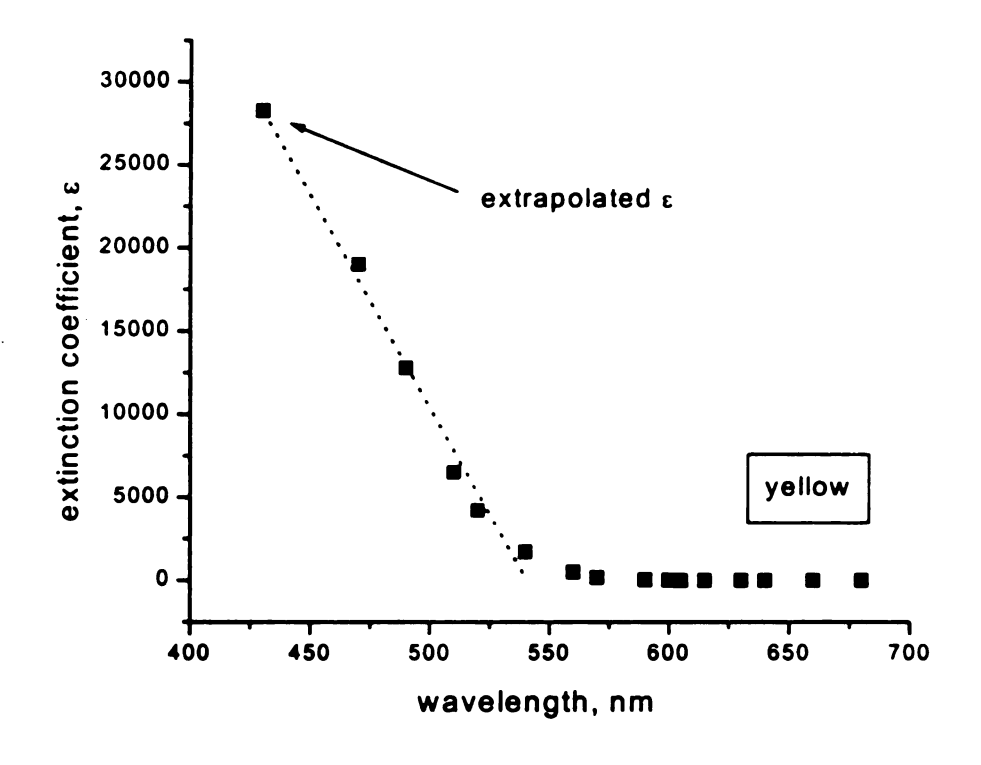


Figure A.2. Extrapolation of extinction coefficients for CV<sup>+</sup> (violet species, top) and H<sub>2</sub>CV<sup>3+</sup> (yellow species, bottom) based upon reported literature values.

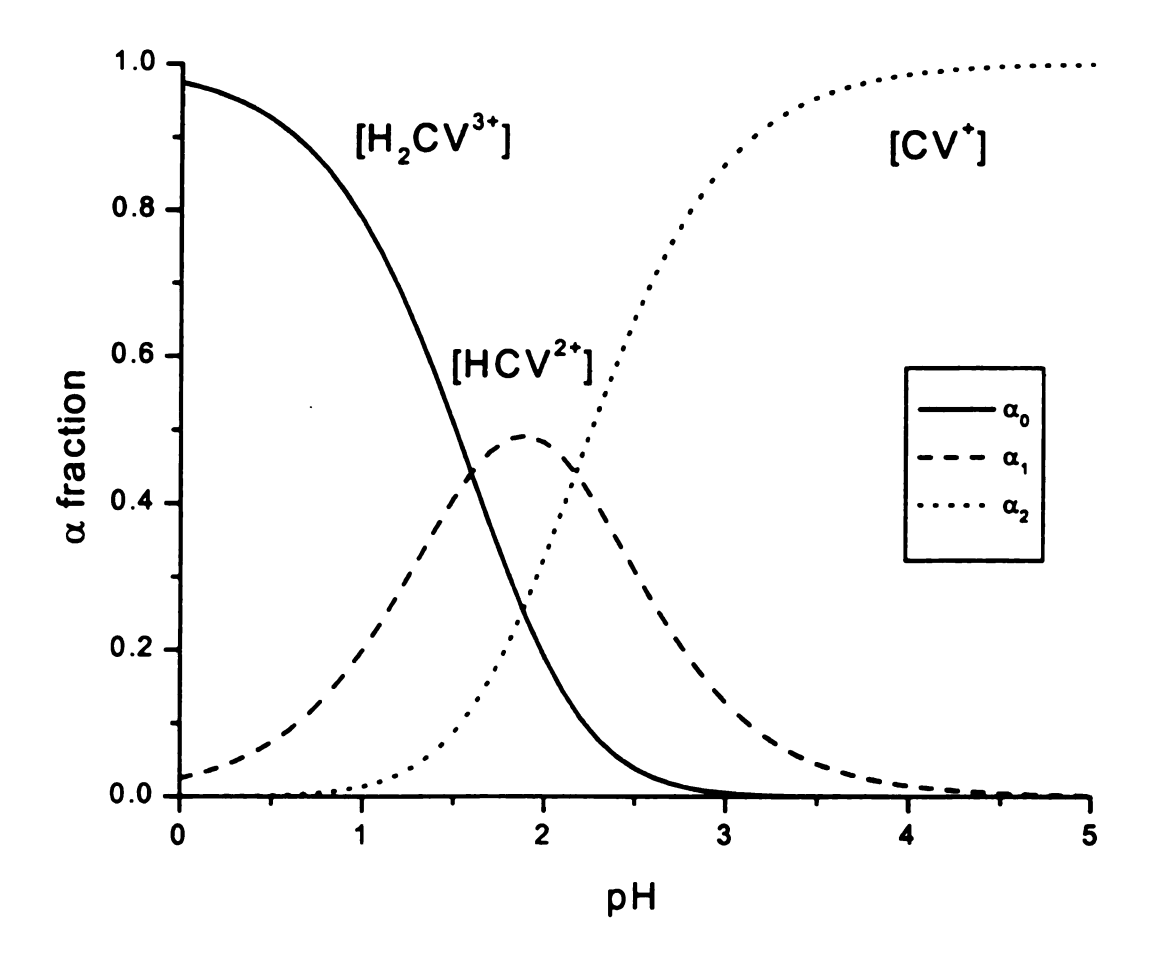


Figure A.3. Change in relative amounts of  $CV^+$  ( $\alpha_2$ ),  $HCV^{2+}$  ( $\alpha_1$ ) and  $H_2CV^{3+}$  ( $\alpha_0$ ) with decreasing acid concentration.

# A.3. REFERENCES

- 1. D.A. Skoog, D.M. West and F.J. Holler, *Analytical Chemistry: An Introduction*, 5<sup>th</sup> ed., Saunders College Publishing, Chicago, 1990.
- 2. J.B. Conant and T.H. Werner, "The determination of the strength of weak bases and pseudo bases in glacial acetic acid solutions," J. Am. Chem. Soc., 52, 4436 (1930).